(200)
R290
no. 85-452

USGS LIBRARY-RESTON
3 1818 00063171 1

UNITED STATES DEPARTMENT OF THE INTERIOR

GEOLOGICAL SURVEY

Geology and geochemistry of the Broken Ridge Area, Southern Wah Wah Mountains, Iron County, Utah

By

Karen A. Duttweiler

U.S. GEOLOGICAL SURVEY
RESTON, VA.
AUG 23 1985
LIBRARY

Open-file report
(Geological Survey
(U.S.))

ocle
#12489963

Open-File Report 85-452

This report is preliminary and has not been reviewed for conformity with U.S. Geological Survey editorial standards and stratigraphic nomenclature. Any use of trade names is for descriptive purposes only and does not imply endorsement by the USGS.

1985

CONTENTS

	Page
Abstract	1
Introduction	1
Previous work	3
Methods of study	3
Sample preparation	3
Sample analysis	4
Acknowledgements	4
Regional geologic setting	7
Structural setting	7
General stratigraphy	7
Oligocene volcanism	9
Miocene volcanism	9
Blawn Formation and associated mineralization	10
Steamboat Mountain Formation	12
Geology of the Broken Ridge area	12
Stratigraphy	12
Paleozoic sedimentary rocks (P, Paleozoic)	12
Needles Range Group; undivided (Tv, Oligocene)	12
Wah Wah Springs Tuff (Tw, Oligocene)	12
Lund Tuff (Tl, Oligocene)	13
Isom Formation (Ti, Oligocene)	13
Hornblende andesite (Tha, Miocene)	13
Bauers Tuff Member of the Condor Canyon Formation (Tcb, Miocene)	13
Andesite (Ta, Miocene)	13
Silicic clastic rocks (Tt, Miocene)	13
Vent breccia (Tbt, Miocene)	14
Steamboat Mountain Formation (Tr, Miocene)	15
Glassy margin (Trv, Miocene)	15
Green glass (Trg, Miocene)	17
Gray rhyolite (Trs, Miocene)	17
Rhyolite of Pine (Trp, Miocene)	29
Alluvium and colluvium (Qac, quaternary)	29
Structural features	31
Rock alteration	32
Silicification	32
Argillic alteration	32
Quartz-fluorite alteration	34
Quartz-alunite alteration	34
Geochemistry	36
Petrology of the Steamboat Mountain Formation	36
Rock geochemistry	40
Bible Spring fault zone	46
Southern Broken Ridge Area	52
Fourmile Wash	53
Heavy-mineral-concentrate geochemistry	53
Distribution of barite and garnet	53
Distribution of Sn and cassiterite	55
Tin mineralization	55
Discussion and conclusions	57
References	61
Appendix A	65

ILLUSTRATIONS

Plate 1. Geologic map of the Broken Ridge area.....in pocket

Figure 1. Map showing location of the study area..... 2

Figure 2. Map of southwest Utah and eastern Nevada showing faults and the extent of Miocene silicic volcanic rocks..... 8

Figure 3. Map showing the locations of mines and prospect pits associated with the Blawn Formation..... 11

Figure 4. Photomicrographs of the glassy margin (Trv)..... 18

Figure 5. Photomicrograph of the green glass (Trg)..... 22

Figure 6. Photograph of the gray rhyolite (Trs) showing steep flow-banding..... 24

Figure 7. Photograph of the gray rhyolite (Trs) with topaz crystals in groundmass..... 25

Figure 8. Microscopic views comparing topaz that is contained in groundmass and clear topaz contained in vugs..... 27

Figure 9. Photograph of the dome of Fourmile Wash..... 28

Figure 10. Photograph showing the rhyolite of Pine (Trp) overlying the gray rhyolite (Trs)..... 30

Figure 11. Simplified geologic map showing areas of alteration..... 33

Figure 12. Photomicrographs of alunite in silicic clastic rocks..... 35

Figure 13. AFM and Na_2O-K_2O-CaO ternary diagram for volcanic rocks in the southern Wah Wah Mountains..... 38

Figure 14. SiO_2 variation diagrams of CaO, Na_2O and K_2O for volcanic rocks in the southern Wah Wah Mountains..... 39

Figure 15. Location map of rock samples from the Broken Ridge area..... 41

Figure 16. Correlation diagrams of selected elements in volcanic rocks from the Broken Ridge area..... 43

Figure 17. Histograms of Sn, Mo, and Be abundances in fresh versus altered rhyolite..... 44

Figure 18. Histograms of Nb, Ba and Cu abundances in fresh versus altered rhyolite..... 45

Figure 19. Distribution of Be and F in rock samples from the Broken Ridge area..... 47

Figure 20. Distribution of Sn and Nb in rock samples..... 48

Figure 21. Distribution of U and Th in rock samples..... 49

Figure 22. Distribution of Cu and Mo in rock samples..... 50

Figure 23. Distribution of Pb and Ba in rock samples..... 51

Figure 24. Heavy-mineral-concentrate sample location map with simplified geology..... 54

Figure 25. Distribution of Sn and cassiterite in heavy-mineral concentrates..... 56

Figure 26. Photomicrographs of cassiterite and hematite in vein in silicified rhyolite..... 58

Figure 27. Schematic diagram showing the relationship between rhyolite tuffs and flows in the Broken Ridge area, and possible mineralization related to them..... 60

TABLES

Table 1. Limits of determination for the spectrographic analysis of stream sediments, heavy-mineral concentrates and rocks..... 5

Table 2. Chemical methods used for selected rock samples..... 6

Table 3. Modal analysis of volcanic rocks in the Broken Ridge area..... 16

Table 4. Chemical composition of selected rhyolite samples from the Broken Ridge area..... 19

ABSTRACT

This study was undertaken to document the geologic, petrologic, and geochemical relationships of the tin-bearing rhyolitic lava flows and domes of the 12 million-year-old Steamboat Mountain Formation in the area of Broken Ridge. Early phases of volcanic activity produced a topaz-bearing rhyolite followed by eruption from many local centers of a crystal-poor rhyolite. The rhyolites contain high Si (>74%) and alkalies, and are enriched in Sn, Be, F, Nb, Li and Rb: Ca, Mg, Ti, P and Ba are low. These characteristics suggest that the rhyolites formed as highly differentiated magmas.

Crystalline cassiterite and wood tin are abundant and widespread in heavy-mineral-concentrate samples. Some of the crystalline cassiterite occurs with specular hematite in veins within the rhyolite which formed either as a result of degassing during cooling of the rhyolite or from a later hydrothermal event.

Reactivation along a 23-m.y. fault zone occurred after emplacement of the rhyolite that resulted in a series of high angle normal faults. Multiple hydrothermal events resulted in widespread alteration along the faults and concentration of Be, F, Sn, Nb, Mo, Cu, Zn, W and Ba.

INTRODUCTION

The geology and geochemistry of high-F or topaz-bearing rhyolites in Nevada and Utah have been of considerable interest in recent years in light of their structural and genetic implications and the moderate to high potential for Be, Sn, Mo, U and F deposits that are commonly associated with them. Two such high-F rhyolites occur in the southern Wah Wah Mountains, a north-south trending mountain range in the eastern part of the Great Basin in southwest Utah (fig. 1).

The presence of a 12-m.y.-old topaz-bearing rhyolite and high Be, Sn and Mo contents in stream-sediment samples collected during a reconnaissance geochemical survey by Miller and others (1980) spurred interest in an area of the Mountain Spring Peak 7 1/2' quadrangle, Iron County, Utah. The area is located about 64 km northwest of Cedar City and 56 km southwest of Milford. Two major dirt roads give access to the area; the north-south Pine Valley road and the east-west county road or Jockey road. Other dirt roads requiring four-wheel drive vehicles make access to the area very good.

Deposits of Be and Sn are commonly associated with high-F rhyolites; rhyolitic flows and tuffs at Spor Mountain, Utah, are host to Be mineralization (Burt and others, 1982) and tin occurs in rhyolite at Sierra Madre Occidental in northern Mexico (Huspeni and others, 1984) and in the Black Range, New Mexico (Eggleston and Norman, 1984).

The purpose of this study is to determine the potential for mineralization of Be, Sn, Mo or F in the area of Broken Ridge by documenting the geologic, petrologic, and geochemical relationships of the high-F lava flows and domes, and the nature and extent of alteration along major faults.

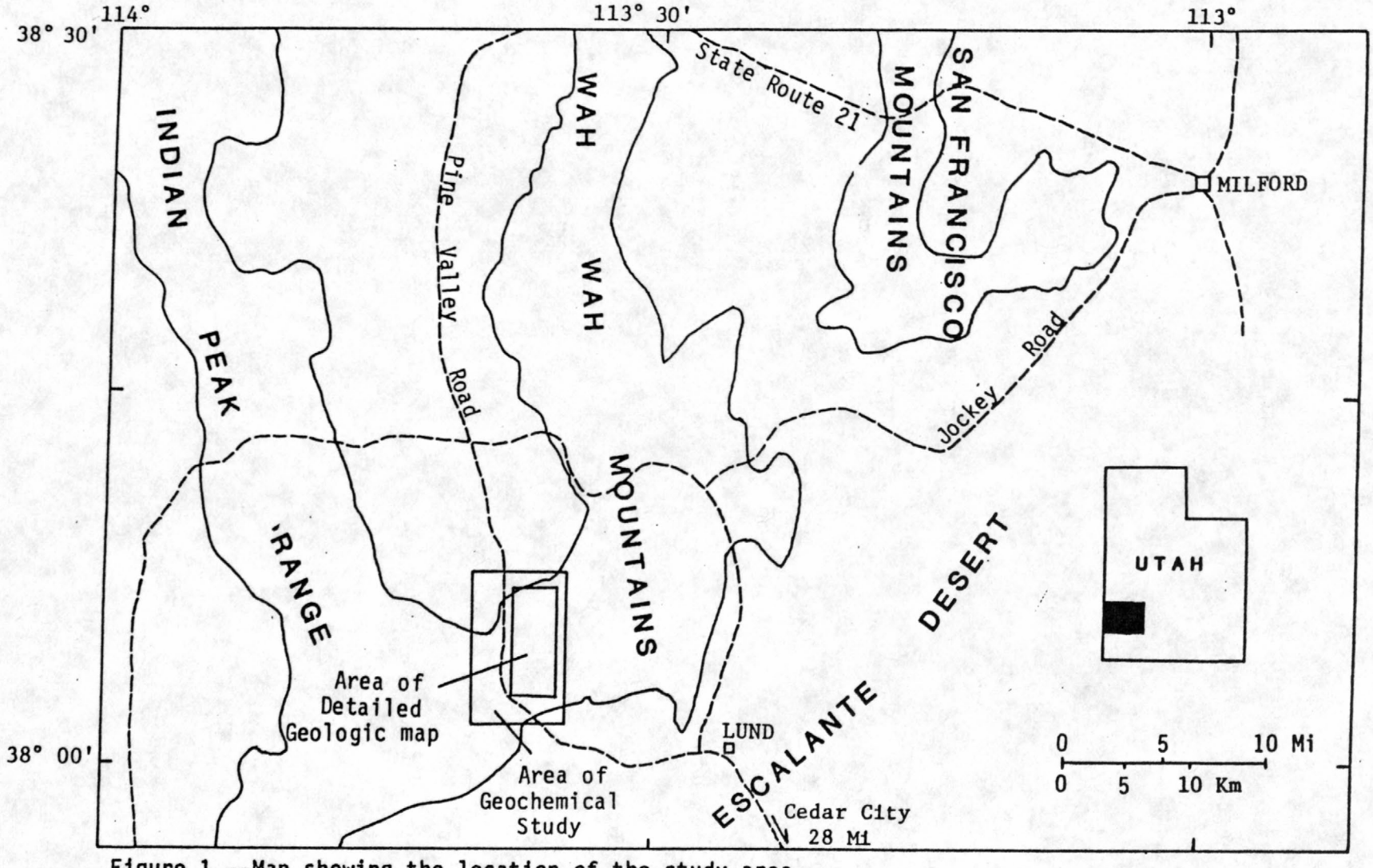

Figure 1.--Map showing the location of the study area.

Previous work

Previous geologic mapping in the Mountain Spring Peak quadrangle was by Best (1979). The Bible Spring quadrangle to the west was mapped by Best and Davis (1981), and the Teton quadrangle to the north by Best and Keith (1979). The mapping at a scale of 1:24,000 and the descriptions of Oligocene and Miocene volcanic rocks in the area provided an excellent background for more detailed work.

A reconnaissance geochemical study of stream-sediment samples in the Richfield 2^{o} sheet by Miller and others (1980) was the first study of its kind in the area. Tucker and others (1981) did a follow-up study using rock geochemistry in parts of the Mountain Spring Peak and Bible Spring 7 1/2' quadrangles. Steven and Morris (1984) compiled all available geologic and geochemical data on the Richfield 2^{o} sheet to determine the mineral resource potential.

Methods of study

Field work, on which this paper is based, was conducted in the summer of 1983 and spring of 1984. Detailed geologic mapping at a scale of 1:24,000 was conducted on a 56 sq km area near Broken Ridge (fig. 1). Detailed petrographic work on thin sections was completed following field work to aid in describing rock units.

In conjunction with the mapping, 41 heavy-mineral-concentrate samples and 204 rock samples were collected for geochemical analysis in the area of Broken Ridge and Fourmile Wash and west-southwestward along the Bible Spring fault zone. About 10 lbs of composite sediment from alluvium in dry washes was collected at each of 41 sites and concentrated by panning in available streams near the study area. Rock samples were largely composite or chip samples collected within a radius of about 2 m at any given site. Samples collected in fresh rock range from $\frac{1}{2}$ km to 2.5 km apart, depending on access and rock exposure. The density of sampling from obviously altered or mineralized rock is much greater; in many altered areas, samples were collected every 8-10 m across an outcrop or zone of alteration. For most rock samples, a representative rock was retained for making thin sections and splits of very fine-grained or altered rocks were made for the purpose of x-ray diffraction studies in an attempt to delineate types of alteration.

Sample preparation

The heavy-mineral concentrates were sieved through a 20-mesh screen, and the +20-mesh fraction was retained for mineralogical analysis. The light minerals (quartz and feldspar) still remaining in the -20-mesh fraction after panning were removed with bromoform (s.g. 2.85). Magnetite was removed with a hand magnet. Using a Frantz Isodynamic Magnetic Separator with a 15^{o} side slope and 25^{o} forward slope setting, three fractions were obtained; the magnetic at 0.5 ampere (M.5), the magnetic at 1.0 ampere (M1), and the nonmagnetic at 1.0 ampere (NM). The M.5 and M1 fractions were used only for mineralogical studies. The NM fraction contains the most common ore-forming sulfide and oxide minerals as well as such accessory minerals as zircon, sphene, topaz, and fluorite. The NM fraction was divided into two splits; one was saved for mineralogical analysis and one was hand-ground for spectrographic analysis.

All rocks were crushed and pulverized to a fine powder. Splits were made of 20 selected samples and one split was analyzed by x-ray fluorescence to obtain major elements not provided by spectrographic analysis. The other split, along with all other rock samples was analyzed by spectrographic and other chemical methods.

Sample analysis

Heavy-mineral concentrates were analyzed for Sn content and rocks were analyzed for 31 elements using a semiquantitative direct-current arc emission spectrographic method (Grimes and Marranzino, 1968). The elements and their limits of determination are listed in Table 1. Spectrographic results were obtained by visual comparison of spectra derived from the sample against those derived from known standards. The semiquantitative spectrographic results are reported as one of six steps per order of magnitude (1, 0.7, 0.5, 0.3, 0.2, 0.15 and multiples of these numbers) and the values are the approximate midpoints of the concentration ranges. The precision of the analytical method is approximately plus or minus 1 reporting interval at the 83 percent confidence level and plus or minus 2 reporting intervals at the 96 percent confidence level (Motooka and Grimes, 1976). Values determined for the major elements (iron, magnesium, calcium, and titanium) are given in weight percent; all others are given in parts per million. Subsequent to analysis of the 31 elements listed in Table 1, all rocks were analyzed for Li, Rb, and Cs using a modification of the semiquantitative emission spectrographic method. The modification consists of a special orange filter to block light below 5000 Å in order to read the Li, Rb, and Cs spectra. Limits of detection for these three elements are also included in Table 1. Other chemical methods of analysis used on selected rocks from the Broken Ridge area are summarized in Table 2.

Major elements for 18 pulverized rock samples were determined using a Siemens set-up for x-ray fluorescence spectrometry. Prior to analysis, 1 gram of sample was dissolved in 7 gm of lithium tetraborate flux by heating to 1100°C in a Claisse fluxer for a minimum of one hour, and then poured into a mold making disk where it was ready for analysis.

All analytical results for rock samples are listed in Appendix A.

Acknowledgements

Discussions with Dr. L. C. Hsu of the University of Nevada throughout this study and guidance from him were greatly appreciated. I wish to thank W. R. Griffitts of the U.S. Geological Survey for aiding in field work and field interpretations, numerous discussions on the geochemistry and alteration and providing continual support. Discussions with M. G. Best and T. A. Steven were very helpful. Belinda Arbogast and B. M. Adrian analyzed all samples for 31 elements while S. J. Sutley analyzed all rock samples for Li, Rb, and Cs. A. E. Hubert analyzed 18 rock samples by x-ray fluorescence. Numerous conversations and discussions with T. Botinelly gave me food for thought. Finally, I wish to thank the people of Lund and adjacent areas, especially Lehi Wood, for being extremely friendly and courteous in giving valuable information concerning the history of mining in the area and other interesting geologic problems.

TABLE 1.--Limits of determination for the spectrographic analysis of heavy-mineral concentrates and rocks. The limits are based on a 10-mg sample for rocks, and a 5-mg sample for heavy-mineral concentrates.

Elements		Lower determination limit		Upper determination limit	
Percent		Concentrates	Rocks	Concentrates	Rocks
1.	Iron (Fe)	.1	.05	50	20
2.	Magnesium (Mg)	.05	.02	20	10
3.	Calcium (Ca)	.1	.05	50	20
4.	Titanium (Ti)	.005	.002	2	1
Parts per million					
5.	Manganese (Mn)	20	10	10,000	5,000
6.	Silver (Ag)	1	.5	10,000	5,000
7.	Arsenic (As)	500	200	20,000	10,000
8.	Gold (Au)	20	10	1,000	500
9.	Boron (B)	20	10	5,000	2,000
10.	Barium (Ba)	50	20	10,000	5,000
11.	Beryllium (Be)	2	1	2,000	1,000
12.	Bismuth (Bi)	20	10	2,000	500
13.	Cadmium (Cd)	50	20	1,000	2,000
14.	Cobalt (Co)	10	5	5,000	5,000
15.	Chromium (Cr)	20	10	10,000	20,000
16.	Copper (Cu)	10	5	50,000	1,000
17.	Lanthanum (La)	50	20	2,000	2,000
18.	Molybdenum (Mo)	10	5	5,000	2,000
19.	Niobium (Nb)	50	20	5,000	5,000
20.	Nickel (Ni)	10	5	10,000	20,000
21.	Lead (Pb)	20	10	50,000	10,000
22.	Antimony (Sb)	200	100	20,000	100
23.	Scandium (Sc)	10	5	200	1,000
24.	Tin (Sn)	20	10	2,000	5,000
25.	Strontium (Sr)	200	100	10,000	10,000
26.	Vanadium (V)	20	10	20,000	10,000
27.	Tungsten (W)	100	50	20,000	2,000
28.	Yttrium (Y)	20	10	5,000	10,000
29.	Zinc (Zn)	500	200	20,000	1,000
30.	Zirconium (Zr)	20	10	2,000	2,000
31.	Thorium (Th)	200	100	5,000	5,000
	Lithium (Li)		1		5,000
	Rubidium (Rb)		10		5,000
	Cesium (Cs)		20		50,000

TABLE 2. Chemical methods used for rock samples

Constituent determined	Analytical method	Determination limit* ppm	Analyst(s)	Reference
Gold (Au)	AA	.05	Roemer and Sharkey	Thompson and others, 1968.
Arsenic (As)	AA	10	Roemer and Sharkey	Modification of Viets, 1978.
Fluorine (F)	Specific ion	100	Roemer and Sharkey	Hopkins, 1977.
Uranium (U)	Fluorometry	.05	Roemer and Sharkey	Modification of Cantanni and others, 1956.

*The determination limit is dependent on sample weight. Given limits imply use of sample weight required by method. Higher limits of determination result from using less than required sample weight.

REGIONAL GEOLOGIC SETTING

Structural setting

The southern Wah Wah Mountains lie on the eastern border of the Basin and Range physiographic province, 50-70 km west of the Colorado Plateau. The area is within the Blue Ribbon lineament as described by Rowley and others (1978). This lineament is described as a prominent east-west structural zone within the Pioche mineral belt in southern Utah and Nevada that cuts across north-south trending mountain ranges and valleys of the Basin and Range province (fig. 2). The lineament, about 25 km wide and several hundred kilometers in length, is marked by volcanic centers, mineral deposits, hydrothermally altered rocks, geophysical anomalies and major faults (Rowley and others, 1978).

As is characteristic of the Basin and Range province in general, high angle normal faults predominate in the southern Wah Wah Mountains. Most of the major faults trend northeast, with the exception of the northwest striking Blawn Wash fault zone northeast of The Tetons (fig. 2). Belts of silicic lava flows, magma centers, and dikes nearly parallel the northeast trending faults. Field evidence suggests the faults are early to mid-Miocene in age (Best and others, 1983), but movement has recurred along the faults since the mid-Miocene. For example, late Miocene rocks of the Steamboat Mountain Formation lie unconformably on tilted and faulted Oligocene rocks. The Steamboat Mountain Formation is not cut by any major throughgoing faults, but it is cut by many small faults. Structural characteristics within the Steamboat Mountain Formation will be discussed in greater detail in later sections of this report.

The general northeast trend of silicic magma centers, dikes, and faults in the southern Wah Wah Mountains suggests a northwest-southeast direction of extension in the early Miocene which is contrary to a west-southwest-east-northeast direction of extension claimed to have prevailed throughout the western United States around 20-10 Ma (million years ago) (Zoback and others, 1981, p. 204). Best and others (1983) suggest that a local perturbation in a regionally otherwise uniform early-mid Miocene stress field may have existed, and note that the northeast trend of faults in the southern Wah Wah Mountains is nearly parallel to and only a few tens of kilometers from the long-standing geologic boundary--the hinge line between the thick craton to the east and the Paleozoic geosyncline to the west, the leading edge of the Sevier orogenic belt, and the transition zone between the Colorado Plateau and the Basin and Range Province.

General stratigraphy

The southern Wah Wah Mountains area consists primarily of Oligocene and Miocene volcanic rocks that overlie and intrude Paleozoic and Mesozoic sedimentary rocks.

During the late Precambrian through the Paleozoic Era, deposition in southwest Utah took place in a miogeosynclinal environment dominated by carbonate strata (Steven and Morris, 1984). The Mesozoic Era was dominated by clastic sedimentation on a plateau-type continental environment (Miller, 1966). The Laramide and Sevier orogenies in the late Mesozoic and early

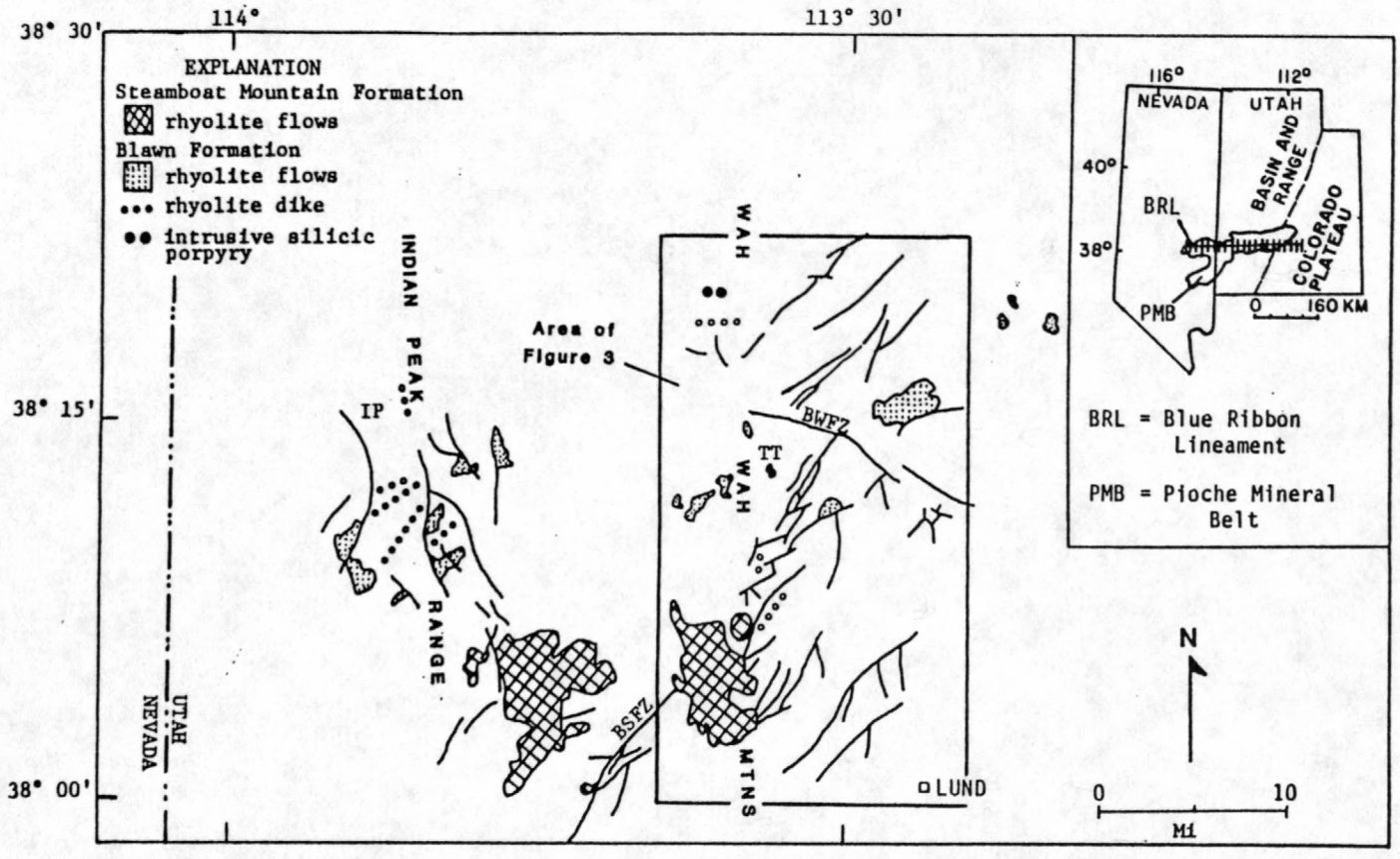

Figure 2.--Map of southwest Utah and eastern Nevada showing faults and the extent of Miocene silicic volcanic rocks (after Best and others, 1983). BSFZ = Bible Spring fault zone; BWFZ = Blawn Wash fault zone; IP = Indian Peak; TT = the Tetons; Rectangular boundary is the area of Figure 3. Inset shows the location of the Pioche mineral belt and the Blue Ribbon lineament (after Rowley and others, 1978).

Tertiary terminated the extensive sedimentation and brought late Precambrian and Paleozoic carbonate rocks over clastic Mesozoic strata (Miller, 1966).

Oligocene volcanism

About 33 Ma, volcanic activity began with deposition of the Sawtooth Peak Formation, a calc-alkalic ash-flow tuff of intermediate-composition. Then, beginning at 30 Ma, ash-flow tuffs of the Needles Range Group were deposited (Best and others, 1983; Best and Keith, 1983). Formerly referred to as the Needles Range Formation (Best, 1979), this unit has recently been classified as a group (Best and Grant, 1985) consisting of four formations: The Escalante Desert Formation, the Cottonwood Wash Tuff, Wah Wah Springs Tuff, and the Lund Tuff. The Escalante Desert Formation consists of crystal-poor, rhyolitic ash-flow tuffs, rhyolite and pyroxene andesite lava flows, and local epiclastic deposits. The Cottonwood Wash Tuff is a crystal-rich dacite tuff which crops out almost entirely in the northern Indian Peak Range (sometimes referred to as the Needle Range or Mountain Home Range) and in eastern Nevada. Following deposition of the Cottonwood Wash Tuff, eruption of the dacitic Wah Wah Springs Tuff produced the Indian Peak caldera, which straddles the Utah-Nevada border. The Wah Wah Springs Tuff is exposed in eastern Nevada and western Utah over an area of almost 25,000 km^2 and its eruption volume is estimated at nearly 5,000 km^3 (Best and Keith, 1983). Later episodes of volcanic activity produced the Lund Tuff, which is very widespread in the Indian Peak Range and the southern Wah Wah Mountains where it generally overlies either Paleozoic sedimentary rocks or older volcanic rocks such as the Wah Wah Springs Tuff.

The Isom Formation is a latitic ash-flow tuff, overlying the Needles Range Group (Mackin, 1960). The Isom is generally only a few tens of meters thick and is very widespread, reflecting the low relief in the area at the time of emplacement. The Isom Formation provides a prominent marker unit in the Oligocene sequence, as it is a distinctive, crystal-poor densely welded tuff. It has been dated at 26-25 m.y. (Armstrong, 1970; Fleck and others, 1975).

Ash-flow sheets of the Quichipa Group were erupted 24-21 Ma from the Caliente caldera south of Pioche, Nevada (Ekren and others, 1977). In the southern Wah Wah Mountains, the Condor Canyon Formation is the only exposed formation from this episode of volcanic activity. It has been dated at 22 m.y. (Fleck and others, 1975).

Miocene volcanism

Beginning about 23 Ma, magmatism shifted from voluminous ash-flow tuff eruptions of intermediate composition to a more bimodal mafic-rhyolite assemblage from many local centers which was approximately coincident with the onset of extensional tectonism in the Basin and Range province (Best and others, 1983). The first pulse from 23-18 m.y. was characterized by high-K mafic lavas with rhyolitic tuffs and flows. Shallow intrusive porphyries accompanied this episode of volcanic activity. These 23- to 18-m.y.-old rocks are grouped together as the Blawn Formation (Best and others, 1983).

At 12 m.y. another bimodal assemblage of less potassic mafic flows with rhyolitic ash-flow tuffs and flows was erupted to the south of the Blawn

Formation. These rocks make up the Steamboat Mountain Formation. Figure 2 shows the distribution of both groups of these Miocene volcanic rocks. Both episodes of volcanic activity define a general east-west trending belt and both were accompanied by alteration and mineralization.

Blawn Formation and associated mineralization

The Blawn Formation consists of intrusive porphyries and high-Si, high-F lava flows which overlie and interfinger with crystal-poor, lithic ash-flow tuffs. Intrusives are contemporaneous with or a little older than the flows (Best and others, 1983). High-K trachyandesite lava flows are less abundant than the rhyolite but are contemporaneous with the eruption of the rhyolitic tuffs and flows. Some of the intrusive porphyries and high-Si flows included in this 23-18 m.y. age bracket have associated mineralization. Figure 3 shows the locations of some mines and prospect pits associated with the Blawn Formation.

The Pine Grove and East End plutons (location B1 on fig. 3) are small stocks of quartz latite and quartz monzonite that were intruded about 24 Ma (Abbott and others, 1983). A stockwork Mo-W porphyry deposit lies at a depth of 900 m to greater than 2000 m in the Pine Grove pluton (Abbott and others, 1983). A garnet-bearing tuff of about 23 m.y. completely surrounds the Pine Grove pluton and is believed to be an eruptive facies of the largely concealed porphyry system (Keith, 1979).

Porphyritic, flow-layered rhyolite of 20.2 m.y. (Rowley and others, 1978) is present in a small intrusive at the Staats mine (location B2). The Staats mine has been an intermittent producer of fluorspar and uranium for many years. The ore minerals occur in brecciated and extremely altered rhyolite at its fault contacts with Paleozoic carbonate rocks. Lindsey and Osmonson (1978) report high concentrations of Be, Ga, Li, Mo, Nb, and Sn in unmineralized rhyolitic rocks from the Staats mine area.

East of the Staats mine, an area about 6 km wide on and near the lower eastern slopes of Blawn Mountain (location B3) consists of large bodies of the Blawn Formation that are altered to alunite, kaolinite, iron oxides, and silicified breccia (Lindsey and Osmonson, 1978). The source of the sulfur to form the alunite appears to be magmatic (R. O. Rye, written communication, 1982; from Steven and Morris, 1984). Whether the alteration at Blawn Mountain and the mineralization at the Staats mine resulted from the same hydrothermal event or two separate episodes is not yet known.

East of Blawn Wash and Willow Creek (location B4) are rhyolite flows with a K-Ar age of 22 ± 0.8 m.y. (Best and others, 1983), which locally contain gem quality red beryl in groundmass or along small fractures or veins. Topaz and bixbyite are also present and the latter forms inclusions in some red beryl crystals.

The Cima (Katie) mine is located 5 km south-southwest of Jockey Spring (location B5). Tuffs of the Blawn Formation are argillized and silicified where they are in fault contact with Paleozoic sedimentary rocks. Native sulfur with small stringers of cinnabar occur within the altered rhyolitic tuffs. The Cima mine is along the projection of the Bible Springs fault zone. Therefore, this deposit may have formed soon after deposition of the

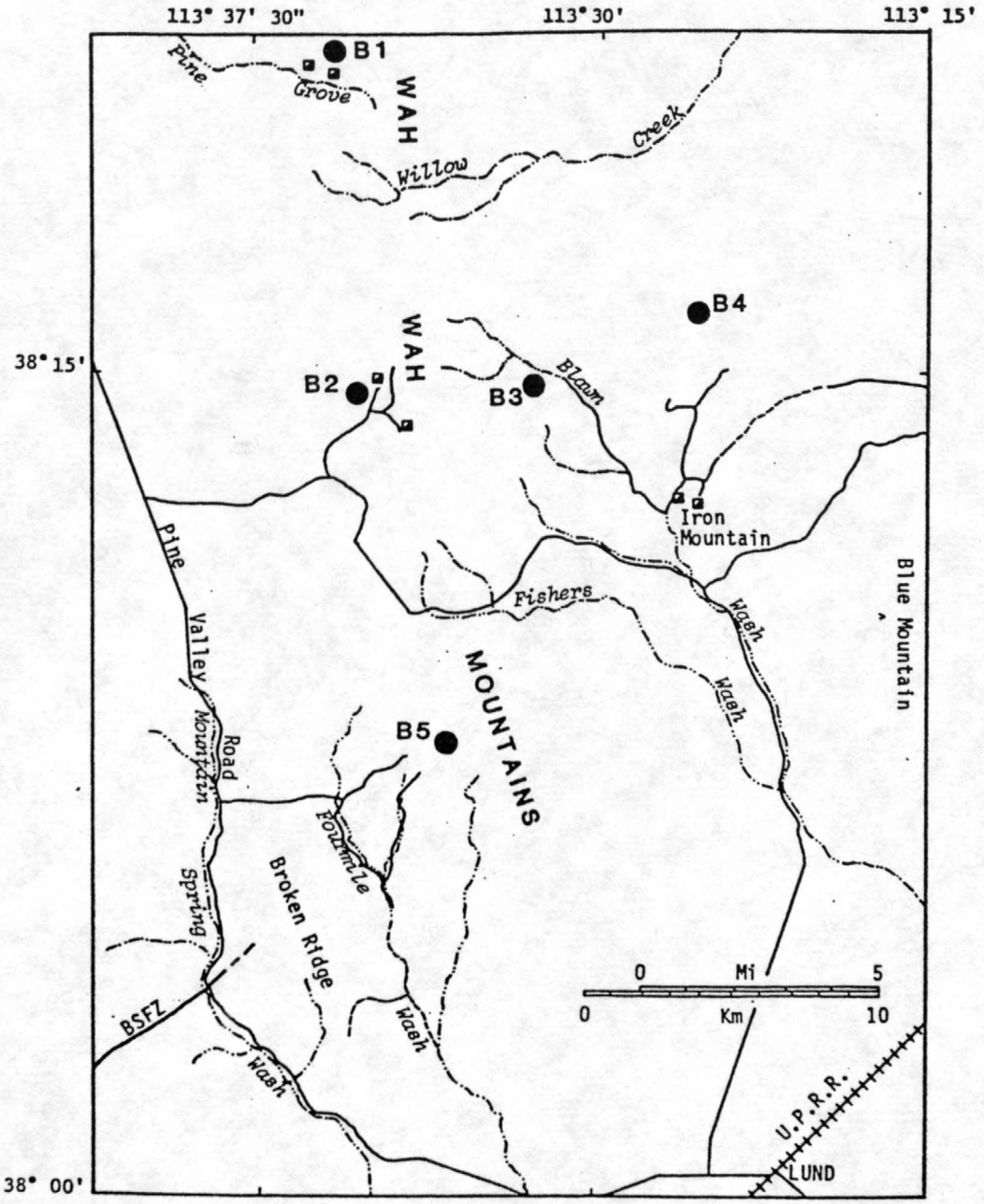

Figure 3.--Map showing the locations of mines and prospect pits associated with the Blawn Formation. U.P.R.R.--Union Pacific Railroad; BSFZ--Bible Spring fault zone.

Blawn Formation as a result of hydrothermal fluids circulating along the Bible Spring fault. On the other hand, it is possible that the mineralization and alteration occurred later in time as a result of hydrothermal activity associated with the Steamboat Mountain Formation (Steven and Morris, 1984).

Steamboat Mountain Formation

The Steamboat Mountain Formation consists of mafic flows, topaz-bearing rhyolite flows and domes, ash-flow tuffs, airfall deposits and reworked water-laid volcaniclastic rocks. The mafic flows are limited in extent in the southern Wah Wah Mountains (Best and others, 1983). The rhyolite flows are extensive in the Wah Wah Mountains and the southern Indian Peak range (fig. 2) where they reach their greatest thickness of 500 m at Steamboat Mountain (Best and Davis, 1981).

Hydrothermal alteration is prominent in several places within the Steamboat Mountain Formation, particularly along faults such as the Bible Spring fault zone. Alteration and mineralization associated with the Steamboat Mountain Formation in the vicinity of Broken Ridge and southwestward along the Bible Spring fault zone will be discussed in detail in later sections of this report.

GEOLOGY OF THE BROKEN RIDGE AREA

Plate 1 is a geologic map of the Broken Ridge area. The area west of latitude 113°37'30" (approximately) was mapped by Best (1979) and Best and Davis (1981). East of this latitude, the geology is represented by mapping as part of this study. The following descriptions of units refer primarily to the area covered by this study. For a more detailed description of units west of latitude 113°37'30", refer to Best (1979) and Best and Davis (1981).

Rhyolite units of the Steamboat Mountain Formation occur in the area of Broken Ridge and Fourmile Wash, where they unconformably overlie Oligocene volcanic rocks or Paleozoic rocks. Numerous north to northeast-trending normal faults characterize the area with minor east-west and northwest trending faults.

Stratigraphy

Paleozoic sedimentary rocks (P, Paleozoic)

This unit consists of undivided Paleozoic sedimentary rocks including limestone and dolomite with some clastic sedimentary rocks.

Needles Range Group; undivided (Tv, Oligocene)

A small area east of Fourmile Wash in the east-central portion of the map area consists of undivided formations of the Needles Range Group. For greater detail, see Best (1979).

Wah Wah Springs Tuff (Tw, Oligocene)

The unit is a crystal-rich dacitic ash-flow tuff characterized by abundant plagioclase, hornblende, and biotite phenocrysts with less than 2% quartz phenocrysts. It has been dated as 29.5 m.y. (Best, 1979).

Lund Tuff (Tl, Oligocene)

The Lund Tuff is a 27.9 m.y. dacitic ash-flow tuff characterized by 25% phenocrysts of quartz, biotite, and lesser amounts of hornblende. Locally, it contains a black basal vitrophyre (Best, 1979).

Isom Formation (Ti, Oligocene)

Dated at 26 m.y., the Isom Formation consists of a densely welded, red-brown to lavender ash-flow tuff with less than 20% phenocrysts of plagioclase and minor pyroxene. It is widespread in the southern part of the map area where it overlies the Lund Tuff. The thickness is generally only a few tens of meters thick. The weathering of this unit to brown plates or grus makes it distinctive. For more detailed description, see Best (1979) and Best and Davis (1981).

Hornblende andesite (Tha, Miocene)

This unit consists of platy, gray rock with abundant black hornblende and lesser green augite phenocrysts in a very fine-grained trachyitic matrix rich in plagioclase. Locally, it is phenocryst-poor or even aphyric. Thickness ranges from 50-100 m (Best, 1979).

Bauers Tuff Member of the Condor Canyon Formation (Tcb, Miocene)

Gray, buff, and lavender, firmly welded ash-flow tuffs containing 10% phenocrysts of plagioclase, sanidine, and biotite make up this unit. Age is 22 m.y. (Fleck and others, 1975; from Best, 1979). It occurs only in the northern portion of the map area.

Andesite (Ta, Miocene)

The unit consists of large plagioclase and smaller pyroxene phenocrysts set in a red-brown felsitic matrix (Best, 1979), occurring only in the far northern portion of the map area.

Silicic clastic rocks (Tt, Miocene)

This unit was first described by Best (1979) as pyroclastic and epiclastic rocks associated with rhyolite units of the Steamboat Mountain Formation and the Blawn Formation covering a very large area in the southern Wah Wah Mountains (Best and Davis, 1981). West of longitude 113°37'30" (Plate 1), the clastic rocks were mapped and described by Best (1979), and Best and Davis (1981). The following description refers only to the silicic clastic rocks in the mapped area of this study.

In the Broken Ridge area, rocks of this unit are associated primarily with rhyolitic flow rocks of the Steamboat Mountain Formation, although the exact age of the rocks is unclear. It is possible that they represent episodes of volcanic activity anywhere from 18-12 m.y. prior to and between emplacements of rhyolitic flow rocks of the Steamboat Mountain Formation. The unit is interfingered with the flow rocks throughout the map area, but for the most part, it underlies the flow rocks and unconformably overlies older volcanic rocks. Thickness in the map area is from a few meters to 30 m. Most

commonly, the unit is gently dipping, from 5-15°, except in areas of faulting where it may reach 35° dips.

The unit consists of a heterogeneous sequence of buff to pink weakly welded ash-flow and minor air-fall tuffs that interfinger with slope wash deposits and reworked water deposited epiclastic rocks. As a whole, it is loosely cemented, though in some places it is silicified or calcified. Because it is less resistant than most of the surrounding rocks, the unit usually occurs in small valleys between the topographically higher ridges of rhyolite. The unit is conspicuous in aerial photographs because of its light color.

The weakly welded ash-flow tuff is light to dark pink containing abundant lithic and pumice fragments with 1-5% phenocrysts of quartz, feldspar, and biotite. Lithic and pumice fragments average 0.5 mm-5 mm in diameter.

In the northern part of the map area, a pumice-lapilli tuff alternates with moderately sorted, mostly sand sized deposits and poorly sorted slope wash deposits. The pumice lapilli tuff contains sparse phenocrysts of quartz, feldspar, and biotite. Pumice, in pieces ranging in size from 0.5-4 cm in diameter, makes up at least 30% of the beds in some places. Other lithic fragments include green and black glass, and clasts of the Lund Tuff (Tl) and Wah Wah Springs Tuff (Tw). East of Fourmile Wash, the pumice lapilli alternates with a buff sandstone exhibiting crude bedding and stratification that locally contains lenses of a unit consisting of angular fragments 20 cm in diameter of the Lund Tuff, probably reflecting a slope wash deposit. The unit as a whole reflects a local source with combined explosive eruption of volcanic debris and water deposited volcanic particles, prior to emplacement of the rhyolite.

In the southern portion of the map area, the unit consists of combined pyroclastic and epiclastic rocks as elsewhere in the map area, but due to the amount of faulting in the area, they are extensively argillized and silicified by hydrothermal solutions.

In the central map area, where green glass (Trg) is present in small outcrops, the clastic rocks consist primarily of fragments of the glass with sparse pumice and lithic fragments of older volcanic rocks. The clastic rocks here represent explosive eruptions from very local centers.

Vent breccia (Tbt, Miocene)

This unit occurs only in the southeast 1/4 of section 23, T31S, R16W and resembles a breccia made up almost entirely of angular fragments of green glass and pumice averaging 1.3 cm in diameter with sparse lithics fragments of rhyolite (Trs). It forms two small apron-like areas underlying the rhyolite of Pine (Trp). The unit in this area represents an explosive vent breccia which formed after emplacement and crystallization of the gray rhyolite (Trs) and before emplacement of the rhyolite of Pine (Plate 1, cross-sections B-B' and C-C').

Some rocks currently classified as silicic clastic rocks (Tt), particularly in the central map area, may be more suitably classified as vent breccias, but the exact petrographic and stratigraphic characteristics of these rocks have not yet been determined.

Steamboat Mountain Formation (Tr, Miocene)

The Steamboat Mountain Formation was first mapped by Best (1979) on Broken Ridge as the Formation of Blawn Wash and later classified as the Steamboat Mountain Formation on the basis of K-Ar dates of 12 m.y. (Best, 1981). The original description included a rhyolite member of Broken Ridge. Included in this rhyolite unit were sequences of gray, red-brown and lavender felsitic lava flows with autobrecciated margins and vitrophyric bases (Best, 1979). A vertically flow-layered green glass was also grouped as part of this formation. The rhyolitic flow rocks as described by Best (Tr) are combined as Tr on Plate 1. More detailed examination during this study showed four separate phases within the rhyolite, called here the glassy margin of the Steamboat Mountain Formation, or just glassy margin (Trv), the gray rhyolite of the Steamboat Mountain Formation, which will be referred to as the gray rhyolite (Trs), the green glass (Trg), and the rhyolite of Pine (Trp). Because the glassy margin (Trv) is a basal glass unit, it is considered to be relatively older than the other rhyolitic phases. The exact relationship between the green glass (Trg) and the gray rhyolite (Trs) is uncertain. The rhyolite of Pine (Trp) is relatively younger than the gray rhyolite. Age determinations on three rhyolite samples in the Broken Ridge area by Best and others (1983) give ages of 13-12 m.y., but qualitative age determinations are lacking for the four separate phases defined in this report.

Glassy margin (Trv, Miocene)

Previously included in the rhyolite member of Broken Ridge (Best, 1979), the unit crops out to the north of Broken Ridge in the far northern portion of the map area and consists of a vitrophyre and a localized underlying ash-flow tuff. The thickness of this unit is about 30 m. The tuff is pink and non-welded with 25-30% phenocrysts of sanidine, plagioclase, and quartz set in a glassy matrix. Locally, the tuff contains angular clasts from 3 mm to 2.5 cm in diameter, some of which are glassy, resembling the overlying vitrophyre, and others that have been devitrified. On weathered surfaces, the clasts are easily removed by erosion, creating a honeycomb appearance in outcrop.

The overlying vitrophyre is light gray to black, and crystal-rich, locally containing abundant chalcedony in small veinlets and cavities, interpreted to be from fluids circulating during cooling of the rhyolite. Phenocrysts in the glass make up 15-25% of the rock, and are mostly between 0.5 and 1.5 mm in diameter. Phenocrysts include (in order of decreasing abundance) moonstone sanidine, plagioclase, quartz, biotite, and opaques with sparse crystals of zircon and apatite. Modal analysis of selected volcanic rocks in the Broken Ridge area are listed in Table 3.

Moonstone sanidine, comprising 7-12% of the rock, ranges in size from 0.8 to 2.5 mm. Twinned plagioclase makes up 6% of the rock. Smoky quartz, comprising 5% of the rock, occurs as euhedral to subhedral grains, ranging from 0.5 to 1 mm in diameter. Many grains are embayed. Red to dark brown biotite, partially oxidized, constitutes 1 percent of the rock. Opaques are present in up to 1 percent of the rock.

The matrix is glassy, with some shard structures visible. Large circular cracks are present, either as a result of cooling or of hydration of the glass. Small spherulites are present in the glass as a result of

Table 3.--Modal analysis of volcanic rocks in the Broken Ridge area.

Latitude	Longitude	Sample no.	Rock type	matrix	quartz	sanidine	plag	bio	opaques	zircon	apatite	other
38 06 34	113 35 54	83K135	vitrophyre Trv	77.9	5.9	7.6	6.0	1.0	1.0	tr	tr	
38 06 34	113 36 00	83K239	vitrophyre Trv	74.9	6.8	10.2	7.6	tr	--	--	--	
38 03 23	113 34 08	83K199	rhyolite Trp	93.0	2.0	3.4	1.0	--	--	--	--	1-2% bio in groundmass
38 05 25	113 36 15	83K105	rhyolite Trp	97.0	1.0	2.0	tr	--	--	--	--	1-2% bio in groundmass
38 05 27	113 35 44	83K102	fl-lyd-rh[1] Trs	88.4	3.7	7.0	0.5	--	0.2	--	--	
38 05 48	113 36 34	83K236	pheno-rich[2] Trs	70.3	8.2	13.9	5.9	0.3	0.9	--	--	
38 04 49	113 34 52	83K191	fl-lyd-rh[1] Trs	90.8	0.9	4.5	1.7	--	1.1	--	tr	
38 03 35	113 34 55	83K265	green glass Trg	96.6	1.1	1.0	1.2	--	--	--	--	

[1]flow-layered rhyolite

[2]phenocryst-rich rhyolite

devitrification. Light brown rims of devitrification minerals surround most of the quartz and sanidine phenocrysts (Figure 4).

This vitrophyre is interpreted to be the glassy margin or base of the rhyolite flow occurring north of Broken Ridge, whereas the tuff represents an explosive eruption just prior to eruption of the rhyolite flow.

The available whole-rock data for the vitrophyre shows high SiO_2, between 76-78% (Table 4). The sample from Best and others (1983) is a vitrophyric base of the Steamboat Mountain Formation further west near Steamboat Mountain (in the Steamboat Mountain 7 1/2 quadrangle), but is probably equivalent to the vitrophyre in the Broken Ridge area.

Green glass (Trg, Miocene)

This unit was first described by Best (1979). Green, partly hydrated, devitrified and locally brecciated glass makes up this unit, which occurs mostly in the south-central part of the map area. The thickness ranges from 5 m to 20 m. About .5 km north of Pine triangulation station (NE 1/4 sec. 35, T31S, R16W), a rough east-west trending zone of small patches of the glass exists as well as moderate amounts about 1 1/2 km west of Fourmile Spring (NE 1/4 sec. 6, T32S, R15W). In every case, it is spatially related to clastic rocks of Tt, which for the most part overlie the glass. A very small outcrop exists to the north in the western half of sec. 24 (T31S, R16W).

The glass is nearly vertically flow-layered. Thick glassy layers alternate with spherulitic layers which are about 2 mm across (Figure 5). Phenocrysts, generally less than 0.5 mm in diameter, total only 1-3% and include plagioclase, quartz, and minor sanidine (Table 3). The matrix is mostly glassy, but small spherulites are present. Large circular cracks due to hydration are in some places filled with clays. Locally, the glass is almost entirely altered to clinoptilolite. Abundant chalcedony and opalline silica are also present as veins or cavity fillings. The bodies of glass grade into lithophysae-rich crystalline rhyolite such as the large body in the eastern part of section 1 (T32S, R16W). It has been suggested by Best (1979) that these bodies of green glass may represent feeder masses for the topographically higher bodies of weakly porphyritic rhyolite; an idea that is also supported by this study. In some places (NW 1/4 sec. 24, T31S, R16W; and SW 1/4 sec. 30, T31S, R15W), the glass forms small dikes that cut the gray rhyolite and run sub-parallel to the trend of normal faults. Cross-section C-C' on Plate 1 illustrates this relationship.

Chemically, the glass has high SiO_2 and relatively low Al_2O_3, MgO, and Na_2O contents compared with the other rhyolitic units (Table 4). Potassium is relatively high while Li and U are low. The high K_2O and low MgO, Na_2O, Li and U in the glass is probably due to the addition of K^+ and subtraction of the other elements that is common during hydration and devitrification of glass (Zielinski and others, 1977).

Gray rhyolite (Trs, Miocene)

This unit was previously described by Best (1979) as part of the rhyolite unit of the Formation of Blawn Wash. Gray and lavender felsitic lava flows and domes make up this unit and occur widely throughout the map area. The

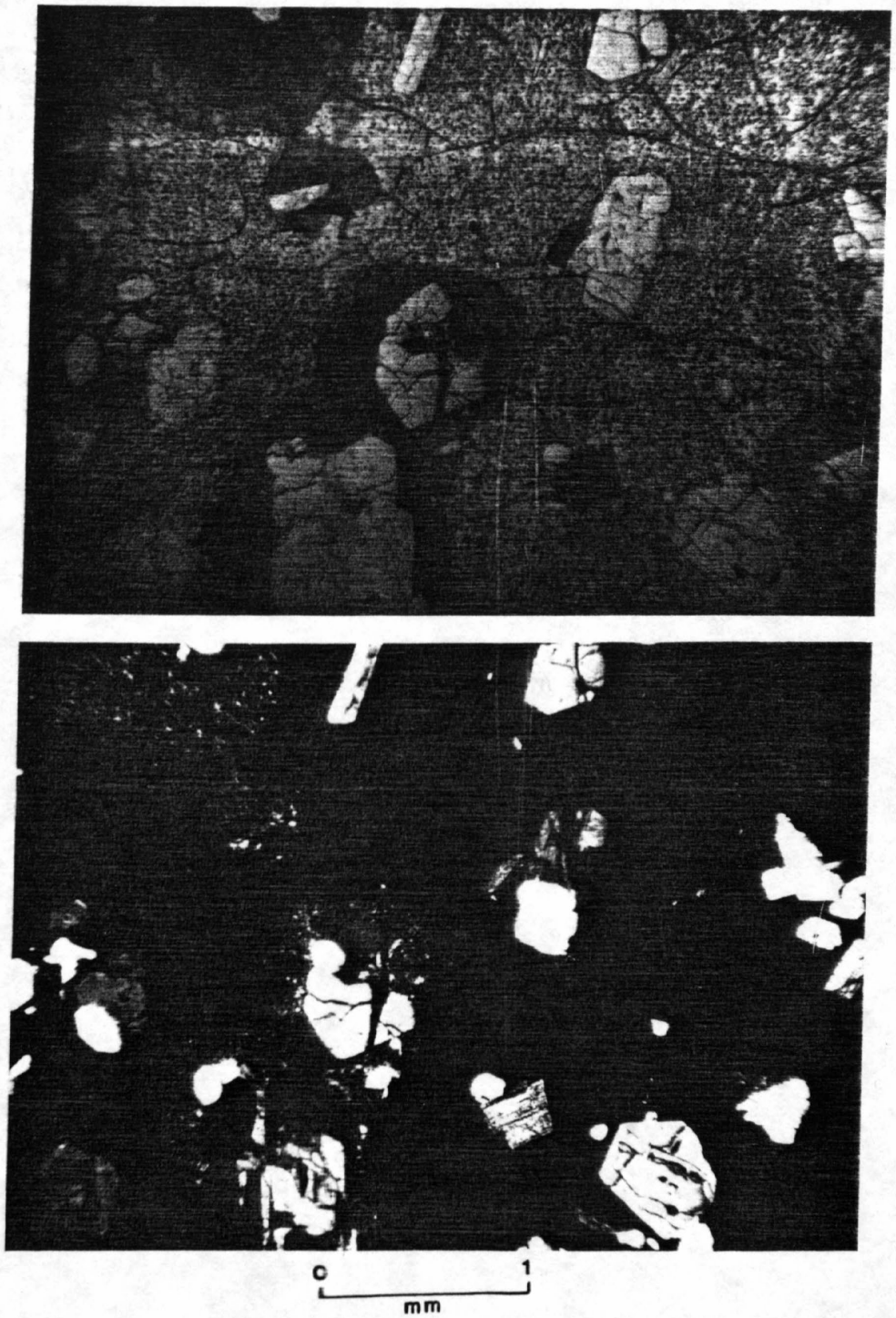

Figure 4. Photomicrographs of the glassy margin (Trv). Pheoncrysts of quartz, sanidine, and plagioclase set in a glassy matrix in plane light (top) and cross-polars (bottom); matrix shows hydration cracks and devitrified rims around the phenocrysts.

Table 4.---Chemical composition of selected volcanic rocks from the southern Wah Wah Mountains
[N, not detected; L, less than the detection limit; ---, not analyzed]

wt. %[1]	Trp 83K199	Trp 83K105	Trs 83K233	Trs 83K236	Trs 83K133	Trs 83K275	Trs 83K281	Trs 83K132	Trs 83K031	Trv 83K135
SiO_2	73.9	72.2	75.1	75.7	76.0	74.8	74.1	74.95	75.8	77.6
TiO_2	0.12	0.08	0.03	0.06	0.06	0.03	0.05	0.07	0.10	0.06
Al_2O_3	12.1	16.0	12.4	12.5	12.9	11.8	13.0	12.4	12.4	11.2
Fe_2O_3	1.1	1.4	1.07	0.91	1.16	1.03	1.01	1.51	1.3	0.94
MgO	0.1	0.1	0.07	0.1	0.03	0.1	0.1	0.1	0.2	0.1
CaO	1.0	0.4	1.78	0.94	0.43	0.90	0.55	0.22	0.2	0.37
Na_2O	3.7	3.6	3.3	3.54	3.06	4.55	3.0	3.09	3.4	3.93
K_2O	4.6	4.1	4.85	4.7	5.13	4.49	4.98	5.60	4.6	4.92
P_2O_5	0.09	0.08	0.03	0.02	0.10	0.04	0.01	0.01	0.10	0.01
Total	96.71	97.96	98.63	98.47	98.87	97.74	96.80	97.90	98.1	99.13
ppm[2]										
F	2800	2100	1100	500	520	300	2000	520	810	800
Be	20	7	15	20	20	15	15	20	10	20
Mo	5	7	10	10	5	L	500	10	20	L
Rb	500	700	500	500	700	500	100	500	---	700
Li	150	150	200	150	150	200	N	70	---	200
Nb	50	50	70	50	50	100	2.3	50	70	20
U	1.7	---	6.3	2.6	3.6	1.2	100	3.4	---	2.7
Y	100	70	100	50	70	100	20	70	100	50
La	20	N	L	N	50	L	20	20	100	L
Ba	N	N	50	20	20	L	20	L	L	20

Table 4 (cont).--Chemical composition of selected volcanic rocks from the southern Wah Wah Mountains

	(Trv)	Trg		ARGILLIZED RHYOLITE-STEAMBOAT MOUNTAIN FM					ALUNITE ALTERATION
wt. %[1]	1*	83K265	2*	83K027	83K037	83K088	83K116	83K115	83K265
SiO_2	76.4	74.4	52.6	73.2	74.2	73.1	73.6	77.5	74.9
TiO_2	0.08	0.04	1.89	0.11	0.11	0.11	0.05	0.06	0.2
Al_2O_3	12.2	11.0	16.4	12.4	10.8	11.6	7.4	10.8	12.1
Fe_2O_3	1.2	1.13	9.72	1.5	2.4	1.33	1.38	1.17	0.9
MgO	0.03	0.02	4.6	0.3	0.2	0.2	0.1	0.1	0.1
CaO	0.48	0.62	6.92	1.2	2.4	1.7	0.63	0.31	1.7
Na_2O	3.2	2.88	3.9	1.5	1.8	3.1	0.89	1.55	0.6
K_2O	4.88	5.08	2.79	5.4	4.0	4.4	3.76	6.63	3.2
P_2O_5	---	0.01	0.84	0.03	0.04	0.05	0.07	0.05	0.09
Total	98.42	95.18	99.82	95.64	93.95	95.56	87.88	98.17	93.79
ppm[2]									
F	---	900	---	820	710	500	700	420	1500
Be	---	10	---	5	10	50	50	20	5
Mo	---	10	---	L	10	150	150	5	N
Rb	270	700	---	---	---	700	700	700	50
Li	---	70	---	---	---	150	150	30	15
Nb	---	70	---	100	100	150	150	100	70
U	---	0.15	---	---	---	2.5	2.5	0.6	---
Y	---	100	---	20	70	100	100	30	15
La	---	20	---	N	70	L	L	N	L
Ba	---	N	---	N	L	N	50	50	300

Table 4 (cont).--Chemical composition of selected volcanic rocks from the southern Wah Wah Mountains

	BLAWN FORMATION						LUND TUFF	
wt. %[1]	3*	4*	5*	6*	7*	8*	83K143	83K264
SiO_2	75.8	75.8	74.5	76.1	60.5	58.7	65.4	65.3
TiO_2	0.06	0.06	0.28	0.05	0.96	0.94	0.7	0.61
Al_2O_3	12.4	12.8	12.8	12.5	15.9	15.4	13.5	13.5
Fe_2O_3	1.1	1.3	1.78	1.17	7.42	7.2	4.9	5.5
MgO	0.05	0.11	0.21	0.05	3.9	3.8	1.7	1.3
CaO	0.62	0.67	0.69	0.62	6.01	6.65	2.4	3.2
Na_2O	3.7	4.06	3.7	4.2	2.9	3.44	2.7	2.6
K_2O	4.72	4.60	5.41	4.64	3.32	3.10	3.4	3.6
P_2O_5	---	---	---	---	0.33	0.34	0.17	0.21
Total	98.56	99.43	99.42	99.47	101.29	99.65	94.87	95.82

[1]Locations of samples are listed in Appendix A.
[1]all whole rock analysis by A. E. Hubert using X-ray fluorescence spectroscopy
[2]F by specific ion electrode; U by fluorometry; all others by emission spectrographic method
*Best and others, 1983
1*vitrophyre from Steamboat Mountain quadrangle but assumed to be equivalent to vitrophyre in study area
2*mugearite flow of 13 m.y.
3*flow-layered felsitic topax-bearing flow at The Tetons in The Tetons quadrangle
4*intrusive plug feeder and extrusive flow at the Staats mine
5*strongly porphyritic felsic flow rock east side of Needle Range 6 km south of Indian Peak, Buckhorn Spring quadrangle
6*felsic, porphyritic flow 5 km west of Miners Hill Resevoir on east flank of Wah Wah Mountains in the Frisco quadrangle (23 m.y.)
7*trachyandesite flow in Frisco quadrangle
8*trachyandesite flow in Willow Creek southeast of Baudino Ranch in the Frisco quadrangle

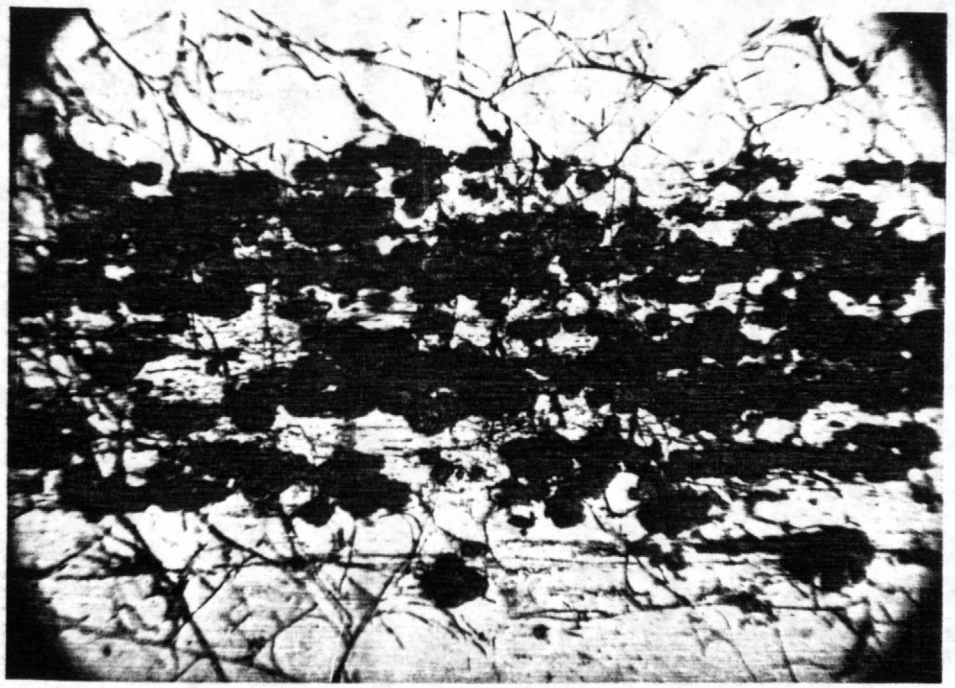

Figure 5.--Photomicrograph of the green glass (Trg). Photomicrograph in plane light; thin laminae of devitrification minerals alternate with glassy layers. Small phenocrysts of quartz (bottom center) are sparse.

thickness of the flows varies greatly; individual lava flows may be as little as 30 m thick, whereas sequences of flows are collectively at least 150 m thick, such as at Pine triangulation station where the gray rhyolite underlies the rhyolite of Pine. The rhyolite flows for the most part overlie but are locally interbedded with silicic clastic rocks of unit Tt. The flow rocks are massive to strongly flow-layered, sometimes giving a pancake-like appearance in outcrop. Flow-layers vary in thickness from thin laminae less than 1 mm up to many centimeters and meters, and are often contorted and isoclinally folded. Small pressure ridges and cracks or "stretch" features were seen at many outcrops. The "stretch" features probably formed during cooling of the rhyolite, and the direction of elongation is interpreted to be perpendicular to the direction of flow. Measurements were taken that were perpendicular to the elongation of these features and noted with an arrow by the strike and dip symbol. The arrow, therefore, is in the direction of flow.

Large thicknesses and consistantly steep flow-banding in the northwest quarter of section 24 (T31S, R16W) suggests a close proximity to a vent for this rhyolite (fig. 6). The north-trending normal fault in the area may have been a fissure vent through which the gray rhyolite vented as is suggested by the flow-banding of the rhyolite which dips moderately to steeply toward it on either side of the fault (Plate 1, cross-section C-C').

Petrographically, the flow-rocks of the gray rhyolite vary greatly. Three basic types can be distinguished: a phenocryst-rich rhyolite, a light gray aphyric rhyolite, and a light purple or lavender flow-layered rhyolite. All three types locally contain abundant lithophysae and vugs.

At the north end of Broken Ridge, the rhyolite contains 30% phenocrysts that are up to 3 mm in diameter of smoky quartz, sanidine, and plagioclase (Table 3). Dark brown biotite is present in small amounts. Groundmass is largely a fine-grained mixture of intergrown quartz and feldspar, with minor disseminated biotite and opaques. Locally, the unit contains numerous lithophysae and vugs that are filled with secondary minerals such as quartz and topaz. Lithophysae average 3-5 mm and the crystals completely fill them. Topaz crystals in the vugs are generally clear with very few inclusions. Just overlying the glassy margin (Trv) north of Broken Ridge, abundant lithophysae and vugs in the rhyolite are filled with chalcedony. Mordenite, a zeolite with a high Si/Al ratio, was identified in a vug in the phenocryst-rich rhyolite (NE 1/4 sec. 14, T31S, R16W). Chalcedony and zeolites as secondary minerals in vugs and lithophysae reflect the presence of fluids circulating during cooling of the rhyolite, and later circulation of groundwater.

Light gray, aphyric rhyolite occurs widely in and south of the area of Broken Ridge. It consists of an equigranular mixture of interlocking quartz and feldspar with some biotite, and up to 5% disseminated needle-like opaques. Locally, it is altered to clays, primarily kaolinite. Massive, in outcrop, it is locally flow-layered. Topaz occurs in groundmass, ranging from 1 cm to 3.5 cm in length (fig. 7). Largely intergrown with the rhyolite, the topaz indicates an extremely high F content in the magma at the time of crystallization. Crystals of topaz in groundmass contain numerous inclusions of rhyolitic material and dark black minerals, largely hematite. The topaz seems to be concentrated locally, perhaps due to entrapment of fluorine-rich fluids near the top of a cooling lava flow by another later overlying flow

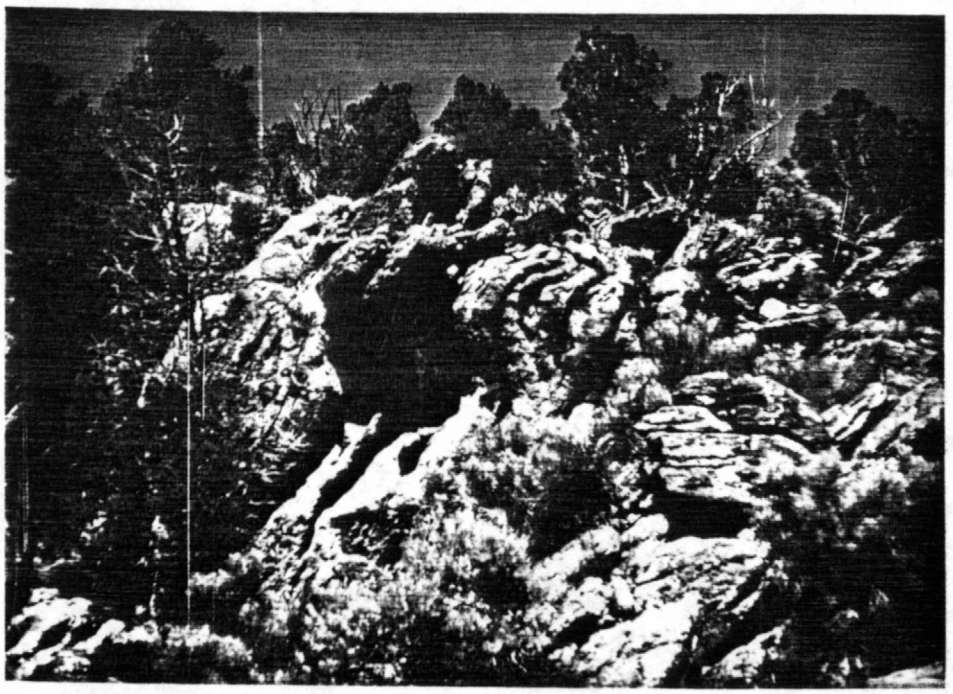

Figure 6. Photograph of the gray rhyolite (Trs) showing steep flow-banding (NW1/4 sec. 24, T31S, R16W). View looking north. Flow-banding has an overall westerly dip.

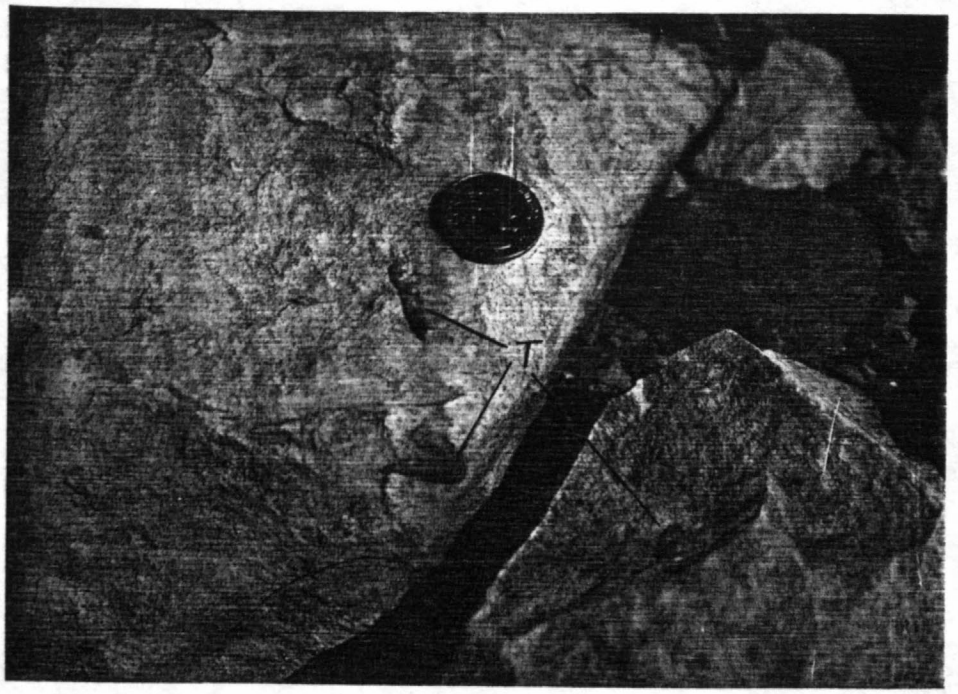

Figure 7. Photograph of the gray rhyolite (Trs) with topaz crystals (T) in groundmass. The quarter is 2.3 cm in diameter.

unit. On either side of Fourmile Wash in section 30, there are places where there are 5-7 topaz crystals per sq ft. A thick sequence of gray, aphyric rhyolite in the southern part of the map area (NE 1/4 sec. 12, T32S, R15W) has also concentrated topaz in groundmass. Vugs are prevalent locally and are commonly lined with quartz and clear topaz crystals interpreted to be products of vapor phase deposition. Small hematite plates are abundant in cavities wherever topaz is abundant. Figure 8 shows microscopic views comparing clear topaz from vugs with those contained in groundmass.

Light purple, flow-layered rhyolite occurs with the aphyric rhyolite. Phenocrysts are 0.5-1 mm in diameter, averaging 10% of quartz, sanidine, plagioclase, minor opaques and sparse apatite (Table 3). Groundmass consists of alternating dark purple compact layers of fine-grained quartz and feldspar aggregates and light gray more porous layers of coarse-grained quartz. Average thickness of layers is 0.5 mm-1.5 mm. Phenocrysts seem to be restricted to the fine-grained layers of quartz and feldspar with the light gray quartz-rich layers "bending" around the phenocrysts. Vugs, where present, occur at the boundary between layers and are filled with secondary quartz and topaz.

In the northeast, east of Fourmile Wash, the rhyolite is an extrusive lava dome, referred to in this paper as the dome of Fourmile Wash (fig. 9). Dips of flow-banding on the west side are generally eastward, at between 15-55^{0}, while those on the east dip westward with a well-defined imaginary line dividing the general directions of dip. Towards the center and top of the structure, dips of flow bands vary greatly, but reach 65-70^{0}. The structure suggests an upward movement in the center where the rhyolite exhibits steep flow-banding, with flaring and lessening of dips along the margins.

The rhyolite of the dome of Fourmile Wash is bounded on the west, north, and south by thin beds of silicic clastic rocks (fig. 9). The clastic rocks average 15 m in thickness in this area. The absence of the clastic rocks on the east side of the dome is due to faulting. The clastic rocks are pumice lapilli tuffs interbedded with moderately sorted sand sized material and slope wash deposits representing a mixture of explosive activity and reworked water-deposited material (page 14).

The rocks in the dome of Fourmile Wash are phenocryst-rich and similar to those north of Broken Ridge directly overlying the glassy margin. Phenocrysts of smoky quartz, sanidine, and plagioclase, up to 3 mm in diameter comprise 25-40% of the rock. Lithophysae are abundant, particularly on the east side of the dome, where a zone trending north to northeast of lithophysae-rich rhyolite contains abundant quartz and topaz, and minor fluorite as vapor phase crystals. It is interesting to note that both the dome of Fourmile Wash and the thick pile of rhyolite flow rocks from the possible fissure vent to the southwest lie along the projection of the Bible Spring fault zone.

About 1/2 km slightly northeast of Mountain Spring Peak in the southern part of the map area, very steep flow-banding over a large area suggests it may also be a dome complex, but erosion, extensive faulting and subsequent alteration have obscured the structure (W. R. Griffitts, personal communication).

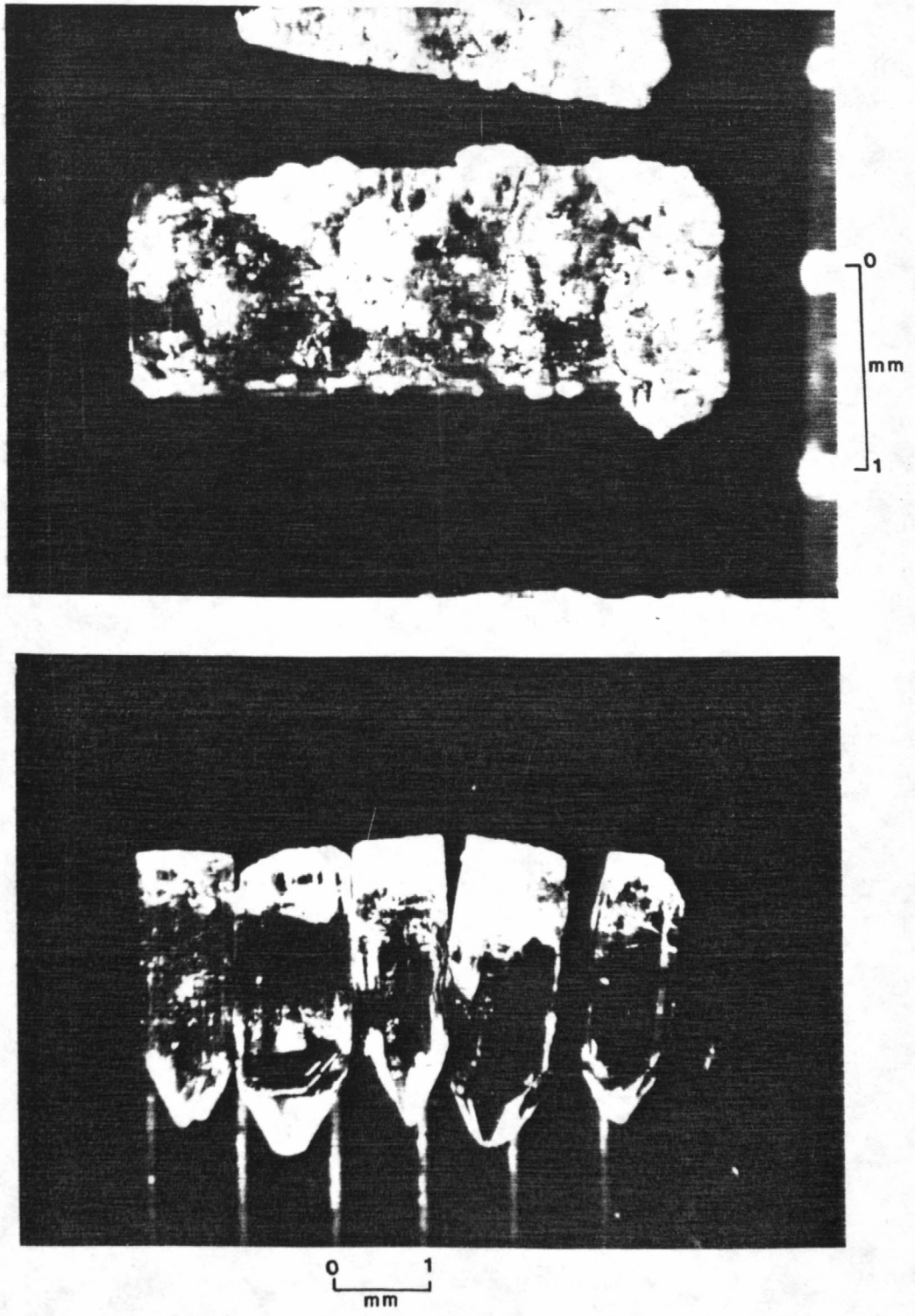

Figure 8. Microscopic views comparing topaz contained in groundmass and clear topaz contained in vugs. The topaz in groundmass (top) contains numerous black and white inclusions. Topaz contained in vugs (bottom) is inclusion free.

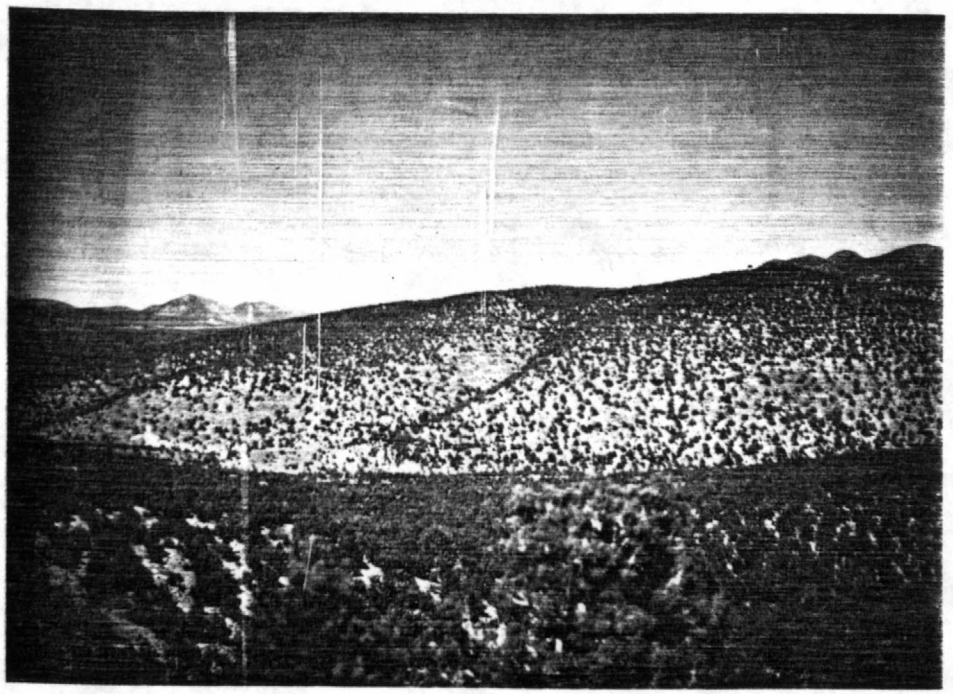

Figure 9. Photograph of the dome of Fourmile Wash. View looking east of the west side of the dome. The light weathering unit where the slope levels out are clastic rocks of unit Tt.

Generally the gray rhyolite is a peraluminous rock containing 75-76% SiO_2 and 12% Al_2O_3 (Table 4). Total alkalies do not exceed 10%. Magnesium is very low, generally less than 0.1 weight percent.

Rhyolite of Pine (Trp, Miocene)

Best (1979) previously included this unit in the rhyolite member of Broken Ridge, Formation of Blawn Wash. The unit occurs in greatest abundance near Pine triangulation station (NE 1/4 sec. 35, T31S, R16W), but is fairly extensive to the east with minor amounts to the north and south. The thickness averages 30 m. The unit consists of a red-brown strongly flow-layered and locally autobrecciated rhyolite. The autobreccia, usually at the base, contains angular clasts of rhyolite set in a felsitic matrix. Clasts range from a few centimeters to large blocks a few meters in diameter. Some clasts are still largely glass while others are more crystalline. The unit as a whole weathers to give honeycomb or mottled outcrops. Massive and resistant, it forms prominent ridges where it generally overlies the gray rhyolite (fig. 10).

Near Pine, the rhyolite caps the ridges, forming a faint circular structure that is particularly obvious on aerial photographs. This circular structure is defined by the east-west trending ridge of Pine, where the rhyolite is near vertical, and the south-trending ridges on either side of Pine. The underlying gray rhyolite, locally interfingered with silicic clastic rocks of unit Tt, forms a small pipe in the center of the circular area. This circular area may be a remnant of a small vent complex.

East of Pine, the rhyolite of Pine is still fairly abundant, but more patchy. It thins out rapidly to the north and south.

Phenocrysts average 3-5% in the rhyolite of Pine (Table 3) and are generally less than 1 mm in diameter. Sanidine, exhibiting nice Carlsbad twinning, comprises 2-3% of the rock with 1-2% subhedral embayed quartz. Plagioclase is present, but sparse. Groundmass is crystalline and flow-layered consisting of interlocking quartz and feldspar with up to 2% disseminated green-brown biotite. Flow-layers are alternating dark red-brown and lavender bands that are less than 1 mm across and are contorted and folded. Very little textural or mineralogical changes exist between layers, though secondary silica has replaced some flow-layers as is evidenced by small vugs and lithophysae filled with secondary quartz crystals. This unit is interpreted to have been a very viscous lava, erupted from local centers as is suggested by its scanty distribution, and the autobrecciated and strongly flow-layered nature of the rock.

Chemical analyses of the rhyolite of Pine show this to be a strongly peraluminous rock with a SiO_2 content between 72-74 wt percent (Table 4). Al_2O_3 content is between 12 and 16% and total alkalies in general do not exceed 10 wt percent. Fluorine, Rb, and Li are all enriched.

Alluvium and colluvium (Qac, Quaternary)

Unconsolidated, poorly sorted stream and slope wash deposits of silt, sand and gravel are included in this unit. Locally, it includes talus and colluvial debris from the gray rhyolite (Trs), the glassy margin (Trv),

Figure 10. Photograph showing the rhyolite of Pine (Trp) overlying the gray rhyolite (Trs). View looking east (eastern 1/2 sec. 36, T31S, R16W). The rhyolite of Pine is the dark-brown unit overlying the light-weathering gray rhyolite.

silicic clastic rocks (Tt), the Lund Tuff (Tl), and Paleozoic sedimentary rocks (P).

Structural features

The Broken Ridge area, as described previously, consists of silicic volcanic materials resulting from explosive eruptions, and silicic lava domes and flows from many local centers. The dome of Fourmile Wash, the fissure vent (NW 1/4 sec. 24, T31S, R16W), the area of Pine (NW sec. 35, T31S, R16W) and an area 1/2 km northeast of Mountain Spring Peak are all possible dome-vent complexes. Vent areas for the rhyolite of Pine must be very close to areas where it crops out, as it appears to have been a very viscous lava. This interpretation is supported by the presence of strongly flow-layered and contorted rhyolite of Pine adjacent to each body of vent breccia, suggesting perhaps that both the rhyolite of Pine and the breccia moved up through the same vent.

In addition to the primary structures just mentioned, post-rhyolite faulting is widespread in the Broken Ridge area. The northeast-trending Bible Spring fault zone is older than the 12 m.y. rhyolitic rocks, but there has been minor movement along the fault since emplacement of the young flow rocks.

Most of the faults in the Broken Ridge area are high angle normal faults trending north to northeast with the exception of a few minor northwest trending faults, which for the most part, cut the northerly trending faults. In the southern map area, the trend of faults is nearly east-west. The result of the faulting in the area of Broken Ridge is a series of horst and graben fault blocks (see cross-sections A-A', B-B' and C-C', Plate 1). These faults are contemporaneous with or post-date the emplacement of the gray rhyolite and clastic rocks of unit Tt. Only in the south-central map area is the rhyolite of Pine cut by faults, most of which are east-west or northwest trending. Otherwise, the faulting seems to be either contemporaneous with or prior to the emplacement of the rhyolite of Pine.

Slickensides can be seen on rock surfaces in the southwest and southern parts of the map area which are sub-horizontal rather than down-dip. Myron G. Best pointed out (personal communication, 1984) that this anomalous presence of gently plunging slickensides on faults with vertical displacement is widespread in the southern Wah Wah Mountains. For instance, along the Bible Spring fault zone (NW 1/4 sec. 8, T32S, R16W and NW 1.4 sec. 4, T32S, R16W) slickensides on altered volcanic rocks trend southwest with a plunge of approximately 10^{0} (Best and Davis, 1981) indicating very slight dipslip movement along the fault. Likewise, in the southern part of the map area, slickensides from a north-trending fault (E 1/2 sec. 12, T32S, R16W) trend nearly due north and plunge only 20^{0}. However, there is no evidence for large scale lateral displacement from offset of map units. In fact, the vertical displacements must be great, as Miocene rocks are in fault contact with Oligocene and Paleozoic rocks as in the eastern map area. Possibly the latest movement along the faults was strike-slip to cause the sub-horizontal slickensides (M. G. Best, personal communication, 1984).

Most faults occur along the margins of the Steamboat Mountain Formation, and are nearly nonexistent in the northern map area at Broken Ridge, where the rhyolite is very thick. Faults of the northeast trending Bible Spring fault

zone die out about 3 km west of Broken Ridge, but can be seen northeast of the map area where they extend from this point for several kilometers (figure 2). The north-trending fault in sec. 24 is nearly perpendicular to the Bible Spring fault zone. This north-trending fault probably at one time was a fissure vent along which a flow of gray rhyolite was emplaced (page 23). An intrusion probably was emplaced just west of the northerly trending normal fault; emplacement of such an intrusion may have been responsible for the formation of the fault along an already weakened zone. The vent breccia (Tbt), the abundance of the rhyolite of Pine, the tin vein mineralization and the green glass (Trg) dike that parallels the fault are all evidence that an intrusion lies directly beneath (cross-section B-B', C-C', Plate 1).

Rock alteration

Basically, there are four types of alteration in the Broken Ridge area: silicification, argillic alteration, quartz-fluorite alteration, and quartz-alunite alteration. Figure 11 is a simplified geologic map showing the areas of alteration. The most intensely altered rocks are along faults; emphasis was placed on these areas in delineating alteration types. Areas between faults may be altered to some extent, but they are not shown on the map.

Silicification

Rhyolitic rocks along faults in the Broken Ridge area are commonly replaced by quartz, chalcedony, and opalline silica. Rhyolitic rocks along the Bible Spring fault zone, about 3 km west of Broken Ridge, are silicified to jasperoid, and mark the limit of the fault in the Steamboat Mountain Formation (location A1 on fig. 11). About 1 km to the north, volcanic rocks overlie Paleozoic limestones and dolomites. A small prospect pit exists in the Paleozoic rocks that have been silicified to jasperoid. Overlying the jasperoid zone are volcanic rocks that are intensely silicified and argillized. Silicification resulted in replacement of the volcanic rocks by chalcedony, opalline silica and local iron and manganese oxide coatings and veins. The zone of silicification grades upward within the volcanics to extensive argillic alteration.

Quartz veining in Oligocene volcanic rocks in the southwest part of the map area (location A2) is widespread. Direct evidence of the faulting in this area is the presence of subhorizontal slickensides on surfaces of the silicified volcanic rocks.

Argillic alteration

The most widespread alteration in the area, argillization resulted in formation of quartz and kaolinite with local introduction of oxidized iron, montmorillonite and minor sericite. Rocks of the Steamboat Mountain Formation and clastic rocks are thoroughly bleached except where oxidized iron is present making the rocks bright red-orange. In most places, the argillized rock is spatially related to silicified fault zones. Intensely argillized rocks along the Bible Spring fault zone (location A1) were explored for uranium by means of pits and adits. The pits are in a red oxidized zone that grades westward to extensive white bleached rock. Going northeast along the fault, argillized rock gives way to silicified rhyolite.

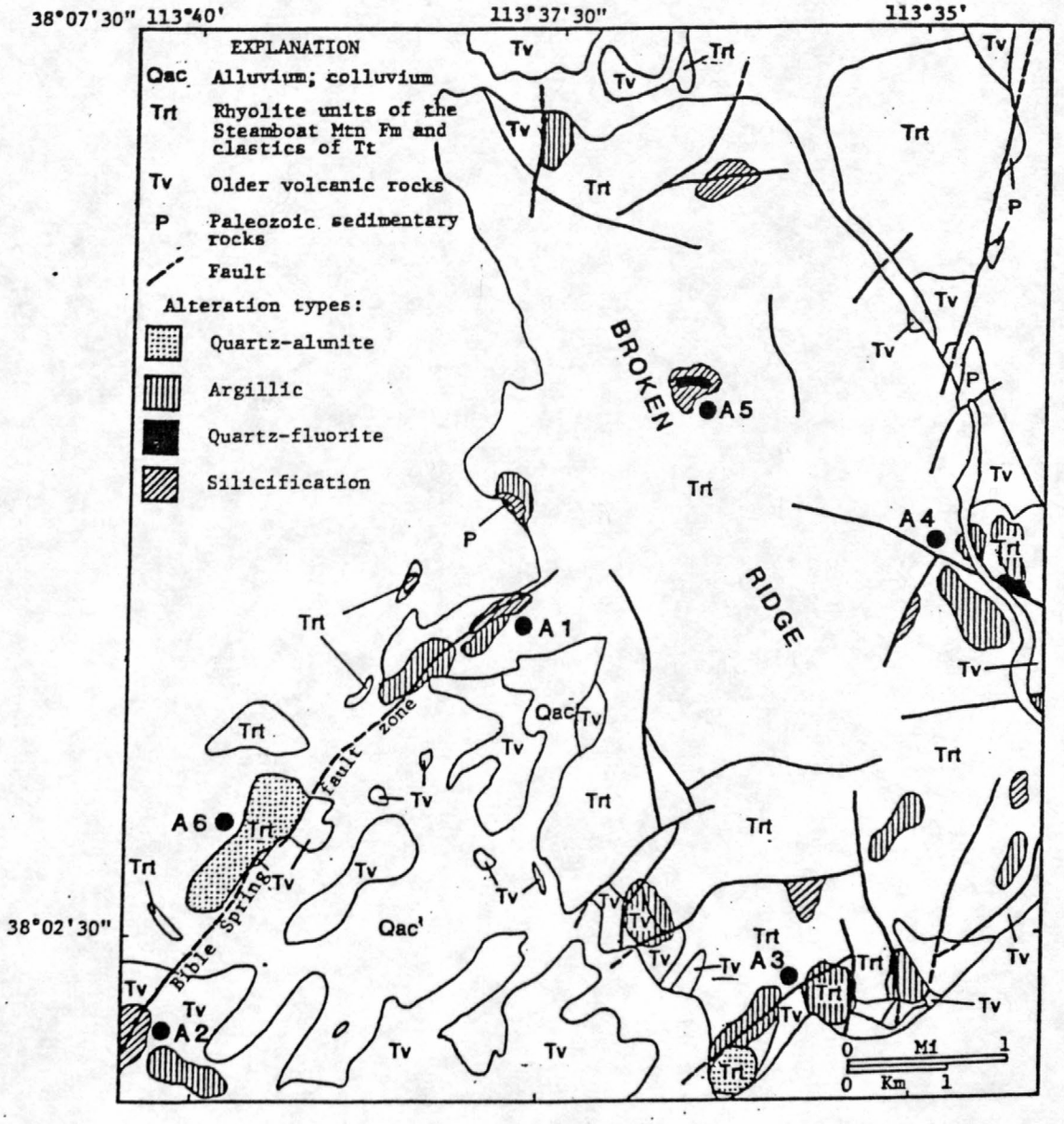

Figure 11. Simplified geologic map showing areas of alteration. Labeled dots are areas of alteration referred to in the text.

Other areas of argillized rock occur to the south and east of Broken Ridge along small faults. Near Mountain Spring (location A3), clastic rocks and gray rhyolite are extensively altered to clays. At Mountain Spring Peak, clastic rocks are argillized, while the overlying rhyolite is silicified and alunitized. A thick pile of gray rhyolite along both sides of a northwest trending fault in Fourmile Wash east of Broken Ridge (location A4), is argillized and contains quartz, kaolinite and oxidized iron.

Quartz-fluorite alteration

This type of alteration is similar to the silicification already described except that fluorine was introduced and fluorite crystals can be found in the silicified rhyolite and on joint surfaces. In the northern Broken Ridge area (location A5 on fig. 11), gray rhyolite is cut by the vent breccia (Tbt) which in turn is overlain by the rhyolite of Pine (SE sec. 23, T31S, R16W, Plate 1). Several small prospect pits expose a highly silicified and fluoritized zone within the flow-layered gray rhyolite adjacent to the vent breccia. Small dark purple fluorite crystals line cavities and vugs in the silicified rhyolite. This silicified and fluoritized rhyolite is also host to tin veining; small cassiterite crystals occur in a vein with specular hematite and quartz (more detail in later sections).

About 3 km east of Broken Ridge on the east side of Fourmile Wash (location A4), a northwest striking normal fault brought Oligocene volcanic rocks in contact with rhyolite (Trt on fig. 11). Specifically, the rhyolite right at the contact is green glass (Trg) that is locally altered to clays and overlain by a thin wedge of clastic rocks of unit Tt (Plate 1). Joint surfaces near the fault in the altered green glass are coated with fine-grained quartz and fluorite.

A partially hydrated and devitrified sample of the green glass in an unfaulted area yielded 900 ppm F (sample 83K265, Table 4) and low Li, U, Na, Al, and Mg compared with other rhyolitic rocks in the area. It is conceivable that these elements are released from the glass during hydration and devitrification, and that at least part of the fluorine responsible for the formation of fluorite by hydrothermal fluids could be released from the glass and picked up by throughgoing fluids.

Quartz-alunite alteration

On the far southwestern part of the Bible Spring fault zone, a thick pile of clastic rocks (Trt on fig. 11) are pervasively altered to quartz, alunite and locally kaolinite with minor montmorillonite (location A6). The rocks are generally weakly welded ash-flow tuffs with as much as 35% of the rock consisting of somewhat flattened and elongated cavities that are interpreted to be relict pumice fragments. Clear euhedral tabular crystals of alunite up to 2 mm in diameter occur with feldspar in the cavities (fig. 12). Quartz, iron oxides, kaolinite, and minor montmorillonite accompany the alunite. In groundmass, fine-grained alunite, quartz and iron oxides are locally abundant.

On the basis of textural relationships, it is reasonable to assume that the tuff first underwent replacement by quartz and feldspar, and then later, introduction of sulfate-rich solutions formed alunite which partially replaced the feldspar.

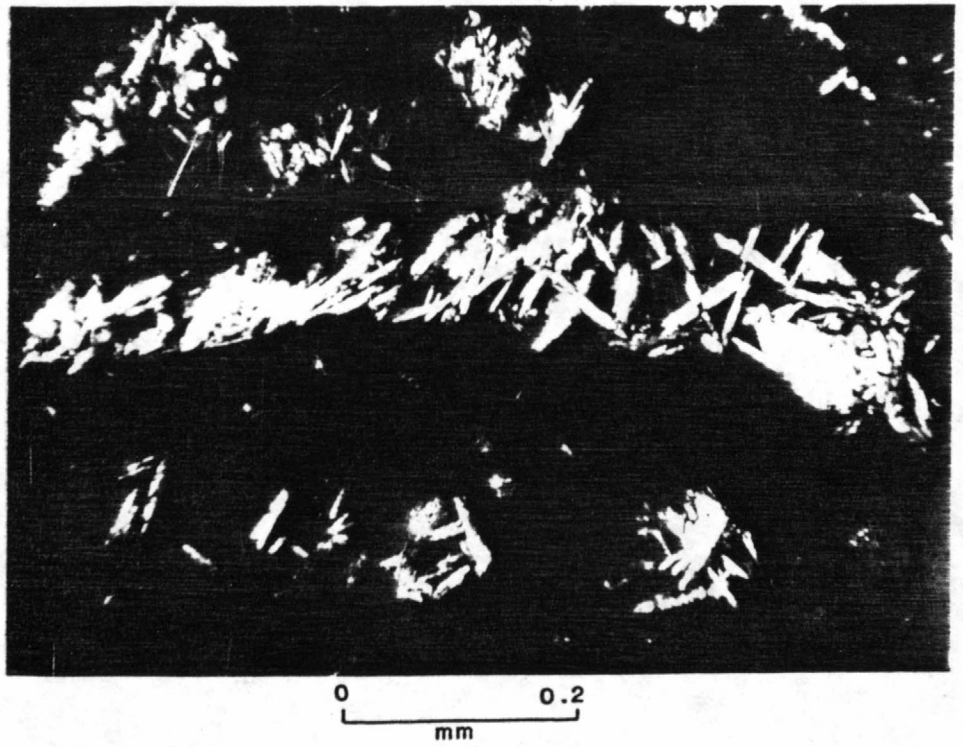

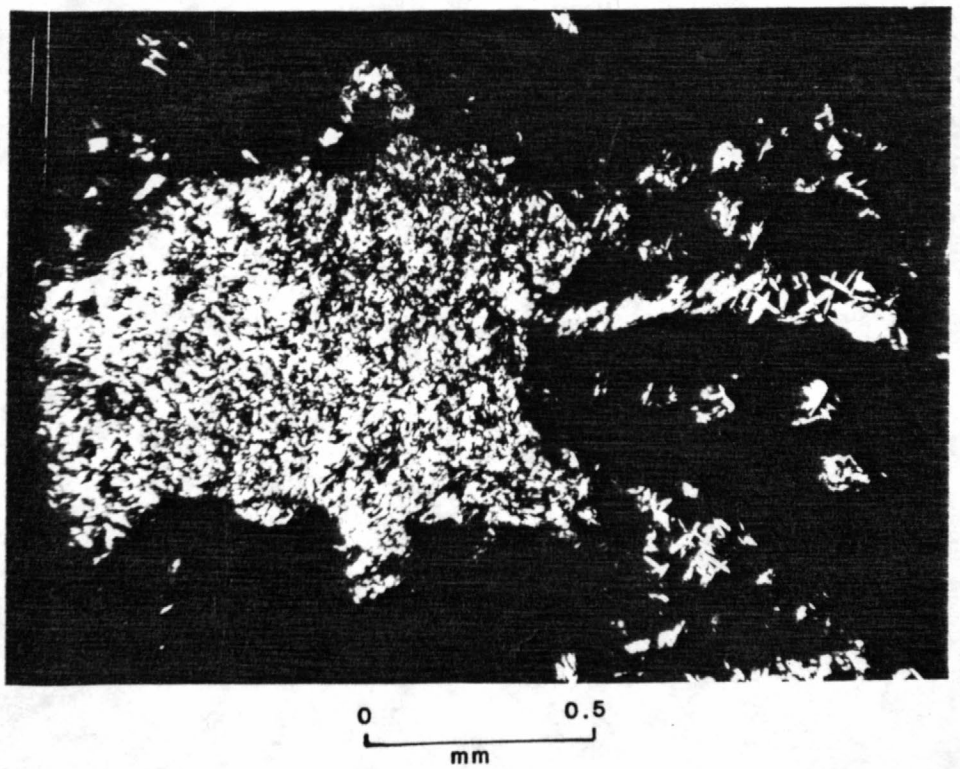

Figure 12. Photomicrographs of alunite in silicic clastic rocks. View with cross-polars of alunite and feldspar occurring in small veins and vugs.

At Mountain Spring Peak (location A3), alunitized rhyolite overlying clastic rocks grades northward to very extensive areas of argillization.

GEOCHEMISTRY

Petrology of the Steamboat Mountain Formation

Table 4 (pages 19-21) lists whole rock major and trace element chemistry for 18 selected fresh and altered rhyolitic rocks of the Steamboat Mountain Formation and 2 samples of the Lund Tuff from the Broken Ridge area. Also included is a sample from Best and others (1983) of a mugearite flow (orthoclase-bearing oligoclase basalt) from the east side of the Wah Wah Mountains dated at 13.3 m.y. which is within the Steamboat Mountain period of igneous activity (Best and others, 1983). For comparative purposes, analyses of 4 fresh rhyolitic rocks and 2 trachyandesite flow rocks of the Blawn Formation (23-18 m.y.) from Best and others (1983) are included in Table 4 (samples 3-8). In the following discussion, only fresh rocks will be considered.

As described briefly before, the rhyolitic rocks of the Steamboat Mountain Formation have greater than 74% SiO_2, except for the rhyolite of Pine which has between 72-74% SiO_2. Total alkali content is high, averaging 8-10%. Average CaO content is low (0.6%), but the concentration shows large variation, ranging from 0.2 to 1.7 wt. percent. In addition, the rocks have very low MgO contents (mostly <0.1%), and low TiO_2 (<0.2%) and P_2O_5 (<0.15%) contents. Of the trace elements, Be, Rb, Li, Nb, Mo, Y, and U are high and Ba is low. Beryllium contents average 10 ppm, with 500 ppm Rb, 150 ppm Li, 50-100 ppm Nb, 10-20 ppm Mo, and 50-100 ppm yttrium. Uranium is variable in amount because it is commonly lost during hydration and devitrification (Zielinski and others, 1977); partially glassy samples that have undergone these processes have low U contents (e.g. sample 83K265, Table 4 has 0.15 ppm U). Fluorine content in the rocks is high as indicated by the presence of topaz, but analyses of whole rocks yield average F values of 500-1000 ppm; such values are low compared with other high-F rhyolites. For instance, Spor Mountain rhyolitic vitrophyres contain up to 1 wt. percent F (Christiansen and others, 1984). The scarcity of fresh vitrophyre samples from the Broken Ridge area makes it difficult to determine F contents that would be representative of the magma itself. Fluorine is lost during high temperature devitrification as well as during eruption of the rhyolite. Therefore, only fresh glassy samples are representative of the true F content.

Whole rock major element chemistry of the Blawn Formation, with SiO_2 contents between 74-76%, high alkalies and low MgO, TiO_2, and P_2O_5, is very similar to that of the Steamboat Mountain Formation. Calcium is low, but does not show the large range of values as the Ca contents in the Steamboat Mountain Formation.

The characteristic high Si and alkalies, low Mg, Ca, Ti and P, and enrichment of lithophile elements are typical of other topaz-bearing rhyolites in the western United States and northern Mexico (e.g. Burt and others, 1982; Huspeni and others, 1984; Christiansen and others, 1984; and Eggleston and Norman, 1984). Many of these high-F rhyolites are host to beryllium and tin mineralization, such as the beryllium deposit at Spor Mountain, Utah (Staatz and Carr, 1964; Christiansen and others, 1984), the tin mineralization in the

Black Range, New Mexico (Eggleston and Norman, 1984) and the tin hosted by rhyolite in the Sierra Madre Occidental, Mexico (Huspeni and others, 1984).

Alkali, iron, and magnesium contents of the Steamboat Mountain Formation, the Blawn Formation and the Lund Tuff are plotted on ternary diagrams (Figure 13). SiO_2 variation diagrams of CaO, Na_2O, and K_2O contents for the volcanic rocks are shown in Figure 14. Rhyolitic rocks of the Blawn Formation are represented by open triangles (analyses from Best and others, 1983); dots represent rhyolitic rocks of the Steamboat Mountain Formation and the Lund Tuff. Mugearite and trachyandesite samples, represented by open circles, are marked as M and T, respectively. For comparison, analyses of rhyolite from the Sierra Madre Occidental, Mexico (Huspeni and others, 1984; Table 3) and Spor Mountain, Utah (Christiansen and others, 1984; Table 1) are also plotted.

The AFM ($Na_2O + K_2O$-Fe_2O_3-MgO) ternary diagram (Fig. 13a) shows the Steamboat Mountain Formation and Blawn Formation to be strongly alkaline, magnesium poor, and very similar in terms of alkalies ($K_2O + Na_2O$), Mg and Fe to rhyolites of the Spor Mountain area and the Sierra Madre Occidental. The mugearite of the Steamboat Mountain Formation is more Fe rich and less alkaline than trachyandesite of the Blawn Formation.

The Na_2O-K_2O-CaO ternary diagram (Fig. 13b) and the SiO_2-CaO variation diagram (Fig. 14a) show the variation and wide range in Ca content for rhyolitic rocks of the Steamboat Mountain Formation compared with the consistently low Ca content of the Blawn Formation, even though average Ca for both suites are similar. Calcium is variable in rhyolite from Sierra Madre Occidental and Spor Mountain, but there is an increase in K_2O with CaO in the former rocks and an increase in Na with increase in Ca in the latter rocks, whereas there is no apparent increase of alkalies with increasing Ca in rhyolite of the Steamboat Mountain Formation. The linear trend toward higher Ca content from the rhyolite of the Steamboat Mountain Formation to the Lund Tuff to the mafic rocks (Fig. 13b) suggests the high Ca in some samples is not an effect of secondary alteration, but is inherent in the primary composition of the rock. In general, Ca content of the Steamboat Mountain Formation and the Blawn Formation increases with a decrease in Si (Fig. 14a).

Na_2O contents of the Steamboat Mountain rhyolite average 3.4 wt. percent and are for the most part lower than the Blawn rhyolites (average 3.9%) and are very similar to those of Sierra Madre Occidental (Fig. 14b). Spor Mountain rhyolites are extremely high in Na and somewhat lower in Si compared with the the other rhyolites. The mugearite flow is higher in Na than the trachyandesite flow rocks. Generally, Na decreases with decreasing Si until intermediate-Si compositions, around 65%, are reached; thereafter with a further decrease in Si, Na increases (Fig. 14b).

Average K_2O contents in the Steamboat Mountain and Blawn rhyolitic rocks are nearly identical, at about 4.8 wt. percent, and the range of K_2O values fall well within the range of K_2O for Sierra Madre Occidental and Spor Mountain rocks (Figs. 13b and 14c). K_2O increases slightly with an increase in Si for the Steamboat Mountain Formation, but it decreases with increasing Si for the Blawn Formation (Fig. 14c), although the scarcity of data for the Blawn Formation makes it difficult to make firm conclusions. The mugearite of the Steamboat Mountain Formation is less potassic than the trachyandesite. Overall, there is a definite trend of increasing K_2O with increasing SiO_2.

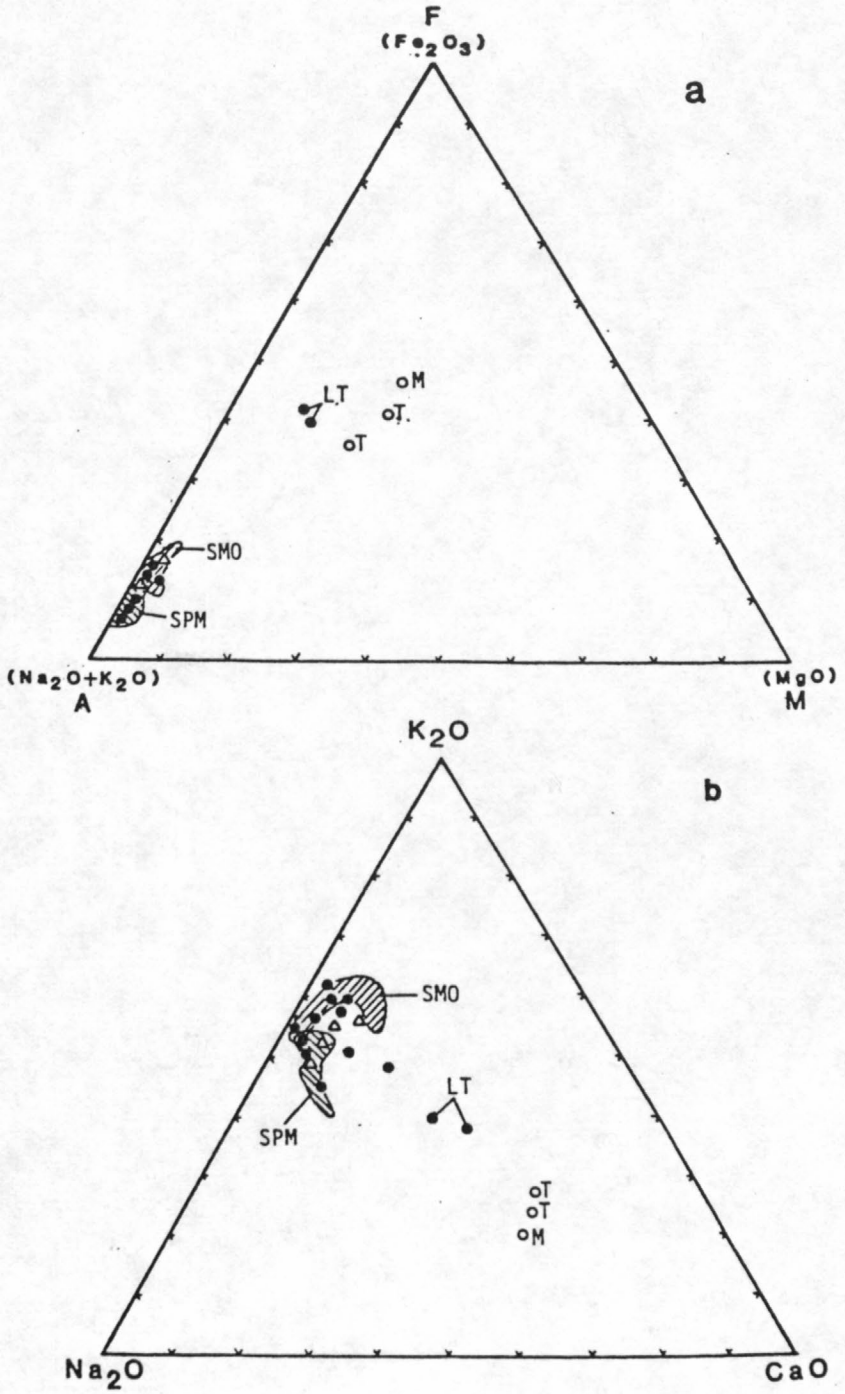

Figure 13.--a) AFM ternary diagram and b) Na_2O-K_2O-CaO ternary diagram for volcanic rocks in the southern Wah Wah Mountains. Open traingles represent analyses of silicic rocks of the Blawn Formation from Best and others (1983); open circles represent analyses of mafic rocks from Best and others (1983); dots represent analyses from this study; M = mugearite flow; T = trachyandesite flow; LT = Lund Tuff; SMO = Sierra Madre Occidental, Mexico (Huspeni and others, 1984; Table 3); SPM = Spor Mountain, Utah (Christiansen and others, 1984; Table 1).

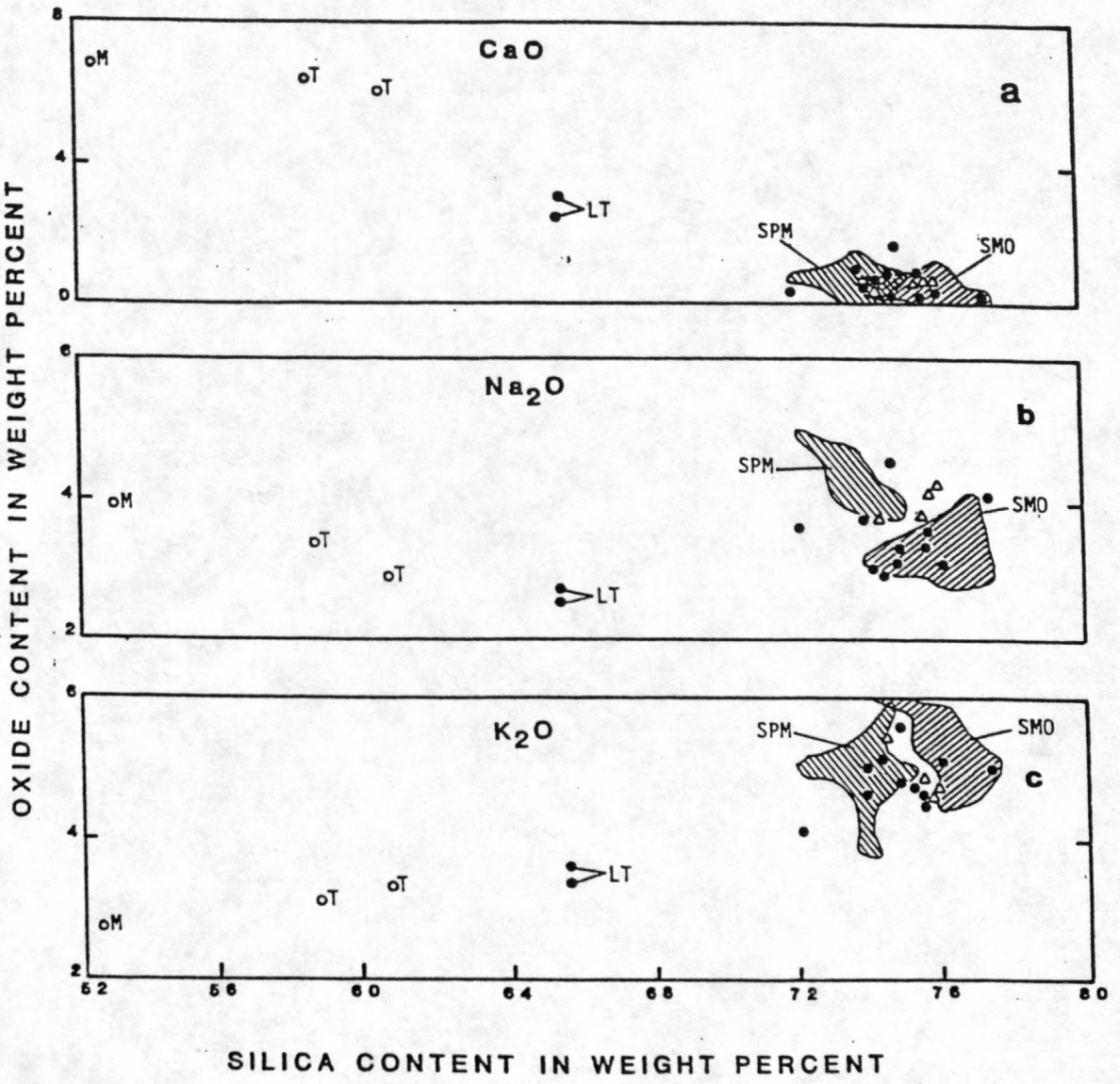

Figure 14.--SiO_2 variation diagrams of a) CaO, b) Na_2O, and c) K_2O for volcanic rocks in the southern Wah Wah Mountains. Open triangles represent analysis of silicic rocks of the Blawn Formation from Best and others (1983); circles represent analyses of mafic rocks from Best and others (1983); dots represent analyses from this study; M = mugearite flow; T = trachyandesite flow; LT = Lund Tuff; SMO = Sierra Madre Occidental, Mexico (Huspeni and others, 1984; Table 3); SPM = Spor Mountain, Utah (Christiansen and others, 1984; Table 1).

Topaz rhyolites from the Thomas Range, Utah and Spor Mountain, Utah (Christiansen and others, 1984), as well as rhyolites from the Sierra Madre Occidental, Mexico (Huspeni and others, 1984) and the Black Range, New Mexico (Eggleston and Norman, 1984) have large negative Eu anomalies and nearly flat chondrite-normalized rare earth element patterns with a slight enrichment of LREE (light rare earth elements) relative to the heavy elements. The REE characteristics just described have been recognized in many highly evolved rhyolitic magmas and have been explained by extreme differentiation of their magmas at relatively shallow crustal depths (Hanson, 1978, from Huspeni and others, 1984). Although rare earth data are not available for this study, the similarity of major element characteristics to other topaz rhyolites suggests that the Steamboat Mountain Formation and Blawn Formation also formed as highly differentiated magmas.

It has been suggested that U.S. topaz rhyolites are equivalent to Soviet ongonites (Burt and others, 1982). Most of the ongonites are topaz-bearing dikes and therefore would be sub-volcanic equivalents of the topaz rhyolites. Glassy portions of ongonites contain up to 3.2 wt. percent F. The lower F content of topaz rhyolites, particularly the Steamboat Mountain Formation, can be attributed to loss during initial eruption and during high temperature devitrification and crystallization.

The geochemistry of high-F rhyolites is similar to that of anorogenic or A-type granites (Loiselle and Wones, 1979) which are distinct from I or S-type granites as defined by Chappel and White (1974). Because of the similarity in geochemical characteristics, the petrogenesis of topaz rhyolites can be likened to that of A-type granites. The petrogenesis occurs late in an orogenic cycle (hence the name "anorogenic"), prior to rifting and after subduction ceases. They are believed to have been derived from partial melting of water-depleted lower crustal rocks from which an earlier partial melt was produced. White and others (1981) propose a similar origin for Climax-type porphyry Mo deposits. Both the geochemistry previously described for the Steamboat Mountain Formation and the extensional tectonic setting in the Broken Ridge area support the proposed link between topaz rhyolites and A-type granites.

Rock Geochemistry

In the area of Broken Ridge and Fourmile Wash and south-southwestward along the Bible Spring fault zone, 204 rock samples were collected for geochemical analyses. Locations of all samples are shown in Figure 15 (for detailed geology, see Plate 1). All analytical results for the rock samples are listed in Appendix A.

Be, F, Sn, Nb, U, and Th are very closely associated with each other and their distribution reflects the rhyolitic rocks of the Steamboat Mountain Formation. The highest values occur along the Bible Spring fault zone and other areas of alteration and faulting within the rhyolitic rocks. High values of Mo, Cu and Pb accompany the lithophile elements in some areas of alteration, but in general are more widely dispersed and not restricted to rhyolitic rocks. For the most part, Ba is low in fresh rhyolitic rock, but is very abundant in alunitized clastic rocks and Oligocene volcanic rocks.

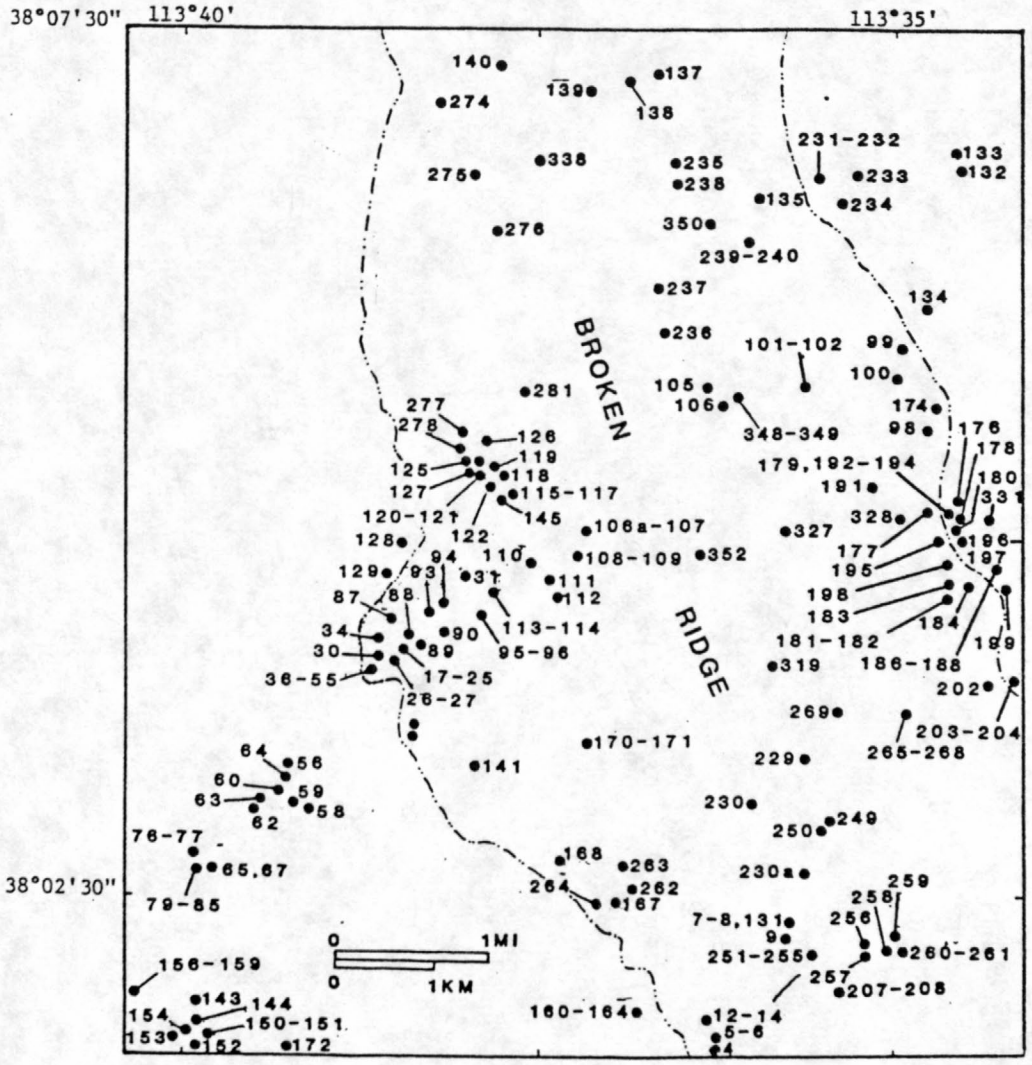

Figure 15.--Location map of rock samples from the Broken Ridge area. The 83K or 84K prefix was dropped for clarity on map. All samples are listed in Appendix A. For geology, see Plate 1. MSP = Mountain Spring Peak.

Correlation diagrams of Be and Nb, Li and Rb, F and Be, and Cu and Mo are shown in Figure 16. Circles represent rhyolitic rocks of the Steamboat Mountain Formation; open circles are fresh samples and closed circles represent altered samples. Triangles, representing Oligocene volcanic rocks, likewise are open for fresh samples and closed for altered samples. As can be seen from the diagrams, Rb, Li, Be, Nb, and F are higher in rhyolitic rocks than in Oligocene volcanic rocks and there is a high correlation between Be and Nb, and Li and Rb in fresh rock. Be and Nb contents in altered rhyolitic rocks vary greatly from fresh rhyolite. Be contents are 50-100 ppm; nearly 5 times greater than average Be contents in fresh rock. Nb increases only slightly. In contrast to the rhyolitic suite, very little change in Be or Nb occurs between fresh and altered Oligocene volcanic rocks.

Li content increases slightly with an increase in Rb in rhyolitic rocks, and both elements are higher in concentration than in Oligocene volcanic rocks. In Oligocene volcanic rocks, Rb contents increase during alteration whereas Li remains fairly constant with the exception of one sample which contains over twice the average content of fresh rock. In general, there is a slight loss of Li and very little loss of Rb during alteration of rhyolitic rocks.

Fluorine contents are highly variable; there is no systematic change in F content with Be content in fresh rhyolite. However, altered samples show a strong correlation between Be and F, indicating Be and F are transported together in solution and precipitated at approximately the same time. Be is commonly carried in solution as BeF_4^- (Griffitts, 1982); if F reacts with Ca to form fluorite or substitutes for OH to form topaz, thereby removing F from solution, Be would consequently precipitate out of solution as well.

The Cu and Mo correlation diagram emphasizes the higher Cu content of intermediate-Si Oligocene volcanic rocks compared with the high-Si rhyolite of the Steamboat Mountain Formation. Cu averages <5 ppm in rhyolitic rocks whereas in Oligocene rocks, Cu averages 20 ppm. Mo contents are <5 to 20 ppm in rhyolite and <5 ppm in the older volcanic rocks. From the diagram, it appears that Cu is very mobile during alteration of Oligocene volcanic rocks. Altered rocks contain anywhere from 10 to 100 ppm Cu. However, Mo remains at <5 ppm for the most part. In altered rhyolitic rocks, both Cu and Mo are highly variable. Mo ranges from 5 ppm to 200 ppm with accompanying 5-100 ppm Cu.

The geochemical data indicate that Sn and Ba, in addition to the elements just described (Be, Nb, F, Li, Rb, and Mo), increase during alteration of the rhyolitic rocks of the Steamboat Mountain Formation. Moreover, the type of alteration strongly influences the behavior of each element. Figures 17 and 18 are histograms of Sn, Mo, Be, Nb, Ba and Cu abundances in fresh rhyolitic rock versus each of three alteration types: argillic; silicic; and alunitic. Samples used for plotting abundances include 18 fresh rhyolite, 25 argillically altered, 6 silicified, and 4 alunitically altered rocks. Argillic alteration results in increases in Sn (up to 30 times the average 10 ppm), Mo (20 times the average of 10 ppm) and Nb (about twice the average of 30-70 ppm).

Although one sample contains 50 ppm Be, Be contents actually decrease in most argillically altered samples; the largest percentage of them containing

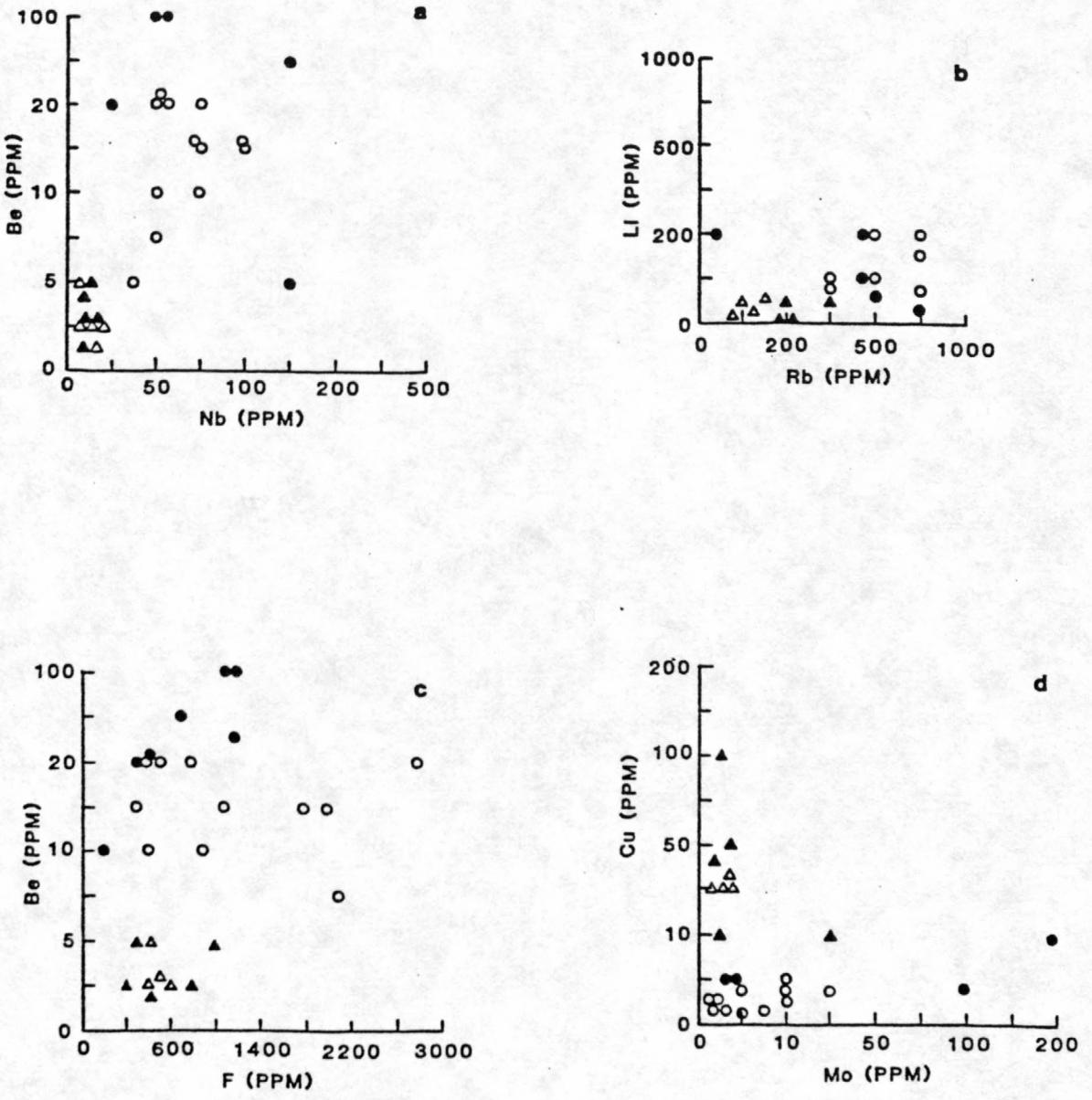

Figure 16.--Correlation diagrams of selected elements in volcanic rocks from the Broken Ridge area. (a) Be and Nb; (b) Li and Rb; (c) F and Be; (d) Cu and Mo. Circles = rhyolite of the Steamboat Mountain Formation; triangles = Oligocene volcanic rocks; open symbols = fresh rock; closed symbols = altered rock.

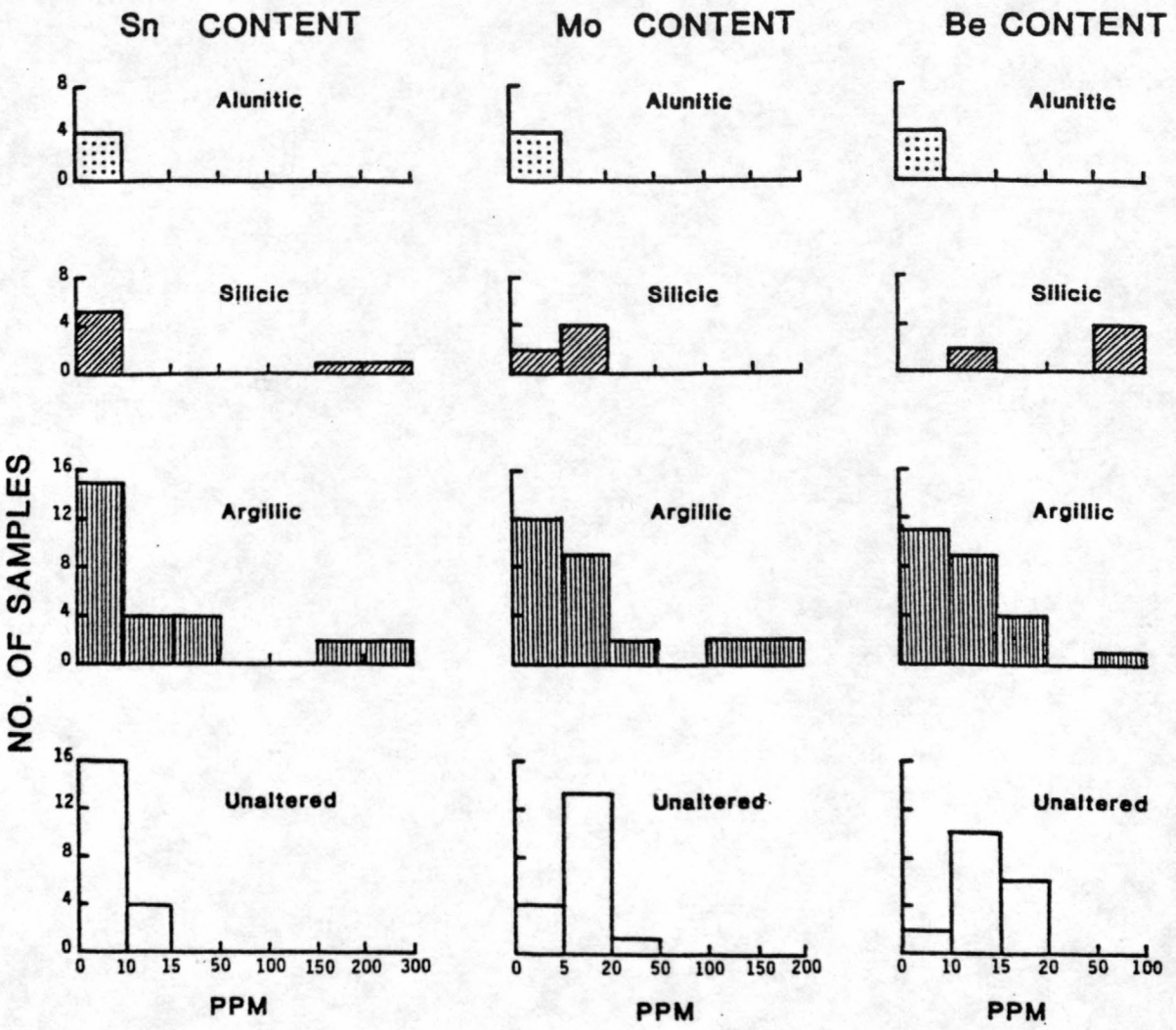

Figure 17.--Histograms of Sn, Mo, and Be abundances in fresh versus altered rhyolite.

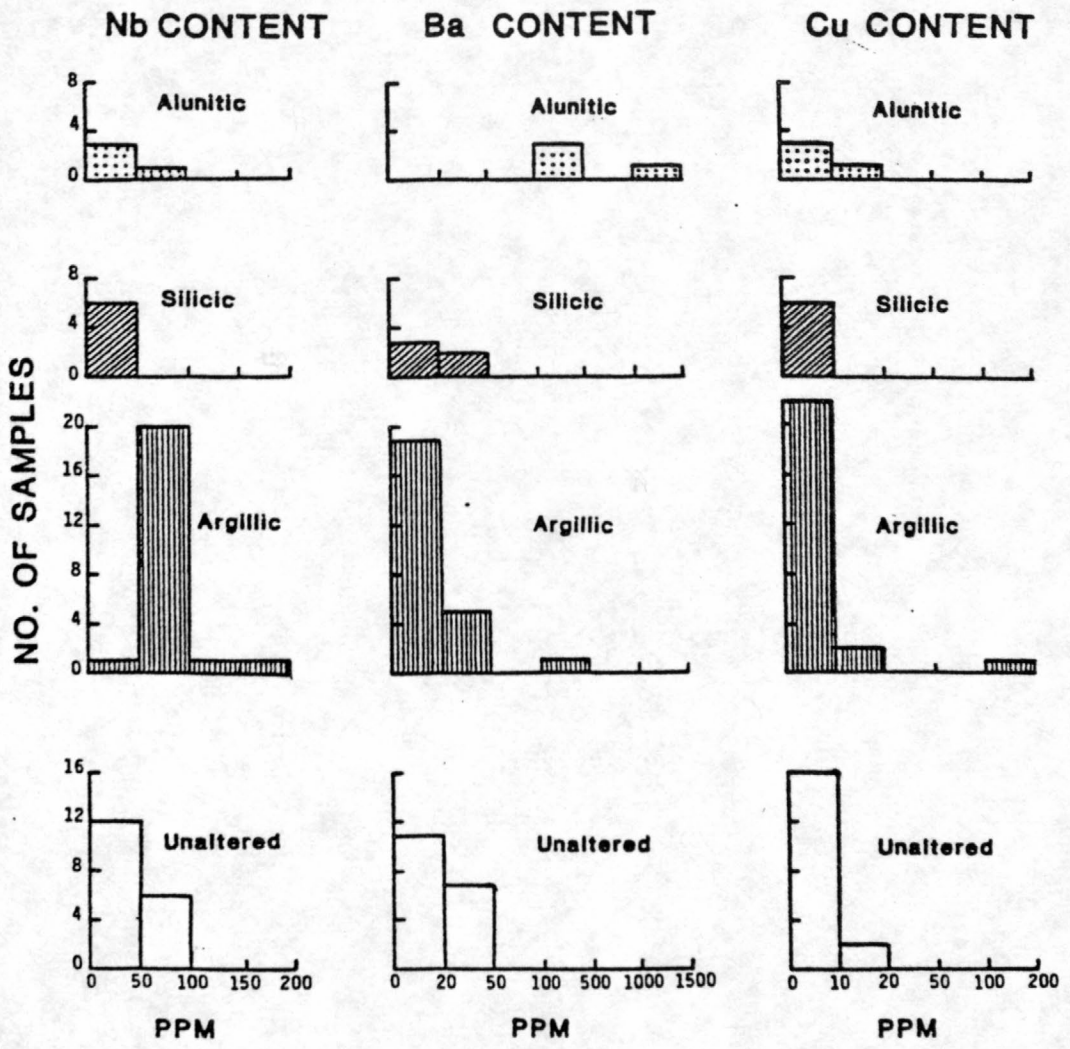

Figure 18.--Histograms of Nb, Ba, and Cu abundances in fresh versus altered rhyolite.

<10 ppm. Likewise, Ba remains low (<20 ppm) in most argillized rock. Silicification, however, results in increases in Be (10 times the average of 10 ppm) and Sn (300 ppm) with virtually no increase in Mo, Nb, or Ba. Alunitcally altered rocks are barren of all metals except Ba which was increased twentyfold over fresh rock contents, and Cu which increased slightly.

Single element plots of Be, F, Sn, Nb, U, Th, Mo, Cu, Pb and Ba are shown in Figures 19 through 23. For each element, four intervals were chosen for plotting. The lowermost interval for each element represents approximately 75% of all samples. The two uppermost intervals are above average or background. At sites with multiple samples, a single symbol is shown if all samples contained the same amount of a particular element. If multiple samples at a given site have different values, each value is shown in brackets.

The distribution of these elements in relation to the zones of alteration associated with faults can be shown by the geochemical maps. Three general areas are defined by the geochemistry: the Bible Spring fault zone; the southern Broken Ridge area; and the Fourmile Wash area.

Bible Spring fault zone

Within the rhyolitic units of the Steamboat Mountain Formation, high Be (50-100 ppm), F (0.4-1.7 wt. %), Sn (30-300 ppm), Nb (100-200 ppm), U (4-10 ppm), and Th (100-200 ppm) occur together in a northeast-trending zone from the southwest part of the map area to the east side of the dome of Fourmile Wash which outlines the Bible Spring fault zone. The most striking geochemical feature is the similarity between Be and F and the extent to which they mark the fault zone (fig. 19). The close association of Be and F is not surprising, because Be is commonly transported by fluorine-rich solutions as a fluoride complex. Furthermore, high fluoride in a melt can cause beryllium to become concentrated in residual solutions, so increases in fluoride in the magma may be accompanied by increases in beryllium (Griffitts, 1982). Beryllium averages 30 ppm and F averages 5000 ppm in this northeast-trending zone whereas north of Broken Ridge, fresh rhyolite contains mostly >10 ppm Be and >1450 ppm F. West of Broken Ridge, the rhyolitic rocks are extensively argillized and silicified (page 32) and contain 50-100 ppm Be and 400-11000 ppm F. East of Broken Ridge, where tin mineralization occurs and evidence suggests an intrusive at depth (page 32), silicified and fluoritized rhyolite contains up to 100 ppm Be and 2100 ppm F, grading northeastward to fresh rhyolite averaging 15 ppm and 1500 ppm F; generally higher than fresh rhyolite outside the Bible Spring fault zone.

Although not as continuous as Be and F, high Sn and Nb also mark the fault zone (fig. 20). Fresh rhyolite north of Broken Ridge contains mostly less than 10 ppm Sn and less than 100 ppm Nb, whereas southwest of Broken Ridge, Sn and Nb are both high (150-200 ppm Nb and 30-300 ppm Sn). East of Broken Ridge, where tin mineralization occurs, silicified rhyolite contains 300 ppm which reduces to 10-20 ppm northeastward in slightly argillized and fresh rhyolite.

Uranium data are not available for all samples, and the detection limit for Th is poor and therefore Th was not detected in most samples.

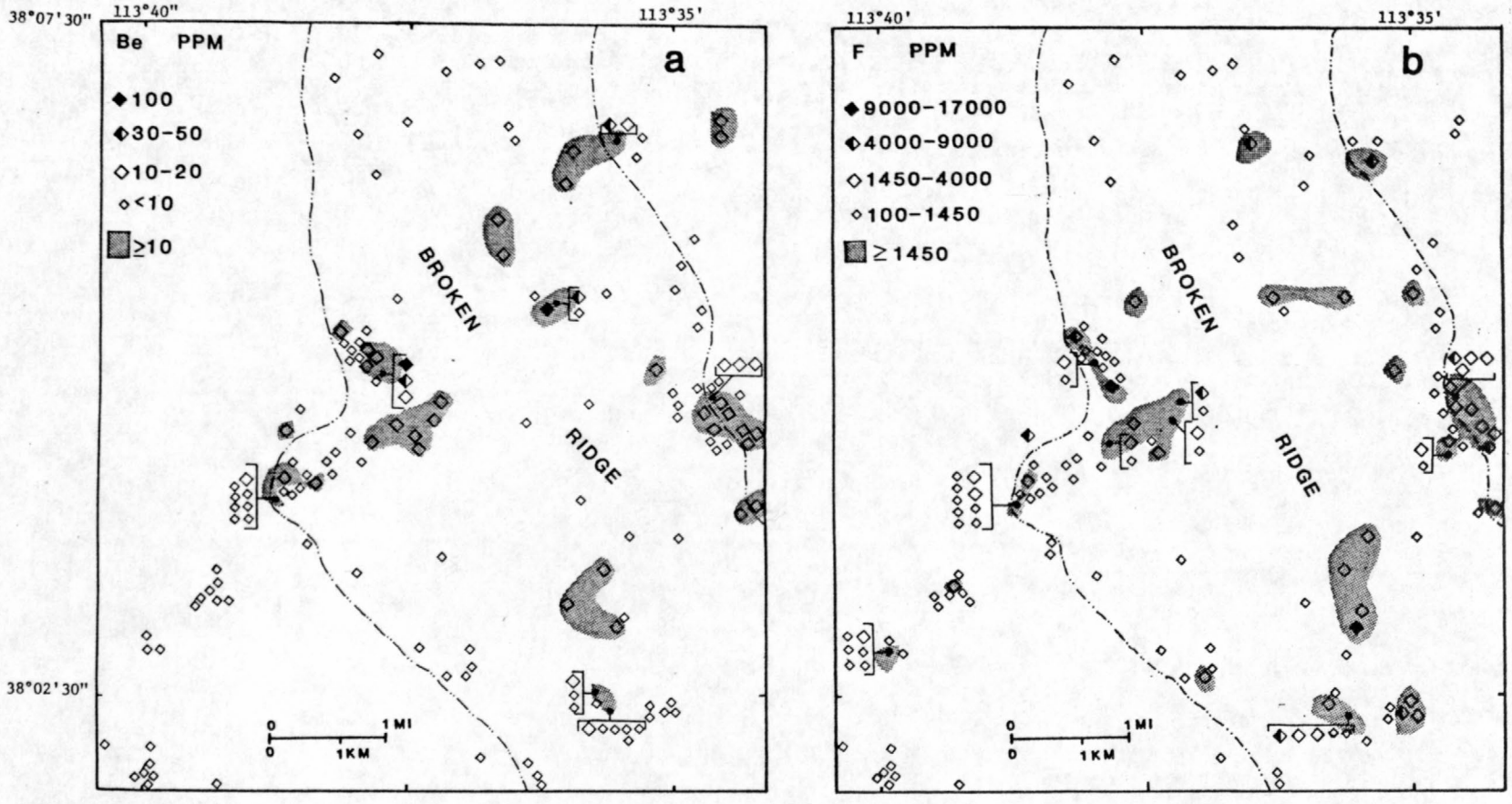

Figure 19.--Distribution of Be and F in rock samples. (a) Be content; (b) F content.

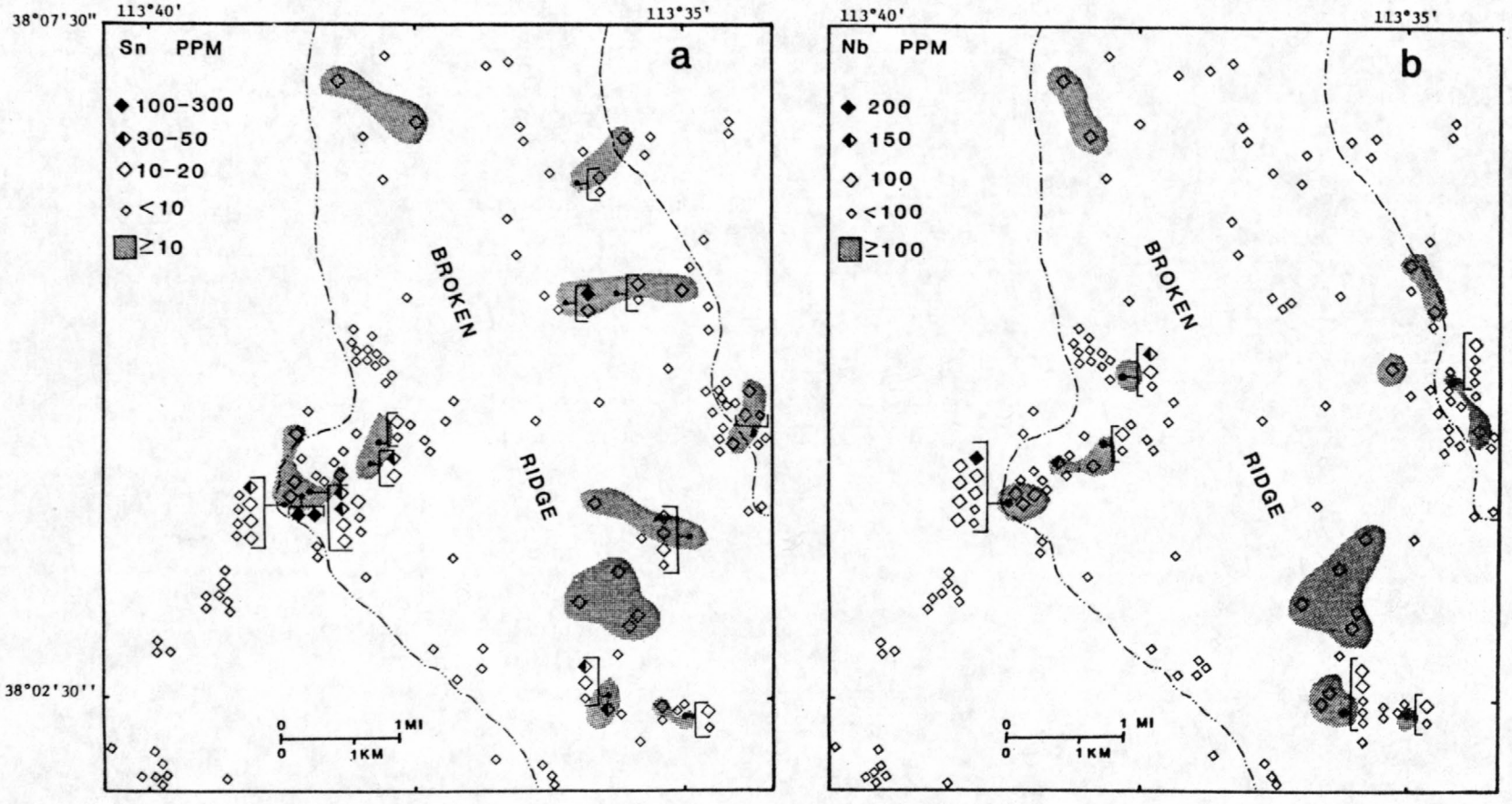

Figure 20.--Distribution of Sn and Nb in rock samples. (a) Sn content; (b) Nb content.

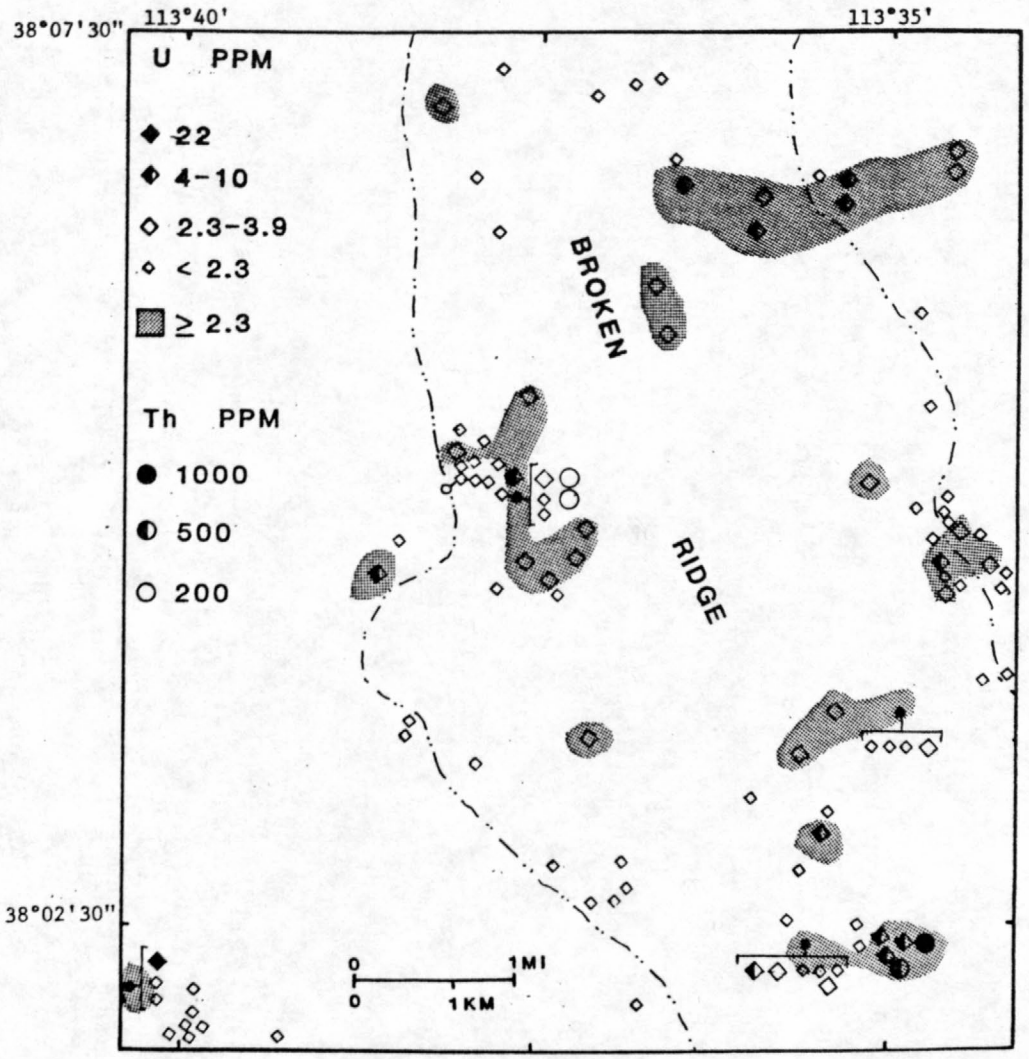

Figure 21.--Distribution of U and Th in rock samples.

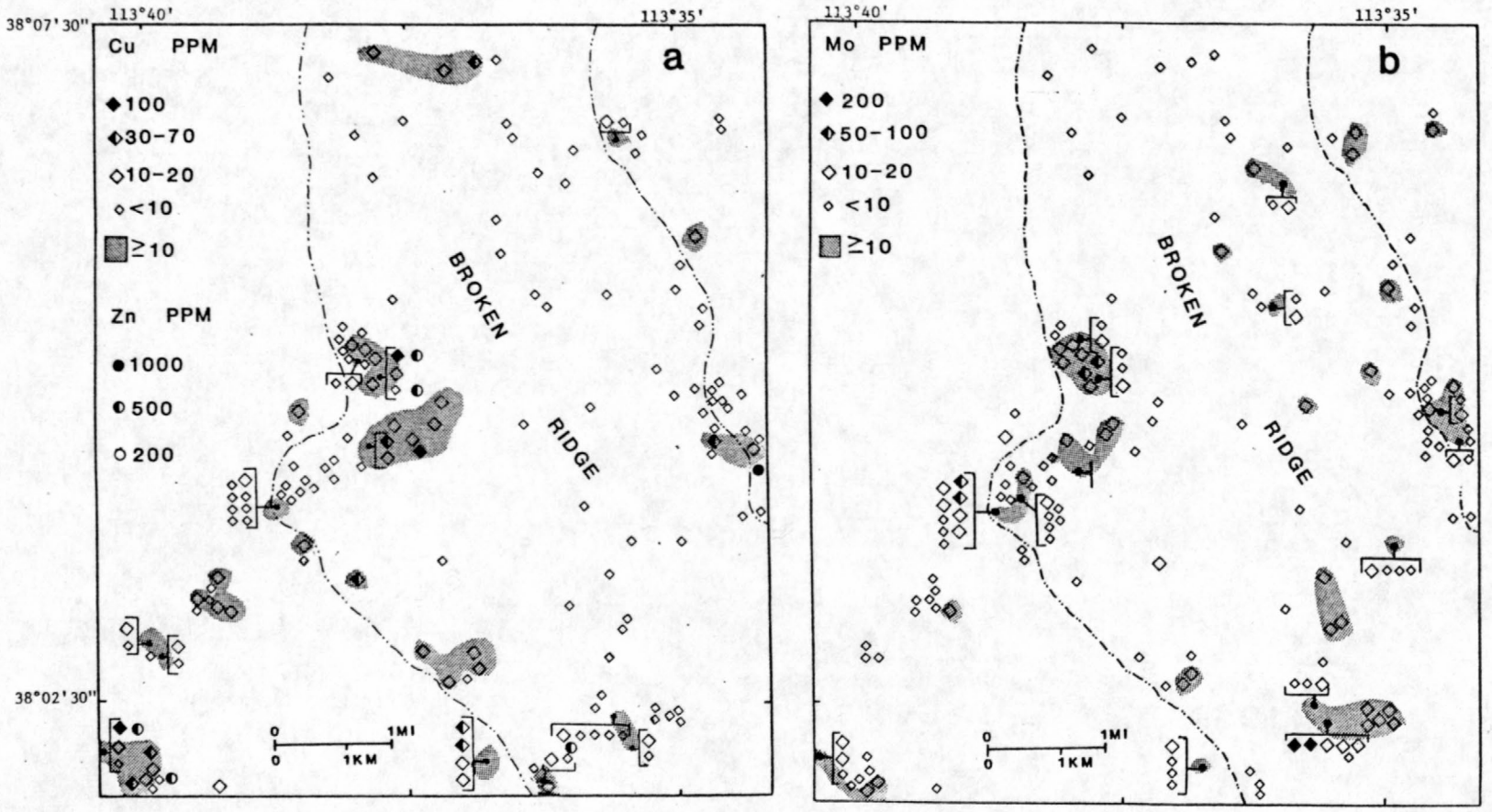

Figure 22.--Distribution of Cu and Mo in rock samples. (a) Cu content; (b) Mo content.

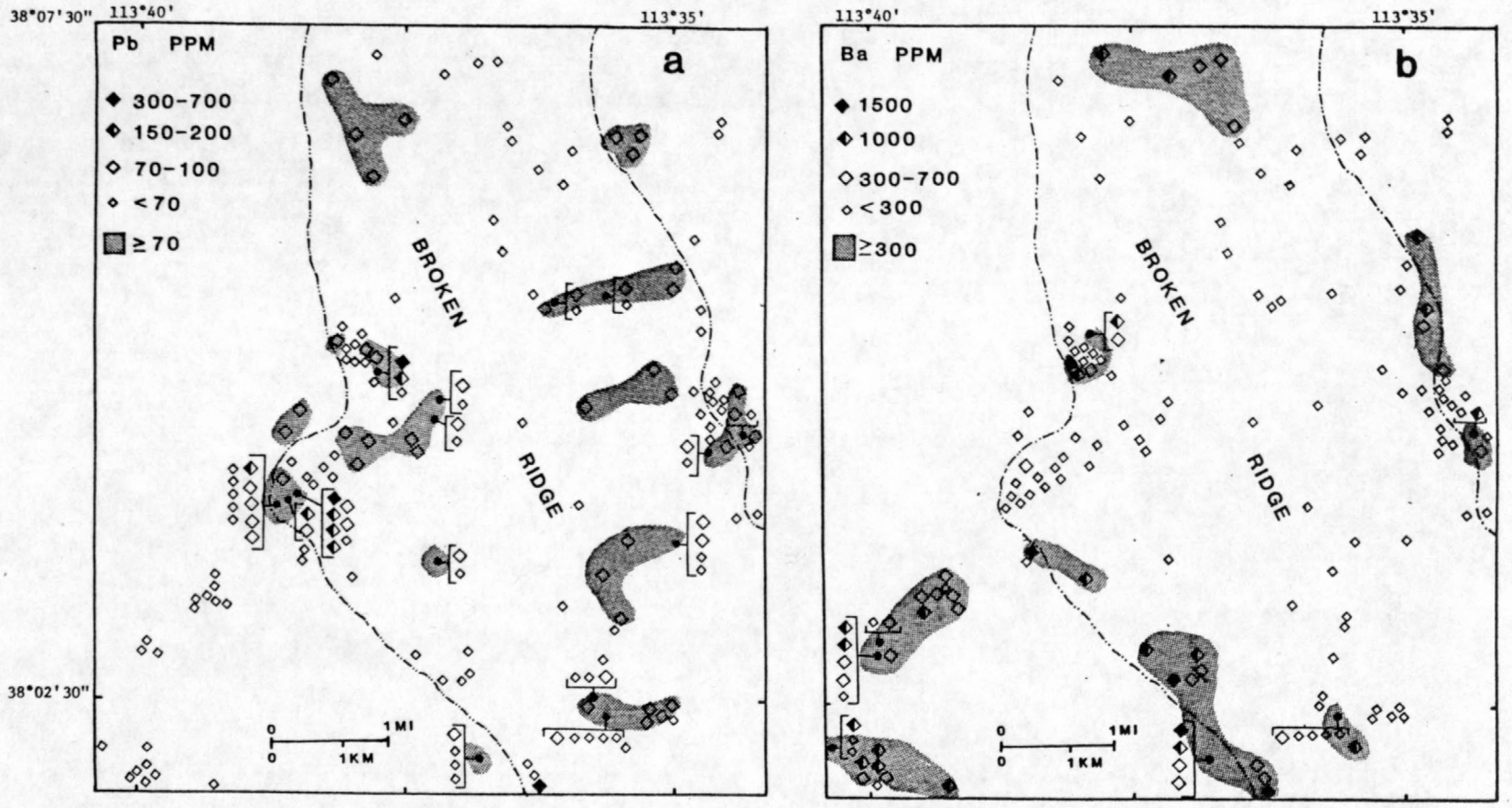

Figure 23.--Distribution of Pb and Ba in rock samples. (a) Pb content; (b) Ba content.

(fig. 21) shows the remarkable similarity to the distribution of Be, F, Sn and Nb (figures 19-20). West of the dome of Fourmile Wash and northeast of Broken Ridge, the fresh rhyolite contains 4-10 ppm U in many samples. Argillized and silicified rhyolite west of Broken Ridge contains abundant Th (100-200 ppm) with moderately high U (2.3-3.9 ppm). In the far southwest part of the map area, 22 ppm U occurs in silicified volcanic rocks with very low Th.

Anomalous Mo and Cu occur along the Bible Spring fault zone, but they are not as restricted to rhyolitic rocks as the lithophile elements and extend southwestward within the Oligocene volcanic rocks (fig. 22). The distribution of Cu clearly marks the trend of the Bible Spring fault zone. In the far southwest part of the map area, faulted Oligocene volcanic rocks are silicified and contain 30-100 ppm Cu and 10-20 ppm Mo. Going northeast along the fault zone in alunitized clastic rocks, Mo content is generally less than 10 ppm, but Cu content is consistently 10-20 ppm. Southwest of Broken Ridge in rhyolitic rocks with anomalous Be, F, Sn, Nb, U and Th, 50-100 ppm Mo occurs with 70-100 ppm Cu. Three samples with up to 100 ppm Cu also contain 200-500 ppm Zn (fig. 22). East-northeast of Broken Ridge and in the dome of Fourmile Wash, Mo and Cu contents decrease, with only a few fresh rhyolite samples containing 10-20 ppm Mo and Cu.

Altered rhyolite southwest of Broken Ridge containing high Sn, Nb, Be, F, Cu and Mo is accompanied by Pb contents of 150-700 ppm (fig. 23). Elsewhere along the northeast-trending fault zone, Pb remains moderately high at 70-100 ppm.

Barium is generally depleted in fresh rhyolite (fig. 23) and enriched in altered rhyolitic rocks and Oligocene rocks where it occurs with high Cu. An extensive area in the southwest part of the map area in the Bible Spring fault zone contains 300-1000 ppm Ba. Alunitically altered silicic clastic rocks that are slightly enriched in Cu (10-20 ppm) but depleted in the lithophile elements, Mo and Pb, are very high in Ba (up to 1000 ppm). Barium also exceeds 1000 ppm west of Broken Ridge, an area high in Be, F, U, Th, Nb, Mo, Cu and Pb.

In general, there is a close association between anomalous Be, F, Sn, Nb, Mo, U and Th. These elements are among the characteristic elements often concentrated in disseminated porphyry Mo deposits (Boyle, 1974). It is not unreasonable to suggest the possibility that the surface anomalies of these elements may reflect a porphyry Mo deposit beneath Broken Ridge (though perhaps at a great depth), particularly with the structural and stratigraphic evidence so strongly in favor of an intrusion.

Southern Broken Ridge area

Approximately 1/2 km - 1 km north-northeast of Mountain Spring Peak, a series of north to northeast-trending faults exist at the margin of the rhyolite flow rocks of the Steamboat Mountain Formation that resulted in extensive areas of argillic alteration that are partly oxidized (see discussion in alteration section). One particularly localized area (samples 251-261) contains very high Mo (200 ppm), W (150-200 ppm), U (4-10 ppm), Th (500-1000 ppm), Zn (500 ppm), F (4000-9000 ppm) and Sn (30-50 ppm).

North of this area of alteration, fresh rhyolite over an area of about 2 km^2 contains 10-20 ppm Sn, 100 ppm Nb, 10-20 ppm Mo, and average F contents of 3000 ppm but reaching 17000 ppm. The enrichment of the lithophile elements in this area may be the result of migration of fluids from the hydrothermal event responsible for the extremely high Mo, W, U, Th, Zn, F and Sn in the argillized rock to the south.

Quartz-alunite alteration of the rhyolite at Mountain Spring Peak contains 1500 ppm Ba, but unlike the alunitically altered clastic rocks in the southwest part of the map area, 300 ppm Pb accompanies the Ba. Barium is consistently high (1000-1500 ppm) west and northwest of Mountain Spring Peak in Oligocene volcanic rocks that are extensively faulted and altered.

Fourmile Wash

West of Broken Ridge and south of the dome of Fourmile Wash, a northwest-trending normal fault juxtaposes rhyolite of the Steamboat Mountain Formation against Oligocene volcanic rocks. Quartz-fluorite alteration of the green glass right at the fault grades north and south into extensive argillic alteration. Fluorine contents of the altered rhyolite are between 4500 and 8800 ppm and nearly every sample in this area has 20 ppm Be. Slight enrichments of Sn (20 ppm), U (10 ppm), Mo (20 ppm) and Cu (30 ppm) are also contained in the rhyolite. Oligocene volcanic rocks south of the fault contain high Zn (2000 ppm) and Ba (500 ppm).

Heavy-mineral concentrate geochemistry

Locations of 41 heavy-mineral-concentrate samples are shown in Figure 24 with generalized geology. All four rhyolite units of the Steamboat Mountain Formation are combined with silicic clastic rocks as Trt on Figure 24. All volcanic rocks older than the 12 m.y. Steamboat Mountain Formation are grouped as Tv. Major washes draining Broken Ridge and the area west of Broken Ridge are shown, but many of the smaller washes are not shown.

Each sample site represents a drainage area of about 2 sq km. Most samples are from drainages within the Steamboat Mountain rhyolitic units, with the exception of those in the southwestern part of the map area which represent older volcanic rocks along the Bible Spring fault zone.

The heavy-mineral concentrates were collected primarily for use in mineralogical studies. Specifically, a mineralogical study of this kind is useful in evaluating the distribution of ore-forming minerals and in locating possible source areas of the minerals. Many times concentrates reveal the presence of minerals not observed in rocks, particularly if it is a minor constituent of the rock.

Distribution of barite and garnet

Barite in the NM (non-magnetic at 1 ampere) fraction and garnet in the M.5 (magnetic at 0.5 ampere) fraction are among the minerals not observed in rocks but of abundance in concentrates. Barite is contained in concentrates from washes draining Oligocene volcanic rocks and alunitically altered clastic rocks. Both areas also have high Ba contents in rock samples (Fig. 23b). Garnet is contained in nearly every sample from areas of rhyolitic flow rocks

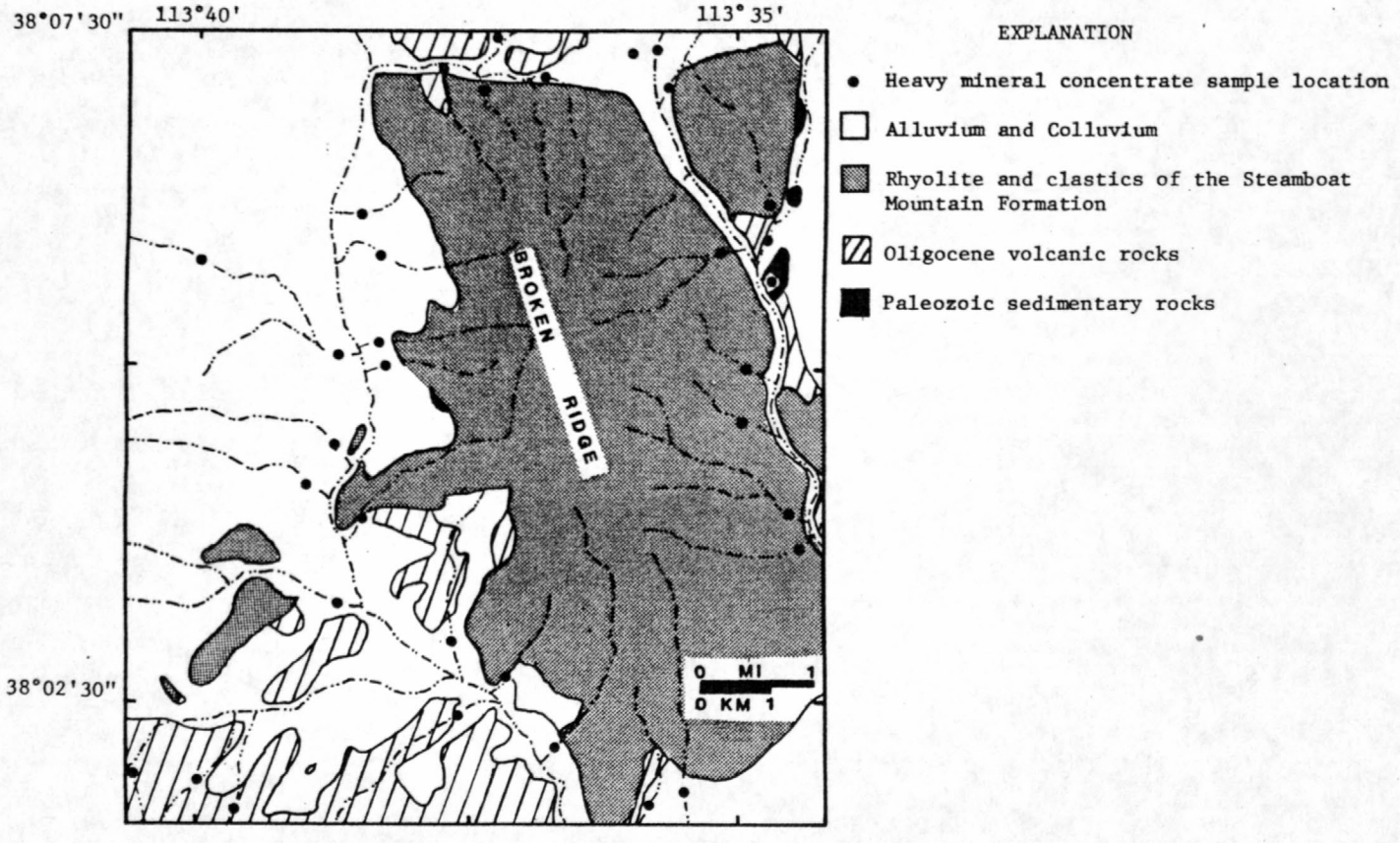

Figure 24. Heavy-mineral-concentrate sample location map with simplified geology. Geology from Best (1979), Best and Davis (1981) and Plate 1 (this report).

silicic clastic rocks of the Steamboat Mountain Formation. Semiquantitative analyses of four garnet samples show the garnet to be Mn-rich (>10,000 ppm or >1%) with 20-30% Fe. Mg and Ca contents are relatively low making the garnet spessartine-almadine in composition. Keith (1980) describes a spessartine-almadine garnet-bearing ash-flow tuff that has an elliptical area of 800 km^2 surrounding the Pine Grove pluton in the northern Wah Wah Mountains (page 10). Keith concludes the ash-flow tuff containing garnet is an eruptive facies of the granitic porphyry system in Pine Grove that is host to disseminated Mo-W at depth. For this reason, the widespread and abundant garnet in the Broken Ridge area, if contained in the rhyolitic flow rocks or clastic rocks, may hold special significance. More detailed sampling is needed to determine direct source areas for the garnet.

Distribution of Sn and cassiterite

Because of the highly silicic and lithophile-rich nature of the Steamboat Mountain Formation and the tin vein occurrence within the silicified rhyolite, attention is focused in this study on determining the distribution of Sn and cassiterite in the heavy-mineral concentrates.

Figure 25 shows the distribution of Sn as determined by emission spectrographic methods with the distribution of cassiterite as observed with a binocular microscope in the -20 mesh fraction. Tin is abundant and widespread in concentrates from the Broken Ridge area and the distribution well defines the extent of the high-silica topaz-bearing Steamboat Mountain rhyolite (for generalized geology, see figure 24).

About 40% of all samples contain 2000 ppm or greater tin, with a mean value of 700 ppm (fig. 25a). The occurrence of cassiterite in the concentrates closely coincides with the distribution of Sn content (fig. 25b). Most of the cassiterite grains are red-brown and crystalline though some wood tin or botryoidal tin is present. If cassiterite is present in trace amounts, it is frequently unrecognized or mistaken for other minerals such as rutile. During splitting, the cassiterite may go into one split and not the other. Therefore, some samples contain high Sn and no recorded cassiterite. However, in nearly all samples containing 2000 ppm or greater Sn, cassiterite was observed in the concentrate, ranging from trace amounts up to 2% of the total sample.

Tin mineralization

As described in the previous section, distribution of cassiterite in heavy mineral concentrates is widespread in areas underlain by rhyolite of the Steamboat Mountain Formation (fig. 25). Some of the crystalline cassiterite is contained in veins within the rhyolite such as in the SE 1/4 sec. 23, but much of it is probably dispersed in the rhyolite or contained in lithophysae and vugs. Crystalline cassiterite in rhyolite in the Black Range, New Mexico occurs in miarolitic cavities and in veinlets along flow-dome margins (Rye and others, 1984). Fluid inclusion and oxygen isotope studies of the rhyolite in the Black Range suggest crystalline cassiterite was deposited at intermediate temperatures (150-200°C) and salinities, suggesting mixed magmatic and meteoric water (Eggleston and Norman, 1984). Eggleston and Norman (1984) suggest that at a later stage, wood tin was formed from short-lived meteoric water-dominated epithermal systems. A scanning electron microscope (SEM)

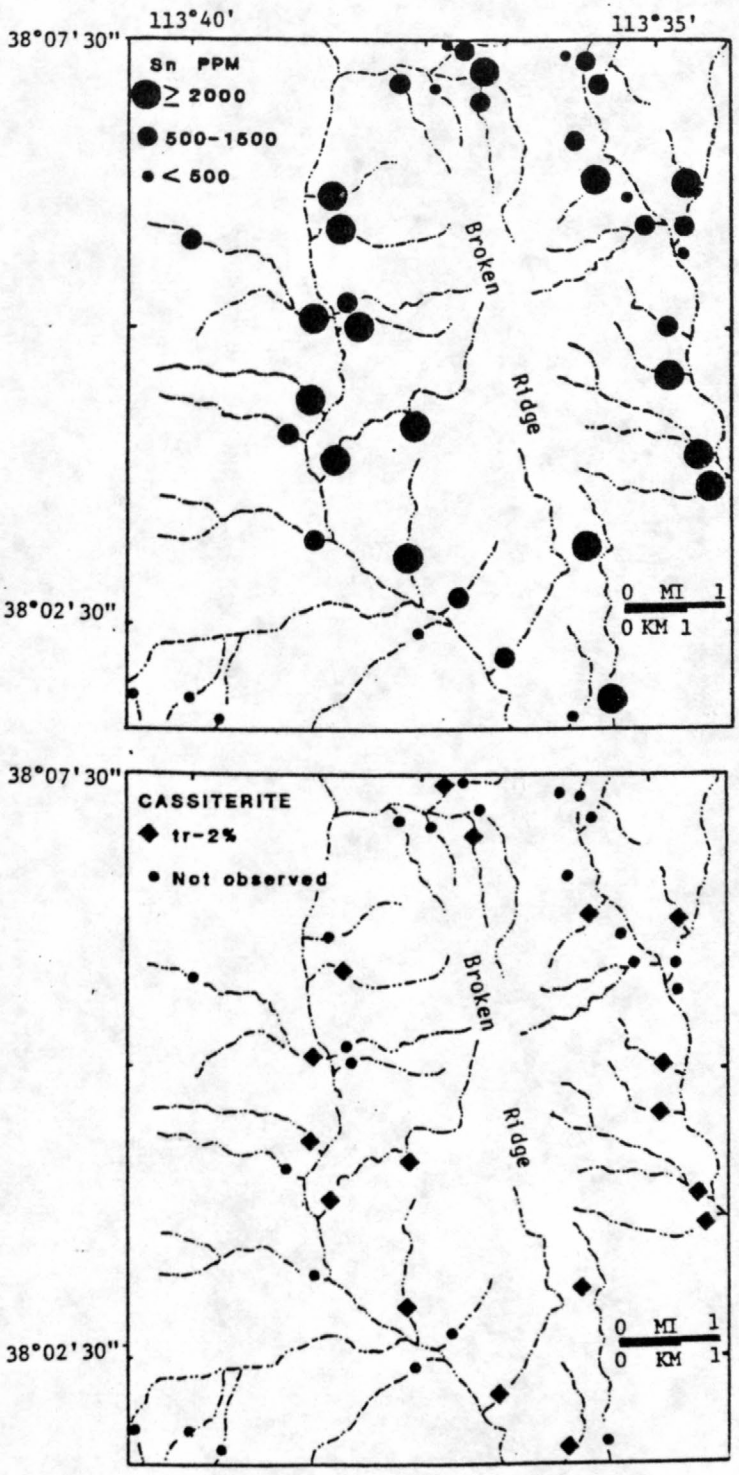

Figure 25. Distribution of Sn and cassiterite in heavy-mineral concentrates. (a) Sn content; (b) cassiterite distribution.

study of cassiterite crystals from tin rhyolites in northern Mexico found that there were four distinct stages of cassiterite development, beginning with the development of large euhedral crystals (0.5 mm) and then growth of smaller crystals on the faces of the large crystals. Later, the cassiterite was partly dissolved and reprecipitated as wood tin and overgrowths on previous crystals (Huspeni and others, 1984).

The only cassiterite observed in the rocks in the Broken Ridge area occurs with quartz and specular hematite in a vein within silicified gray rhyolite of the Steamboat Mountain Formation (SE Sec 23, T31S, R16W). Hematite is abundant and occurs as long bladed crystals. The cassiterite crystals are small (<0.1 mm) and appear to be overgrowths on the hematite crystals (fig.26). The veining in the rhyolite is in close proximity to a vent area and a possible intrusive at depth. The silicified rocks hosting the tin vein contain 50-100 ppm Be, 300 ppm Sn and 10-20 ppm Mo. The extent of the veining in this area or the presence of veining elsewhere in the Broken Ridge area has not yet been determined.

Much of the cassiterite in the Steamboat Mountain rhyolite was probably precipitated as a result of degassing during cooling of the rhyolite. During the evolution of topaz rhyolites, tin and other lithophile elements become enriched. This has been attributed, in part, to the ability of fluorine in the magma to form stable complexes with many elements, including tin; the roofward streaming of volatiles and complexed metals results in accumulation of these metals in a stagnant zone at the top of silicic magma chambers (Kovalenko and Kovalenko, 1976, p.104, from Burt and others, 1982). In addition to fluorine, chlorine also plays an important role as a complexing agent for tin and the lithophile elements (R.L. Smith, personal commun., 1985).

During and shortly after emplacement of the rhyolitic magma, volatiles and complexed metals, as a vapor phase, rise upward through the rhyolite depositing cassiterite as dispersed crystals in vugs and lithophysae. Later hydrothermal solutions may also have been responsible for some of the cassiterite in the Steamboat Mountain rhyolite. Recent studies by Jackson and Helgeson (1985) suggest that Sn is soluble in hydrothermal solutions up to 350°C and exists as hydroxide, chloride or fluoride complexes. The type of complex is dependant on pH, temperature, fugacity of oxygen, and concentration of Cl and F in solution. The solutions may have dissolved some of the cassiterite in the Steamboat Mountain rhyolite that was deposited during cooling of the rhyolite, and reprecipitated it as crystalline cassiterite in veins with hematite, or at lower temperatures as wood tin. It is conceivable, therefore, that cassiterite was deposited due to a combination of deposition during cooling of the rhyolite and from later hydrothermal solutions.

DISCUSSION AND CONCLUSIONS

Volcanic activity in the area of Broken Ridge began with explosive eruptions of silicic airfall and ash-flow tuffs (Tt) followed by eruption from many local centers of rhyolitic lava flows and domes (Trs and Trp) of the 12 m.y. Steamboat Mountain Formation. Field evidence suggests several dome-vent complexes exist: the dome of Fourmile Wash, the fissure vent complex east of Broken Ridge, and an obscured dome-vent complex south of Broken Ridge. In addition, stratigraphic and structural relationships suggest an intrusive may exist at depth beneath Broken Ridge.

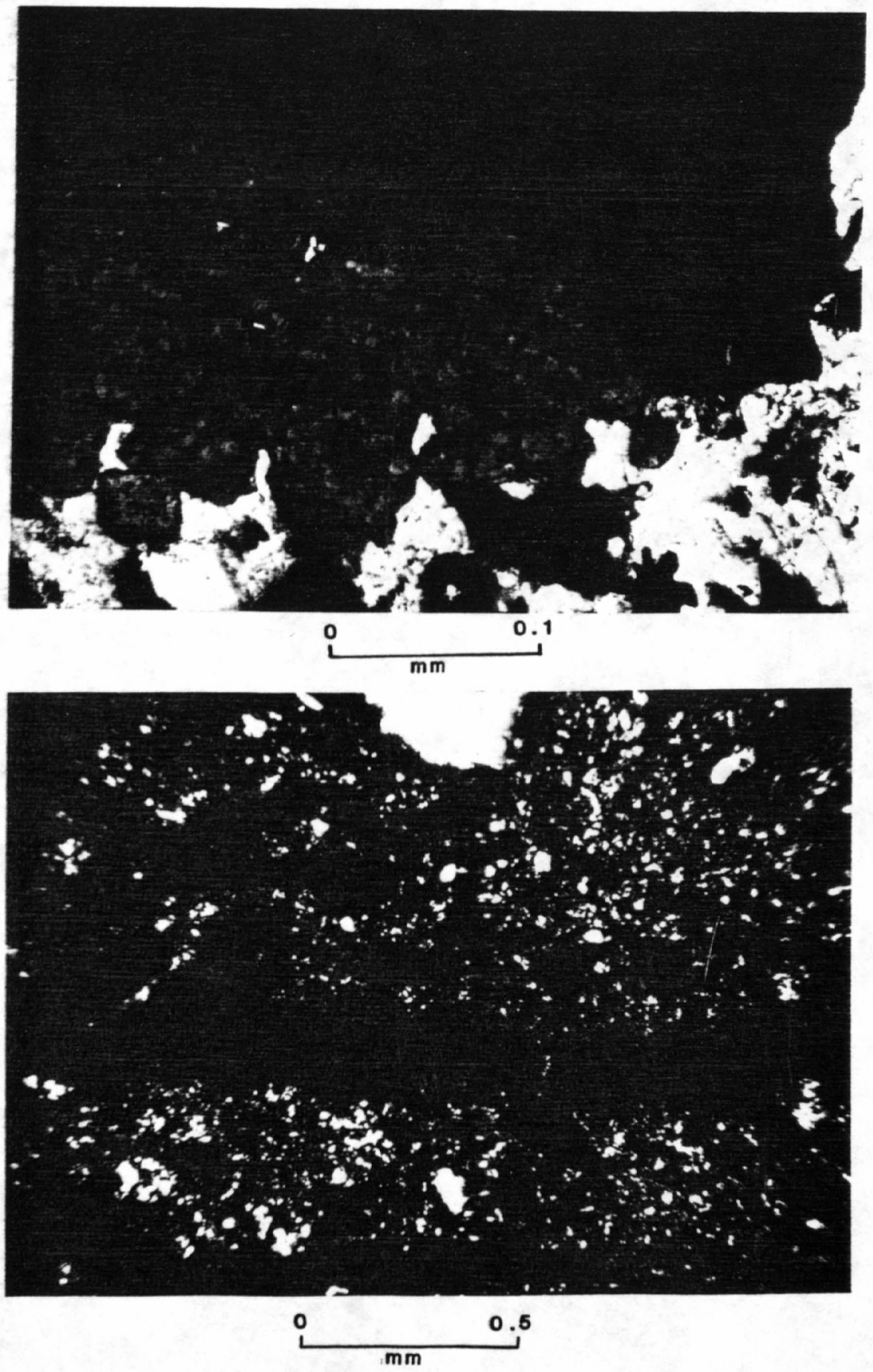

Figure 26. Photomicrographs of cassiterite and hematite in vein in silicified rhyolite. Crystalline cassiterite is coating hematite.

The high Si, alkalies, Sn, Be, F, and other lithophile elements, and low Ca, Mg, Ti, and P contents of the rhyolite are typical of other topaz rhyolites in areas such as Spor Mountain, Utah and Sierra Madre Occidental, northern Mexico. The characteristic major and trace element chemistry of the Steamboat Mountain rhyolite suggests that it formed as a highly differentiated magma. Some authors have suggested that topaz rhyolites are similar in chemistry to A-type or anorogenic granites (Burt and others, 1982) which implies the petrogenesis of the rhyolites is similar to that of A-type granites. This petrogenesis occurs prior to rifting but after subduction ceases in an environment of very high heat flow and involves partial melting of water-depleted Precambrian crustal rocks. White and others (1981) have suggested this model for the Climax-type porphyry Mo deposits as well.

Crystalline cassiterite and wood tin are abundant in the Steamboat Mountain rhyolite as suggested by greater than 2000 ppm Sn and widespread cassiterite in heavy-mineral-concentrate samples. Some of the crystalline cassiterite occurs in veins with hematite, but much of it is probably dispersed in the rhyolite as small crystals in vugs and lithophysae.

Recurrent movement along the mid-Miocene northeast-trending normal faults of the Bible Spring fault zone occurred after the emplacement of the Steamboat Mountain Formation. Numerous other north to northwest-trending faults south and southeast of Broken Ridge resulted in a series of horst and graben structures.

Figure 27 is a schematic diagram depicting the relationship between the rhyolitic tuffs and flows in the Broken Ridge area, and the types of mineralization possibly associated with them. On the surface, airfall and ash-flow tuffs alternate with lava flows and domes suggesting several episodes of volcanic activity separated by periods of surface erosion and weathering which produced epiclastic and reworked water-deposited sediments. During or shortly after emplacement of the rhyolite domes and flows, vapor phase deposition of cassiterite, topaz and fluorite occurred in lithophysae and vugs within the rhyolite. Later hydrothermal fluids may have concentrated metals as is evident by the close association of faults, alteration and geochemical anomalies.

Hydrothermal alteration along the Bible Spring fault zone and other faults south and east of Broken Ridge resulted in high concentrations of Be, F, Sn, Nb, U, Th, Mo, Cu, Zn, Pb and Ba. Argillic alteration resulted in very high Sn, Mo, Nb, U, Th, and to some extent Be, whereas silicification concentrated Sn and Be. Quartz-alunite alteration resulted in low contents of most metals with the exception of Ba and Cu. The lithophile element anomalies are restricted to rhyolite; Mo, Cu, Pb, Zn, and Ba occur with the lithophile elements but are more widely dispersed and not restricted to rhyolitic rocks. The Be, F, Sn, Nb, Mo and Cu distributions well define the Bible Spring fault zone. Most likely there were multiple hydrothermal events; much of the Ba, Cu and Zn, for instance, may be related to an early event, prior to emplacement of the rhyolite, and remobilized during later hydrothermal episodes.

There is a close association of Be, F, Sn, Nb, Mo, U, and Th anomalies within the rhyolitic rocks of the Steamboat Mountain Formation. These are characteristic elements typically associated with porphyry Mo deposits

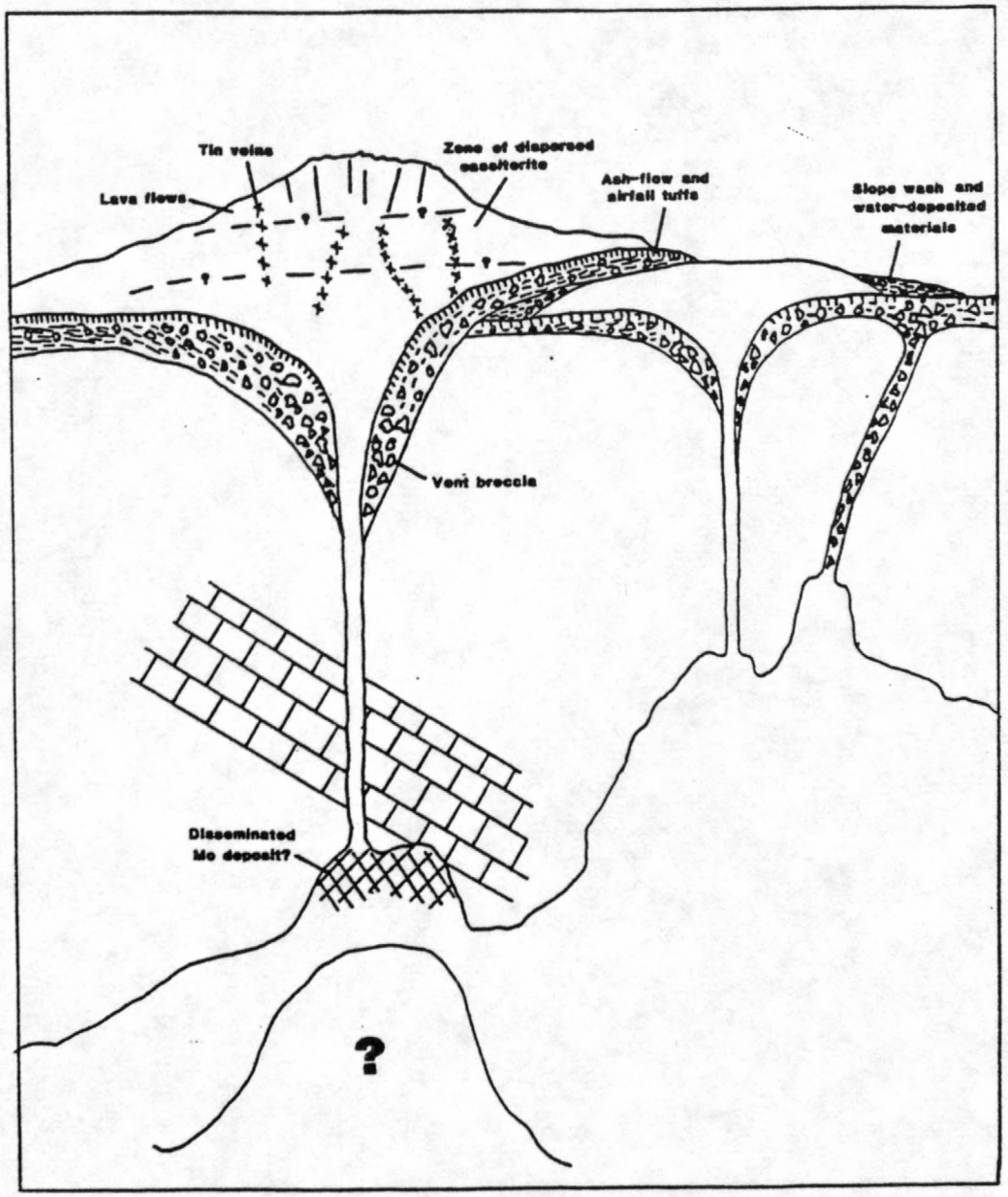

Figure 27.--Schematic diagram showing the relationship between rhyolite tuffs and flows in the Broken Ridge area, and possible mineralization related to them.

(Boyle, 1974), and may be representative of such a deposit at depth beneath Broken Ridge.

Mineralization at the surface consists primarily of cassiterite, either dispersed in the rhyolite or contained in veins within the rhyolite. If the dispersed cassiterite formed as a result of cooling shortly after emplacement of the rhyolite, presumably there would be a zone within the rhyolite which is most favorable for depositing cassiterite from a vapor phase. This zone, the limits of which are arbitrary on Figure 27, would be dependant on many factors, two of which might be temperature of the fluids and porosity of the rock. Vein tin may have also formed during cooling, or it may have been precipitated by later hydrothermal fluids that partly dissolved the dispersed cassiterite.

Suggested areas for further exploration for tin mineralization include the area immediately surrounding the Sn vein occurrence in the SE 1/4 sec. 23, the area of extensive argillic alteration immediately east of Mountain SpringWash along the Bible Spring fault zone and 1 km northeast of Mountain Spring Peak at the margin of the Steamboat Mountain Formation where extensive faulting resulted in intense silicification and argillic alteration, and geochemical anomalies of Be, F, Sn, Mo, W, Zn, U, and Th.

If an intrusion exists beneath Broken Ridge, concentrations of a number of metals such as Mo, W, or Sn are possible in a disseminated porphyry-type deposit or F and W concentrations in skarn deposits. Perhaps the alteration and geochemical anomalies along faults (which provide excellent conduits for fluids) are a reflection of these types of mineralization. Although the presence of an intrusion and associated mineral deposits is hypothetical, it is possible on the basis of the stratigraphic, structural, and geochemical data as defined in this report.

REFERENCES

Abbott, J. T., Best, M. G., and Morris, H. T., 1983, Geologic map and cross sections of the Pine Grove-Blawn Mountain area, Beaver County, Utah: U.S. Geological Survey Miscellaneous Investigations Series Map I-1479, scale 1:24,000.

Armstrong, R. L., 1970, Geochronology of Tertiary igneous rocks, eastern Basin and Range Province, western Utah, eastern Nevada, and vicinity, U.S.A.: Geochimica et Cosmochimica Acta, v. 34, p. 203-232.

Best, M. G., 1979, Geologic map of Tertiary volcanic rocks in the Mountain Spring Peak quadrangle, Iron County, Utah: U.S. Geological Survey Open-File Report 79-1610.

Best, M. G., Davis, R. L., 1981, Geologic map of the Steamboat Mountain and Bible Spring quadrangles, western Iron County, Utah: U.S. Geological Survey Open-File Report 81-1213.

Best, M. G., Grant, S. K., 1985, Stratigraphy of the volcanic Oligocene, Needles Range Group in southwestern Utah: U.S. Geological Survey Professional Paper, in press.

Best, M. G., Mehnert, H. H., Keith, J. D., and Naesar, C. W., 1983, Miocene magmatism and tectonism in and near the southern Wah Wah Mountains, southwestern Utah: U.S. Geological Survey Bulletin, in press.

Best, M. G., Shuey, R. T., Caskey, C. F., and Grant, S. K., 1973, Stratigraphic relations of members of the Needles Range Formation at type localities in southwestern Utah: Geological Society of American Bulletin, v. 84, p. 3269-3278.

Boyle, R. W., 1974, Elemental associations in mineral deposits and indicator elements of interest in geochemical prospecting in Geol. Society of Canada Paper 74-45, revised.

Burt, D. M., Sheridan, M. F., Bikun, J. V., and Christiansen, E. H., 1982, Topaz rhyolites--distribution, origin, and significance for exploration: Econ. Geology, v. 77, p. 1818-1836.

Cantanni, F. A., Ross, A. M., and DeSesa, M. A., 1956, Fluorometric determination of uranium: Analytical Chemistry, v. 28, p. 1651.

Chappel, B. W., and White, A. J. R., 1974, Two contrasting granite types: Pacific Geol., v. 8, p. 173-174.

Christiansen, E. H., 1981, Uranium mineralization associated with fluorine-rich rhyolites in southwestern Utah: U.S. Department of Energy Open-File Report GJBS-225 (80), p. 415-458.

Christiansen, E. H., Bikun, J. V., Sheridan, M. F., and Burt, D. M., 1984, Geochemical evolution of topaz rhyolites from the Thomas Range and Spor Mountain, Utah: American Mineralogist, v. 69, p. 223-236.

Christiansen, E. H., Burt, D. M., Sheridan, M. F., and Wilson, R. T., 1983, The petrogenesis of topaz rhyolites from the Western United States: Contrib. Mineral. Petrol., v. 83, p. 16-30.

Eggleston, T. L., and Norman, D. I., 1984, Geochemistry and origin of rhyolite-hosted tin deposits, southwestern New Mexico: Geol. Soc. of Amer. Abstracts with Programs, 97th annual meeting, v. 16, no. 6, p. 499.

Ekren, E. B., Orkild, P. P., Sargent, K. A., and Dixon, G. L., 1977, Geologic map of Tertiary rocks, Lincoln County, Nevada: U.S. Geological Survey Miscellaneous Investigations Map I-1041.

Fleck, R. J., Anderson, J. J., and Rowley, P.D., 1975, Chronology of mid-Tertiary volcanism in High Plateaus region of Utah: Geological Society of America Special Paper 160, p. 53-61.

Grant, S. K., and Best, M. G., 1979, Geologic map of the Pinto Spring and part of the Atchison Creek quadrangle, Beaver and Iron Counties, Utah: U.S. Geological Survey Open-File Report 79-1656.

Griffitts, W. R., 1982, Diagnostic features of fluoride-related beryllium deposits in Erickson, R. L., compiler, Characteristics of mineral deposit occurrences: U.S. Geological Survey Open-File Report 82-795, p. 62-66.

Grimes, D. J., and Marrangino, A. P., 1968, Direct-current arc and alternating-current spark emission spectrographic field methods for the semiquantitative analysis of geologic materials: U.S. Geological Survey Circular 591, 6 p.

Hanson, G. N., 1978, The application of trace elements to the petrogenesis of igneous rocks of granitic composition: Earth and Planetary Science Letters, v. 38, p. 26-43.

Hopkins, D. M., 1977, An improved ion-selective electrode method for the rapid determination of fluorine in rocks and soils: U.S. Geological Survey Journal of Research, v. 5, p. 583-593.

Huspeni, J. R., Kesler, S. E., Ruiz, J., Tuta, Z., Sutler, J. F., and Jones, L. M., 1984, Petrology and geochemistry of rhyolites associated with tin mineralization in northern Mexico: Econ. Geol., v. 79, p. 87-105.

Jackson, K. J., and Helgeson, H. C., 1985, Chemical and thermodynamic constraints on the hydrothermal transport and deposition of tin: I. Calculation of the solubility of cassiterite at high pressures and temperatures: Geoch. et Cosmoch. Acta, v. 49, p. 1-22.

Keith, J. D., 1980, Miocene porphyry intrusions volcanism, and mineralization, southwestern Utah and eastern Nevada: M.S. thesis, University of Wisconsin, Madison, 166 p.

Kovalenko, V. I., and Kovalenko, N. I., 1976, Ongonites - (topaz-bearing quartz keratophyre) - subvolcanic analogue of rare metal Li-F granites [in Russian], in Joint Soviet-Mongolian Sci. Research Geol. Expedition, Trans., v. 15: Moscow, Nauka Press, 128 p.

Lemmon, D. M., Silberman, M. L., and Kistler, R. W., 1973, Some K-Ar ages of extrusive and intrusive rocks of the San Francisco and Wah Wah Mountains, Utah: Utah Geological Association Publication 3, p. 23-26.

Lindsey, D. A., 1982, Tertiary volcanic rocks and uranium in the Thomas Range and northern Drum Mountains, Juab county, Utah: U.S. Geological Survey Professional Paper 1221.

Lindsey, D. A., and Osmonson, L. M., 1978, Mineral potential of altered rocks near Blawn Mountain, Wah Wah Range, Utah: U.S. Geological Survey Open-File Report 78-114, 18 pages.

Loiselle, M. C., and Wones, D. R., 1979, Characteristics and origin of anorogenic granites: Geol. Soc. of Amer. Abstracts with Programs, v. 11, p. 468.

Lufkin, J. L., 1977, Chemistry and mineralogy of wood-tin, Black Range, New Mexico: Amer. Miner., v. 62, p. 100-106.

Mackin, J. H., 1960, Structural significance of Tertiary volcanic rocks in southwestern Utah: American Journal of Science, v. 258, p. 81-131.

Miller, G. M., 1966, Structure and stratigraphy of the southern part of the Wah Wah Mountains, southwest Utah: American Association of Petroleum Geologists Bulletin, v. 50, p. 858-900.

Motooka, J. M., and Grimes, D. J., 1976, Analytical precision of one-sixth order semiquantitative spectrographic analyses: U.S. Geological Survey Circular 738, 25 p.

Rowley, R. D., Lipman, P. W., Mehnert, H. H., Lindsey, D. A., and Anderson, J. J., 1978, Blue Ribbon lineament, an east trending structural zone within the Pioche mineral belt of southwestern Utah and eastern Nevada: Journal of Research U.S. Geological Survey, v. 6, p. 175-192.

Rye, R. O., Lufkin, J. L., and Wasserman, M. D., 1984, Genesis of tin occurrences in the Black Range, New Mexico, as indicated by oxygen isotope studies: Geol. Soc. of Amer. Abstracts with Programs, 97th annual meeting, v. 16, no. 6, p. 499.

Shuey, R. T., Caskey, C. F., and Best, M. G., 1976, Distribution and paleomagnatism of the Needles Range Formation, Utah and Nevada: American Journal of Science, v. 276, p. 954-968.

Staatz, M. H., and Carr, W. J., 1964, Geology and mineral deposits of the Thomas Range and Dugway Ranges, Juab and Toole Counties, Utah: U.S. Geological Survey Professional Paper 415, 187 p.

Steven, T. A., and Morris, H. T., 1984, Mineral resource potential of the Richfield 1^{o} x 2^{o} quadrangle, southwest-central Utah: U.S. Geological Survey Open-File Report 84-521, 53 p.

Thompson, C. E., Nakagawa, H. M., and Van Sickle, G. H., 1968, Rapid analysis for gold in geologic materials, in Geological Survey research 1968: U.S. Geological Survey Professional Paper 600-B, p. B130-B132.

Viets, J. G., 1978, Determination of silver, bismuth, cadmium, copper, lead, and zinc in geological materials by atomic-absorption spectrometry with tricaprylylmethylammonium chloride: Analytical Chemistry, v. 52, p. 1097-1101.

Weaver, C. L., 1980, Geology of the Blue Mountain quadrangle, Beaver and Iron Counties, Utah: Brigham Young University Studies, 27, no. 3, 116-132.

White, W. H., Bookstrom, A. A., Kamilli, R. J., Ganster, M. W., Smith, R.P., Ranta, D.E., and Steininger, R. C., 1981, Character and origin of Climax-type molybdenum deposits in Seventy-fifth Anniversary Volume, Econ. Geol, Brian J. Skinner, ed.

Zielinski, R. A., Lipman, P. W., and Millard, H. T., 1977, Minor element abundances in obsidian, perlite, and felsite of calc-alkalic rhyolites: American Mineralogist, v. 62, p. 426-437.

Zoback, M. L., Anderson, R. E., and Thompson, G. A., 1981, Cainozoic evolution of the state of stress and style of tectonism of the Basin and Range Province of the western United States: Royal Society of London, Philosophical Transactions, series A, p. 407-434.

APPENDIX A. ROCK DATA FROM THE BROKEN RIDGE AREA, UTAH--Continued

Sample	Y-ppm s	Zn-ppm s	Zr-ppm s	Li-ppm s	Th-ppm s	Cs-ppm s	Rb-ppm s	Au-ppm aa	As-ppm aa	F-ppm si	U-inst
83K4	50	<200	700	--	N	--	--	--	--	160	--
83K5	<10	<200	100	--	N	--	--	--	--	380	--
83K6	<10	<200	100	--	N	--	--	--	--	540	--
83K7	30	<200	200	--	N	--	--	--	--	860	--
83K8	50	<200	200	--	N	--	--	--	--	1,060	--
83K9	200	<200	200	--	N	--	--	--	--	3,860	--
83K12	30	<200	500	--	N	--	--	--	--	220	--
83K13	30	<200	200	--	N	--	--	--	--	180	--
83K14	30	<200	200	--	N	--	--	--	--	240	--
83K17	10	<200	200	--	N	--	--	--	--	1,060	--
83K18	10	<200	200	--	N	--	--	--	--	740	--
83K19	30	<200	200	--	N	--	--	--	--	660	--
83K20	20	<200	200	--	N	--	--	--	--	700	--
83K21	10	N	200	--	N	--	--	--	--	380	--
83K22	<10	N	200	--	N	--	--	--	--	420	--
83K25	15	N	200	--	N	--	--	--	--	460	--
83K26	10	N	200	--	N	--	--	--	--	780	--
83K27	20	N	200	--	N	--	--	--	--	820	--
83K30	70	N	200	--	N	--	--	--	--	460	--
83K31	100	N	200	--	N	--	--	--	--	810	--
83K34	100	N	200	--	N	--	--	--	--	3,460	--
83K36	50	N	200	--	N	--	--	--	--	1,360	--
83K37	70	N	200	--	N	--	--	--	--	710	--
83K38	10	N	500	--	N	--	--	--	--	460	--
83K39	10	N	300	--	N	--	--	--	--	1,060	--
83K40	N	N	200	--	N	--	--	--	--	560	--
83K42	<10	N	150	--	N	--	--	--	--	960	--
83K43	N	N	200	--	N	--	--	--	--	380	--
83K44	<10	N	200	70	N	N	20	--	--	300	--
83K45	<10	N	200	70	N	N	<10	--	--	1,200	--
83K46	<10	N	200	100	N	N	20	--	--	1,700	--
83K47	<10	N	50	100	N	20	30	--	--	3,600	--
83K48	<10	N	200	100	N	N	10	--	--	1,100	--
83K49	<10	N	200	100	N	N	<10	--	--	1,000	--
83K50	<10	N	200	100	N	N	15	--	--	900	--
83K51	<10	N	200	100	N	<20	20	--	--	1,300	--
83K52	<10	N	200	150	N	<20	30	--	--	1,300	--
83K53	<10	N	200	150	N	N	10	--	--	1,000	--
83K54	<10	N	200	20	N	N	15	--	--	900	--
83K55	20	N	200	30	N	N	50	--	--	600	--
83K56	10	N	150	70	N	N	15	--	--	740	--
83K58	10	N	100	<1	N	N	20	--	--	900	--
83K59	20	N	500	1	N	N	200	--	--	500	--
83K60	15	N	150	1	N	N	20	--	--	1,100	--
83K62	10	N	150	<1	N	N	20	--	--	500	--

APPENDIX A. ROCK DATA FROM THE BROKEN RIDGE AREA, UTAH--Continued

Sample	Cr-ppm s	Cu-ppm s	La-ppm s	Mo-ppm s	Nb-ppm s	Ni-ppm s	Pb-ppm s	Sc-ppm s	Sn-ppm s	Sr-ppm s	Y-ppm s	W-ppm s
83K4	<10	30	100	N	20	<5	300	10	N	100	50	N
83K5	15	7	N	N	N	5	50	<5	N	<100	50	N
83K6	10	10	N	N	N	5	50	<5	N	<100	20	N
83K7	10	<5	N	N	100	5	50	N	20	N	10	N
83K8	10	<5	N	N	100	5	100	N	30	N	20	N
83K9	10	<5	<20	<5	100	5	100	<5	30	N	20	N
83K12	20	7	20	N	<20	10	50	5	N	N	50	N
83K13	15	5	<20	N	<20	10	30	5	N	100	50	N
83K14	10	<5	20	N	<20	10	20	<5	N	<100	50	N
83K17	<10	<5	N	N	100	5	100	N	50	N	10	N
83K18	<10	<5	N	N	70	5	50	N	<10	N	10	N
83K19	<10	5	N	N	100	5	200	N	30	N	10	N
83K20	<10	5	N	10	100	5	300	<5	<10	N	10	N
83K21	<10	<5	N	N	100	5	150	<5	20	N	10	N
83K22	<10	<5	N	N	100	<5	200	N	15	N	<10	N
83K25	<10	5	N	N	100	5	100	N	10	N	15	N
83K26	<10	<5	N	<5	100	<5	100	N	300	N	10	N
83K27	<10	<5	N	<5	100	<5	200	N	150	<100	15	N
83K30	<10	<5	20	7	100	<5	100	N	20	N	20	N
83K31	<10	<5	100	20	70	<5	70	N	N	N	10	N
83K34	<10	7	50	<5	70	5	70	N	15	N	15	N
83K36	<10	<5	<20	5	70	<5	70	N	N	N	10	N
83K37	10	15	70	10	100	<5	100	N	10	N	10	N
83K38	10	N	N	50	200	N	70	N	N	N	30	N
83K39	<10	<5	N	10	70	N	50	N	N	100	15	N
83K40	<10	<5	N	10	100	N	100	N	N	N	15	N
83K42	10	<5	N	10	50	N	100	N	15	N	20	N
83K43	<10	N	N	N	100	<5	10	N	15	<100	10	N
83K44	<10	<5	N	N	100	5	50	N	30	N	10	N
83K45	<10	<5	N	20	100	5	70	N	<10	N	10	N
83K46	<10	<5	N	<5	50	5	20	N	<10	N	10	N
83K47	<10	<5	N	10	<20	5	150	N	<10	N	10	N
83K48	<10	<5	N	5	100	5	20	N	N	N	10	N
83K49	<10	<5	N	5	100	5	20	N	N	N	<10	N
83K50	<10	<5	N	10	100	5	50	N	10	N	10	N
83K51	<10	<5	N	N	100	5	<10	N	N	N	10	N
83K52	<10	5	N	5	70	5	50	N	N	N	10	N
83K53	<10	<5	N	N	100	5	30	N	N	N	10	N
83K54	<10	<5	N	50	100	5	70	N	20	N	20	N
83K55	<10	<5	N	20	100	5	20	N	N	N	20	N
83K56	10	10	70	N	<20	<5	20	<5	N	700	50	N
83K58	15	15	100	10	N	<5	30	10	N	500	70	N
83K59	N	15	70	N	<20	<5	30	10	N	200	70	N
83K60	10	<5	<20	N	N	<5	20	10	N	700	70	N
83K62	20	7	50	N	N	<5	30	5	N	500	70	N

APPENDIX A. ROCK DATA FROM THE BROKEN RIDGE AREA, UTAH

[N, not detected; <, detected but below the limit of determination shown; >, determined to be greater than the value shown.]

Sample	Latitude	Longitude	Fe-pct. s	Mg-pct. s	Ca-pct. s	Ti-pct. s	Mn-ppm s	Ag-ppm s	B-ppm s	Ba-ppm s	Be-ppm s	Co-ppm s
83K4	38 1 35	113 36 16	5.00	.20	.20	.500	500	N	10	1,500	2.0	N
83K5	38 1 38	113 36 16	.70	.10	.50	.150	10	N	20	500	2.0	N
83K6	38 1 38	113 36 16	.70	.70	.20	.100	20	N	70	700	2.0	N
83K7	38 2 23	113 35 42	2.00	.05	.05	.100	50	N	10	100	<1.0	N
83K8	38 2 23	113 35 42	2.00	.02	.05	.100	50	N	10	100	<1.0	N
83K9	38 2 17	113 36 17	3.00	.50	.20	.150	200	N	30	100	5.0	N
83K12	38 1 52	113 36 25	3.00	1.00	.20	.300	100	N	30	500	2.0	<5
83K13	38 1 52	113 36 25	3.00	.70	3.00	.200	1,000	N	30	700	3.0	<5
83K14	38 1 52	113 36 25	1.50	.50	.10	.300	50	N	100	700	2.0	N
83K17	38 3 56	113 38 26	1.00	.10	.10	.100	70	N	20	N	10.0	N
83K18	38 3 56	113 38 26	.50	.10	.10	.100	70	N	20	N	10.0	N
83K19	38 3 56	113 38 26	5.00	.05	.05	.100	100	N	30	<20	10.0	N
83K20	38 3 56	113 38 26	7.00	.07	.05	.100	100	N	30	<20	10.0	N
83K21	38 3 56	113 38 26	1.00	.10	.50	.100	100	N	50	N	7.0	N
83K22	38 3 56	113 38 26	.20	.10	.50	.100	70	N	50	N	5.0	N
83K25	38 3 56	113 38 26	1.00	.15	.50	.100	100	N	70	<20	5.0	N
83K26	38 3 53	113 38 30	1.50	.05	.10	.070	100	N	100	N	7.0	N
83K27	38 3 53	113 38 30	1.50	.10	1.00	.100	50	3.0	100	N	5.0	N
83K30	38 3 54	113 38 36	1.50	.05	.05	.100	700	N	50	<20	5.0	N
83K31	38 4 24	113 37 59	1.50	.05	.07	.100	1,000	N	30	<20	10.0	N
83K34	38 3 58	113 38 36	1.50	.30	.50	.070	1,000	N	50	100	20.0	N
83K36	38 3 51	113 38 41	1.00	.30	.50	.070	200	N	70	N	7.0	N
83K37	38 3 51	113 38 41	3.00	.10	.10	.070	300	N	50	<20	10.0	N
83K38	38 3 51	113 38 41	1.00	.10	.05	.150	100	N	50	<20	20.0	N
83K39	38 3 51	113 38 41	.30	.30	.70	.100	100	<.5	100	50	15.0	N
83K40	38 3 51	113 38 41	.20	.10	.50	.100	100	N	20	<20	5.0	N
83K42	38 3 51	113 38 41	.50	.10	.07	.050	50	N	70	<20	10.0	N
83K43	38 3 51	113 38 41	.05	.10	.30	.070	50	N	20	<20	7.0	N
83K44	38 3 51	113 38 41	.15	.20	.20	.100	100	N	70	50	5.0	<5
83K45	38 3 51	113 38 41	.50	.03	<.05	.070	70	N	70	<20	5.0	<5
83K46	38 3 51	113 38 41	.10	.10	.15	.050	70	N	50	<20	2.0	<5
83K47	38 3 51	113 38 41	.20	.10	.05	.020	20	N	100	<20	1.0	N
83K48	38 3 51	113 38 41	.10	.30	.20	.100	70	N	100	<20	5.0	<5
83K49	38 3 51	113 38 41	.10	.02	.05	.100	200	N	100	20	5.0	<5
83K50	38 3 51	113 38 41	.10	.10	.10	.100	70	N	100	20	2.0	<5
83K51	38 3 51	113 38 41	.10	.10	.05	.070	100	N	100	<20	10.0	<5
83K52	38 3 51	113 38 41	.10	.50	.50	.070	200	N	100	100	5.0	<5
83K53	38 3 51	113 38 41	.10	.20	.50	.070	200	N	100	30	7.0	<5
83K54	38 3 51	113 38 41	.50	.10	.05	.070	100	N	100	20	2.0	<5
83K55	38 3 51	113 38 41	.20	.10	.20	.050	100	N	100	30	5.0	<5
83K56	38 3 11	113 39 17	.05	.10	.05	.500	10	N	20	500	1.5	N
83K58	38 3 5	113 39 17	1.50	.10	.30	.300	70	<.5	10	700	N	N
83K59	38 3 3	113 39 15	.30	.05	.05	.300	20	.5	10	500	1.0	N
83K60	38 3 4	113 39 20	.70	.05	.10	.500	30	.7	10	300	N	N
83K62	38 2 55	113 39 30	5.00	.07	.20	.300	200	<.5	<10	1,000	1.0	<5

APPENDIX A. ROCK DATA FROM THE BROKEN RIDGE AREA, UTAH--Continued

Sample	Latitude	Longitude	Fe-pct.	Mg-pct.	Ca-pct.	Ti-pct.	Mn-ppm	Ag-ppm	B-ppm	Ba-ppm	Be-ppm	Co-ppm
			%	%	%	%	%	%	%	%	%	%
83K63	38 3 7	113 39 20	10.00	.15	.70	.500	20	1	15	700	N	N
83K64	38 3 7	113 39 20	.10	.07	.50	.070	100	N	<10	100	5.0	N
83K65	38 2 41	113 39 47	2.00	.20	.70	.200	50	N	20	300	3.0	N
83K67	38 2 41	113 39 47	1.50	.15	.70	.300	50	N	10	700	3.0	N
83K76	38 2 44	113 39 55	.30	.50	1.00	.100	300	N	15	300	<1.0	<5
83K77	38 2 44	113 39 55	<.05	.10	.20	.050	70	N	<10	200	<1.0	N
83K79	38 2 40	113 39 58	.70	.20	.50	.150	300	.7	15	300	N	<5
83K80	38 2 40	113 39 58	1.50	.15	.20	.200	500	N	15	1,000	3.0	<5
83K81	38 2 40	113 39 58	.20	.30	.70	.150	70	N	10	500	N	N
83K82	38 2 40	113 39 58	2.00	.10	.05	.300	50	.5	15	1,000	N	N
83K84	38 2 40	113 39 58	.50	.07	.30	.070	30	N	10	200	N	N
83K85	38 2 40	113 39 58	.30	.05	.07	.100	20	N	15	200	<1.0	N
83K87	38 3 59	113 38 28	.30	.20	.50	.030	200	N	50	500	5.0	N
83K88	38 4 1	113 38 27	1.00	.20	.70	.050	700	N	20	N	10.0	N
83K89	38 4 1	113 38 26	1.00	1.00	1.00	.070	700	N	<10	50	20.0	N
83K90	38 4 5	113 38 17	2.00	.10	.07	.150	70	N	20	100	1.0	N
83K93	38 4 8	113 38 17	.15	.15	.70	.100	100	N	30	150	5.0	N
83K94	38 4 13	113 38 10	<.05	.20	1.00	.050	50	N	30	100	2.0	N
83K95	38 4 13	113 38 1	1.50	.15	.07	.020	1,500	N	50	20	10.0	<5
83K96	38 4 13	113 38 1	1.00	.05	.20	.020	1,000	N	70	N	7.0	N
83K98	38 5 13	113 34 35	3.00	1.00	.70	.200	700	N	N	500	1.5	7
83K99	38 5 36	113 34 47	1.50	.20	.20	.070	1,000	N	<10	<20	10.0	<5
83K100	38 5 31	113 34 50	1.00	.30	.50	.070	1,000	N	50	N	10.0	N
83K101	38 5 27	113 35 44	1.50	1.00	1.00	.070	1,000	N	70	<20	10.0	N
83K102	38 5 27	113 35 44	1.00	.15	.20	.070	1,000	N	70	20	15.0	N
83K105	38 5 25	113 36 15	.70	.05	.10	.020	500	N	30	N	7.0	N
83K106	38 5 21	113 36 8	1.00	.05	.10	.050	700	N	20	N	100.0	N
83K106A	38 4 32	113 37 25	1.00	.05	.15	.050	1,000	N	50	20	20.0	<5
83K107	38 4 32	113 37 25	1.00	.10	.70	.050	1,500	N	20	50	20.0	<5
83K108	38 4 27	113 37 25	1.00	.07	.20	.050	1,000	N	20	20	20.0	<5
83K109	38 4 27	113 37 25	1.00	.10	.20	.050	1,000	N	20	<20	20.0	<5
83K110	38 4 28	113 37 35	1.00	.10	.20	.050	1,000	N	30	20	20.0	<5
83K111	38 4 25	113 37 40	1.50	.10	.10	.070	1,000	N	30	N	20.0	<5
83K112	38 4 18	113 37 38	1.00	.10	.20	.070	1,500	N	30	<20	20.0	<5
83K113	38 4 19	113 37 46	1.00	.07	.20	.050	1,000	N	50	50	20.0	<5
83K114	38 4 17	113 37 46	1.00	.15	.20	.030	1,500	N	50	100	20.0	<5
83K115	38 4 52	113 37 45	1.00	.10	.15	.070	200	N	20	50	20.0	<5
83K116	38 4 52	113 37 45	2.00	.07	.20	.020	>5,000	N	30	50	50.0	<5
83K117	38 4 52	113 37 45	1.00	.02	.20	.020	>5,000	N	10	<20	100.0	<5
83K118	38 4 59	113 37 50	2.00	.50	.50	.050	700	N	50	50	20.0	<5
83K119	38 4 59	113 37 54	2.00	.20	.10	.100	500	N	50	30	20.0	<5
83K120	38 4 58	113 37 56	.50	.05	.10	.070	200	N	20	20	2.0	<5
83K121	38 4 58	113 37 56	5.00	.07	.50	.100	200	N	50	50	2.0	<5
83K122	38 4 57	113 37 54	.10	.02	.10	.700	200	N	20	500	20.0	<5
83K125	38 5 2	113 38 4	.20	.05	.10	.500	1,000	N	20	200	1.5	<5

APPENDIX A. ROCK DATA FROM THE BROKEN RIDGE AREA, UTAH--Continued

Sample	Cr-ppm	Cu-ppm	La-ppm	Mo-ppm	Nb-ppm	Ni-ppm	Pb-ppm	Sc-ppm	Sn-ppm	Sr-ppm	V-ppm	W-ppm
83K63	50	20	70	N	N	N	20	15	N	N	300	N
83K64	N	5	<20	N	70	<5	50	N	10	<100	15	N
83K65	10	10	70	N	N	<5	20	<5	N	200	50	N
83K67	10	5	70	<5	<20	<5	30	5	N	500	50	N
83K76	<10	15	50	N	N	<5	20	N	N	200	20	N
83K77	N	<5	50	N	70	<5	20	N	<10	200	20	N
83K79	<10	7	N	<5	20	<5	20	<5	N	200	50	N
83K80	20	10	70	7	<20	<5	50	7	N	300	70	N
83K81	<10	5	50	N	N	<5	30	N	N	200	50	N
83K82	10	5	70	<5	20	<5	20	5	N	<100	70	N
83K84	<10	<5	N	5	50	<5	10	N	<10	<100	15	N
83K85	N	<5	50	7	N	<5	50	N	N	200	30	N
83K87	N	<5	N	N	20	<5	N	N	N	300	<10	N
83K88	N	<5	70	10	50	<5	50	N	N	N	<10	N
83K89	N	<5	50	N	50	<5	20	N	<10	1,500	<10	N
83K90	10	5	50	<5	70	<5	50	5	15	200	30	N
83K93	<10	<5	N	5	150	<5	10	N	N	<100	<10	N
83K94	N	<5	N	N	70	<5	N	N	N	<100	<10	N
83K95	N	N	N	10	100	<5	100	N	30	N	<10	N
83K96	N	<5	50	5	100	<5	100	N	10	N	10	N
83K98	<10	5	50	N	<20	<5	30	7	N	200	50	N
83K99	N	<5	50	7	100	<5	70	N	N	N	<10	N
83K100	N	N	50	10	70	<5	70	N	10	N	<10	N
83K101	N	7	50	7	50	<5	100	N	10	<100	15	N
83K102	N	<5	50	5	50	<5	50	N	<10	N	15	N
83K105	N	N	N	7	50	<5	50	N	<10	N	<10	N
83K106	N	N	<20	5	50	<5	100	N	N	N	<10	N
83K106A	N	20	50	5	50	10	50	N	N	N	20	N
83K107	N	20	50	N	50	10	100	N	N	N	10	N
83K108	<10	20	50	5	20	10	50	N	N	N	20	N
83K109	<10	10	50	5	20	10	70	N	N	N	10	N
83K110	N	20	50	10	20	10	50	N	N	N	10	N
83K111	N	10	<20	10	50	10	100	N	N	N	15	N
83K112	N	100	50	<5	50	10	70	N	N	N	15	N
83K113	N	10	20	5	50	10	70	N	20	N	10	N
83K114	N	30	N	5	100	10	70	N	<10	N	20	N
83K115	N	10	N	5	100	10	50	N	N	N	10	N
83K116	N	100	<20	10	150	10	700	N	N	N	20	N
83K117	<10	<5	50	<5	50	10	200	N	N	N	10	N
83K118	<10	20	200	50	50	10	70	N	N	N	50	N
83K119	<10	15	N	10	50	10	70	N	N	N	20	N
83K120	<10	10	N	10	70	10	20	N	N	N	10	N
83K121	<10	5	100	20	50	5	50	N	N	N	70	N
83K122	<10	5	N	50	20	5	50	<5	N	N	50	N
83K125	<10	<5	N	10	<20	5	<10	<5	N	N	20	N

APPENDIX A. ROCK DATA FROM THE BROKEN RIDGE AREA, UTAH--Continued

Sample	Y-ppm s	Zn-ppm s	Zr-ppm s	Li-ppm s	Th-ppm s	Cs-ppm s	Rb-ppm s	Au-ppm aa	As-ppm aa	F-ppm si	U-inst
83K63	20	N	150	10	N	<20	50	--	--	460	--
83K64	15	N	100	15	N	<20	50	--	--	1,500	--
83K65	10	N	100	50	N	<20	100	--	--	340	--
83K67	20	N	200	15	N	N	30	--	--	800	--
83K76	10	N	200	20	N	N	30	--	--	450	--
83K77	10	N	100	<1	N	N	200	--	--	650	--
83K79	10	N	150	15	N	N	50	--	--	900	--
83K80	20	N	200	10	N	N	50	--	--	800	--
83K81	<10	N	70	10	N	N	30	--	--	550	--
83K82	15	N	300	15	N	N	15	--	--	1,700	--
83K84	20	N	150	10	N	N	70	--	--	650	--
83K85	<10	N	150	1	N	N	50	--	--	800	--
83K87	20	N	100	20	N	N	100	--	--	300	--
83K88	70	N	100	150	N	N	700	--	--	500	--
83K89	50	N	150	100	N	N	300	--	--	600	--
83K90	50	N	150	30	N	20	30	--	--	800	--
83K93	<10	N	300	70	N	N	<10	--	--	100	--
83K94	<10	N	150	15	N	N	10	--	--	120	--
83K95	70	N	100	200	N	<20	700	--	--	1,000	--
83K96	70	N	150	70	N	N	700	--	--	500	--
83K98	15	N	150	15	N	N	200	--	--	320	--
83K99	70	N	150	200	N	N	700	--	--	1,800	--
83K100	70	N	150	150	N	N	700	--	--	1,900	--
83K101	100	N	100	100	N	N	700	--	--	1,900	--
83K102	50	N	150	100	N	N	500	--	--	1,100	--
83K105	70	N	100	150	N	N	700	--	--	2,100	--
83K106	50	N	100	100	N	N	500	--	--	1,100	--
83K106A	70	<200	200	70	N	N	300	N	<5	700	3.10
83K107	100	<200	200	150	N	<20	700	N	5	7,700	3.30
83K108	70	<200	200	200	N	N	500	N	N	1,100	2.70
83K109	70	<200	200	200	N	N	500	N	N	2,000	3.40
83K110	50	<200	200	150	N	N	500	N	10	2,400	3.40
83K111	50	<200	200	150	N	N	500	N	<5	700	2.90
83K112	100	<200	200	200	N	N	500	N	<5	2,200	1.60
83K113	100	<200	200	200	N	N	700	N	5	1,600	2.20
83K114	100	<200	200	200	N	N	500	N	10	600	2.00
83K115	30	<200	200	30	N	N	700	N	N	820	.60
83K116	100	500	100	150	200	<20	700	N	10	700	2.50
83K117	50	500	20	30	200	N	100	N	5	1,200	1.00
83K118	100	<200	200	100	N	20	700	N	25	1,200	6.20
83K119	50	<200	200	50	N	N	700	N	10	1,400	1.40
83K120	10	<200	200	30	N	N	20	N	5	1,200	.90
83K121	70	<200	200	15	100	<20	50	N	5	2,200	2.00
83K122	20	<200	700	20	N	N	N	N	20	300	2.00
83K125	<10	<200	500	20	N	N	10	N	25	200	.15

APPENDIX A. ROCK DATA FROM THE BROKEN RIDGE AREA, UTAH--Continued

Sample	Latitude	Longitude	Fe-pct. S	Mg-pct. S	Ca-pct. S	Ti-pct. S	Mn-ppm S	Ag-ppm S	B-ppm S	Ba-ppm S	Be-ppm S	Co-ppm S
83K126	38 5 2	113 38 2	2.00	.20	.20	.100	1,000	N	20	100	2.0	<5
83K127	38 4 58	113 38 0	.05	.10	.20	1.000	150	N	20	1,500	<1.0	<5
83K128	38 4 35	113 38 31	2.00	.20	1.00	.100	2,000	N	50	200	15.0	<5
83K129	38 4 23	113 38 34	2.00	.05	.50	.050	1,000	N	50	20	20.0	<5
83K131	38 2 23	113 35 42	2.00	.05	<.05	.070	500	N	50	<20	20.0	<5
83K132	38 6 44	113 34 31	2.00	.10	.05	.100	1,000	N	50	<20	20.0	<5
83K133	38 6 47	113 34 31	2.00	.20	.10	.100	1,000	N	50	20	20.0	<5
83K134	38 5 54	113 34 41	2.00	.20	.20	.200	500	N	50	1,000	5.0	<5
83K135	38 6 34	113 35 54	1.00	.10	.10	.050	1,000	N	50	20	20.0	<5
83K137	38 7 15	113 36 36	1.00	.50	.20	.150	500	N	20	300	15.0	<5
83K138	38 7 12	113 36 49	5.00	1.00	1.50	.500	1,000	N	20	700	5.0	30
83K139	38 7 10	113 37 7	2.00	.20	.70	.500	700	N	30	1,000	5.0	<5
83K140	38 7 18	113 37 45	5.00	.50	1.00	.500	200	N	50	1,000	2.0	20
83K141	38 3 18	113 37 57	5.00	1.00	1.00	.500	1,000	N	20	1,000	2.0	20
83K143	38 1 40	113 39 50	5.00	1.00	1.00	.500	1,000	N	50	1,000	2.0	20
83K144	38 1 48	113 39 59	7.00	1.00	1.00	.500	1,000	N	50	1,000	2.0	20
83K145	38 4 57	113 37 50	5.00	.70	2.00	.500	3,000	N	50	1,000	2.0	10
83K150	38 1 46	113 39 57	7.00	.50	20.00	.100	>5,000	N	20	500	1.0	200
83K151	38 1 46	113 39 57	5.00	.70	20.00	.100	2,000	N	20	100	2.0	50
83K152	38 1 44	113 39 56	.70	.20	15.00	.050	500	N	20	100	2.0	10
83K153	38 1 45	113 40 5	1.00	.10	1.00	.050	3,000	1.0	50	500	5.0	10
83K154	38 1 44	113 40 10	5.00	.50	.50	.500	2,000	N	50	1,000	5.0	20
83K156	38 1 54	113 40 35	1.00	.20	.10	.100	300	.5	50	100	5.0	<5
83K157	38 1 55	113 40 33	.50	.20	<.05	.200	50	N	50	50	2.0	<5
83K159	38 1 53	113 40 36	20.00	.50	.20	.300	100	N	100	1,000	5.0	10
83K160	38 1 55	113 36 44	5.00	.70	1.00	.500	1,000	N	50	1,500	2.0	20
83K161	38 1 55	113 36 44	.50	.50	20.00	.050	3,000	N	10	500	<1.0	<5
83K163	38 1 55	113 36 44	5.00	.10	.20	.500	100	N	30	500	2.0	N
83K164	38 1 55	113 36 44	1.50	.20	.10	.300	200	N	20	1,000	2.0	N
83K167	38 2 24	113 37 0	.50	1.00	10.00	.070	200	N	50	300	5.0	<5
83K168	38 2 42	113 37 25	2.00	.50	1.00	.200	700	N	50	1,000	2.0	<5
83K170	38 2 55	113 37 20	1.00	.20	.50	.050	500	N	30	N	10.0	<5
83K171	38 2 55	113 37 20	1.00	.10	.50	.050	1,000	N	50	N	10.0	N
83K172	38 1 38	113 39 45	2.00	.20	.10	.300	100	N	20	1,000	2.0	<5
83K174	38 5 19	113 34 34	2.00	.70	1.00	.300	500	N	20	1,000	3.0	10
83K177	38 4 44	113 34 41	1.00	.10	.10	.050	500	N	50	<20	10.0	<5
83K178	38 4 43	113 34 36	1.00	.10	.20	.030	500	N	30	N	10.0	<5
83K179	38 4 37	113 34 35	1.00	.10	.10	.050	1,000	N	50	20	10.0	<5
83K180	38 4 36	113 34 34	1.00	.10	.20	.050	500	N	50	<20	20.0	<5
83K181	38 3 20	113 34 34	.70	.05	.20	.050	200	N	50	N	10.0	<5
83K182	38 3 20	113 34 34	2.00	.20	.20	.050	200	N	50	N	10.0	<5
83K183	38 3 22	113 34 35	1.00	.20	.20	.050	500	N	50	20	10.0	<5
83K184	38 3 17	113 34 27	1.00	.10	.10	.050	500	N	20	N	10.0	<5
83K186	38 3 23	113 34 20	1.50	.50	.70	.050	1,000	N	200	200	20.0	<5
83K187	38 3 23	113 34 20	.70	.70	1.00	.050	500	N	200	1,000	20.0	<5

APPENDIX A. ROCK DATA FROM THE BROKEN RIDGE AREA, UTAH--Continued

Sample	Cr-ppm s	Cu-ppm s	La-ppm s	Mo-ppm s	Nb-ppm s	Ni-ppm s	Pb-ppm s	Sc-ppm s	Sn-ppm s	Sr-ppm s	Y-ppm s	Yb-ppm s
83K126	<10	10	<20	10	50	10	10	N	N	N	10	N
83K127	<10	5	N	10	50	5	<10	10	N	N	50	N
83K128	N	20	50	5	70	10	70	N	N	N	20	N
83K129	N	<5	50	10	70	10	70	N	20	N	10	N
83K131	N	<5	N	10	70	10	30	N	N	N	10	N
83K132	N	<5	20	10	50	10	50	N	N	N	10	N
83K133	N	5	50	5	50	10	50	N	N	N	20	N
83K134	N	10	20	N	N	10	30	<5	N	100	50	N
83K135	N	5	<20	<5	50	10	50	<5	N	N	10	N
83K137	N	5	N	N	20	10	10	<5	N	200	50	N
83K138	200	70	100	N	<20	200	20	20	N	300	100	N
83K139	N	15	100	<5	<20	5	50	10	N	200	50	N
83K140	20	20	50	N	N	10	20	20	N	200	200	N
83K141	50	50	50	N	N	20	20	20	N	500	200	N
83K143	50	20	50	N	N	20	30	20	N	300	200	N
83K144	100	50	50	N	N	30	30	20	N	<100	300	N
83K145	20	10	50	10	N	5	50	10	N	500	200	N
83K150	20	7	N	20	N	200	10	<5	N	500	50	N
83K151	<10	5	N	20	N	50	10	N	N	500	20	N
83K152	<10	<5	N	10	N	<5	<10	N	N	500	20	N
83K153	<10	50	N	N	N	10	<10	N	N	N	20	N
83K154	50	20	N	N	N	10	20	10	N	N	200	N
83K156	20	10	N	20	N	5	<10	N	N	N	100	N
83K157	<10	5	N	10	N	5	<10	<5	N	N	100	N
83K159	50	100	N	N	N	20	10	20	N	<100	200	N
83K160	50	50	100	N	N	20	30	20	N	200	200	N
83K161	<10	10	N	20	N	5	<10	<5	N	500	20	N
83K163	N	30	100	N	<20	10	70	10	N	N	100	N
83K164	<10	10	50	N	N	5	20	5	N	N	50	N
83K167	N	5	N	20	N	10	20	<5	N	300	20	N
83K168	N	15	<20	N	N	10	20	<5	N	100	50	N
83K170	N	<5	<20	10	50	10	50	N	N	N	10	N
83K171	N	<5	<20	10	50	20	70	N	N	N	10	N
83K172	10	20	<20	N	N	20	20	5	N	100	100	N
83K174	<10	5	50	N	100	10	30	10	N	200	100	N
83K177	N	<5	100	<5	20	15	50	N	N	N	10	N
83K178	N	<5	20	N	50	10	50	N	N	N	10	N
83K179	<10	<5	50	N	100	10	50	N	N	N	10	N
83K180	<10	<5	20	10	50	10	50	N	N	N	10	N
83K181	<10	<5	<20	N	50	20	30	N	N	N	20	N
83K182	<10	<5	<20	N	50	10	100	N	N	N	10	N
83K183	<10	30	<20	N	50	10	50	N	N	N	10	N
83K184	N	<5	20	N	50	5	100	N	20	N	20	N
83K186	N	<5	20	10	100	10	100	N	10	200	10	N
83K187	N	<5	<20	N	50	10	20	N	N	5,000	10	N

APPENDIX A. ROCK DATA FROM THE BROKEN RIDGE AREA, UTAH--Continued

Sample	Y-ppm s	Zn-ppm s	Zr-ppm s	Li-ppm s	Th-ppm s	Cs-ppm s	Rb-ppm s	Au-ppm aa	As-ppm aa	F-ppm si	U-inst
83K126	20	<200	200	20	N	N	15	N	5	800	.25
83K127	10	<200	700	3	N	N	N	N	5	300	.20
83K128	100	<200	200	150	N	N	500	N	10	1,400	2.00
83K129	100	<200	200	150	N	N	500	N	15	7,400	5.00
83K131	20	<200	200	200	<100	N	700	N	N	1,000	.90
83K132	70	<200	100	70	N	N	500	N	N	520	3.40
83K133	70	<200	100	150	N	<20	700	N	N	520	3.60
83K134	20	<200	300	70	N	N	300	N	<5	400	.90
83K135	50	<200	100	200	N	N	700	N	10	800	2.70
83K137	50	<200	100	200	N	N	200	N	10	1,100	1.10
83K138	50	<200	300	30	N	N	150	N	10	1,100	.35
83K139	50	<200	500	20	N	N	300	N	15	600	.50
83K140	20	<200	200	20	N	<20	100	N	N	600	.45
83K141	20	<200	200	30	N	N	150	N	N	700	.25
83K143	20	<200	200	20	N	N	100	N	N	600	.45
83K144	20	<200	200	50	N	N	500	N	5	700	.55
83K145	20	200	200	50	N	<20	500	N	<5	11,000	1.30
83K150	<10	500	100	15	N	N	200	N	30	500	1.00
83K151	10	<200	50	2	N	N	100	N	15	600	1.00
83K152	<10	<200	20	3	N	N	100	N	N	400	.25
83K153	<10	<200	10	150	N	N	50	N	50	300	.25
83K154	10	<200	100	50	N	N	500	N	15	400	1.00
83K156	<10	<200	50	200	N	N	50	N	40	300	1.30
83K157	<10	<200	70	200	N	N	150	N	30	400	1.30
83K159	20	500	100	50	N	<20	300	N	65	1,200	22.00
83K160	30	<200	300	50	N	<20	200	N	5	800	.30
83K161	<10	<200	20	15	N	N	50	N	10	300	.30
83K163	50	<200	100	7	N	N	200	N	15	200	2.10
83K164	20	<200	300	7	N	N	200	N	15	300	2.20
83K167	20	<200	50	30	N	N	200	N	5	1,500	1.20
83K168	10	<200	200	50	N	N	300	N	<5	400	.45
83K170	70	<200	200	100	N	N	300	N	5	400	2.50
83K171	70	<200	200	70	N	N	300	N	N	400	2.10
83K172	N	<200	100	50	N	N	500	N	<5	500	.70
83K174	20	<200	200	20	N	N	200	N	5	500	.65
83K177	100	<200	200	100	N	N	500	N	<5	1,200	1.70
83K178	70	<200	100	100	N	N	500	N	N	2,200	1.60
83K179	50	<200	100	150	N	N	700	N	N	8,800	.90
83K180	100	<200	100	150	N	N	500	.10	N	3,200	2.30
83K181	70	<200	150	70	N	N	700	N	<5	1,000	2.50
83K182	70	<200	100	100	N	N	700	N	<5	1,800	1.10
83K183	70	<200	100	70	N	N	700	N	<5	1,900	1.30
83K184	70	<200	100	70	N	N	700	N	N	1,200	.80
83K186	100	<200	150	100	N	150	700	N	N	1,900	1.30
83K187	100	<200	100	200	N	20	200	N	N	1,700	3.80

APPENDIX A. ROCK DATA FROM THE BROKEN RIDGE AREA, UTAH--Continued

Sample	Latitude	Longitude	Fe-pct.	Mg-pct.	Ca-pct.	Ti-pct.	Mn-ppm	Ag-ppm	B-ppm	Be-ppm	Be-ppm	Co-ppm
			S	S	S	S	S	S	S	S	S	S
83K188	38 3 17	113 34 17	5.00	1.00	.70	.300	1,000	N	100	500	20.0	10
83K190	38 4 50	113 34 34	1.00	.50	.50	.100	300	N	20	500	5.0	<5
83K191	38 4 49	113 34 52	1.00	.20	.50	.050	1,000	N	20	N	20.0	<5
83K192	38 4 37	113 34 35	2.00	.30	.50	.070	1,000	N	20	<20	20.0	<5
83K193	38 4 37	113 34 35	1.00	.20	.20	.050	1,000	N	20	N	20.0	<5
83K194	38 4 37	113 34 35	.50	.10	.50	.050	200	N	20	<20	5.0	<5
83K195	38 4 34	113 34 38	2.00	.20	.30	.050	1,000	N	50	<20	20.0	N
83K196	38 4 35	113 34 27	.70	.50	.10	.050	200	N	50	N	20.0	<5
83K197	38 4 35	113 34 27	1.00	.20	.30	.050	500	N	50	N	20.0	<5
83K198	38 3 27	113 34 33	1.00	.30	.20	.050	700	N	50	N	20.0	<5
83K199	38 3 23	113 34 8	1.00	.30	.50	.050	1,000	N	50	N	20.0	<5
83K202	38 3 47	113 34 16	1.00	.50	1.00	.070	700	N	50	100	20.0	<5
83K203	38 3 42	113 34 5	2.00	.70	1.00	.200	500	N	50	200	20.0	<5
83K204	38 3 42	113 34 5	1.00	.70	1.00	.100	700	N	20	200	20.0	<5
83K207	38 1 38	113 35 22	2.00	.20	.20	.500	200	N	50	1,000	2.0	<5
83K208	38 1 38	113 35 22	2.00	.20	.50	.500	100	N	20	1,000	3.0	<5
83K229	38 3 18	113 35 39	1.00	.15	.50	.050	1,000	N	20	50	20.0	N
83K230	38 2 58	113 35 50	1.00	.15	.10	.050	1,000	N	30	100	20.0	N
83K230A	38 2 40	113 35 36	.20	.10	.20	.070	300	N	20	30	10.0	N
83K231	38 7 37	113 35 27	1.50	1.00	.50	.100	1,000	N	30	50	30.0	N
83K232	38 7 37	113 35 27	1.50	.70	.50	.100	1,000	N	20	100	20.0	N
83K233	38 6 42	113 35 15	1.00	.15	1.00	.070	1,500	N	30	50	15.0	N
83K234	38 6 37	113 35 17	1.00	.10	1.00	.070	1,000	N	30	70	15.0	<5
83K235	38 6 45	113 36 31	1.00	.30	3.00	.100	300	N	<10	300	15.0	<5
83K236	38 5 48	113 36 34	1.00	.20	.50	.070	700	N	30	20	20.0	N
83K237	38 6 0	113 36 41	1.00	.10	.20	.070	1,000	N	30	<20	20.0	N
83K238	38 6 41	113 36 27	.70	.10	.70	.070	700	N	30	20	15.0	N
83K239	38 6 41	113 36 26	1.00	.07	.20	.070	700	N	50	20	20.0	<5
83K240	38 6 17	113 44 56	.50	.10	.30	.050	700	N	30	50	20.0	<5
83K247	38 3 29	113 38 24	5.00	1.00	2.00	.500	700	N	10	1,500	2.0	20
83K248	38 3 27	113 38 25	2.00	.10	.10	.020	150	N	10	200	15.0	5
83K249	38 2 56	113 35 27	1.00	.10	.30	.070	1,000	N	50	<20	10.0	N
83K250	38 2 55	113 35 30	1.50	.15	5.00	.070	1,000	N	50	50	20.0	N
83K251	38 2 13	113 35 36	3.00	.20	.10	.070	>5,000	N	30	500	20.0	N
83K252	38 2 13	113 35 35	1.00	.10	.10	.070	1,500	N	20	<20	10.0	N
83K253	38 2 13	113 35 34	1.00	.05	.05	.100	1,000	N	30	N	3.0	<5
83K254	38 2 13	113 35 37	5.00	.05	.20	.050	1,000	N	50	20	10.0	<5
83K255	38 2 13	113 35 37	3.00	.10	<.05	.200	200	.5	30	50	2.0	<5
83K256	38 2 8	113 35 11	1.00	.10	.20	.070	1,500	N	30	200	15.0	<5
83K257	38 2 7	113 35 11	1.00	.10	.50	.070	1,000	N	30	<20	15.0	<5
83K258	38 2 12	113 35 6	1.00	1.00	.50	.070	700	N	70	<20	10.0	<5
83K259	38 2 13	113 35 6	1.00	.05	.05	.070	500	<.5	50	100	10.0	<5
83K260	38 2 10	113 35 5	2.00	.15	1.00	.070	500	N	100	<20	10.0	<5
83K261	38 2 10	113 35 5	1.00	.10	.07	.070	700	<.5	100	<20	15.0	5
83K262	38 2 33	113 36 57	1.50	.20	.07	.500	70	N	20	500	2.0	<5

APPENDIX A. ROCK DATA FROM THE BROKEN RIDGE AREA, UTAH--Continued

Sample	Cr-ppm	Cu-ppm	La-ppm	Mo-ppm	Nb-ppm	Ni-ppm	Pb-ppm	Sc-ppm	Sn-ppm	Sr-ppm	V-ppm	W-ppm
83K188	20	10	<20	<5	N	50	20	10	N	100	100	N
83K190	N	<5	<20	N	N	20	20	5	N	N	20	N
83K191	N	<5	20	10	100	20	100	N	N	N	10	N
83K192	N	<5	50	<5	50	10	50	N	N	N	20	N
83K193	N	<5	20	N	20	10	50	N	N	N	10	N
83K194	<10	<5	N	N	50	20	20	N	N	N	10	N
83K195	N	5	20	N	50	10	50	N	N	N	15	N
83K196	N	<5	N	10	20	10	50	N	N	N	10	N
83K197	N	5	50	<5	50	15	50	N	N	N	10	N
83K198	N	<5	20	<5	50	20	50	N	N	N	10	N
83K199	N	<5	20	5	50	10	70	N	N	N	10	N
83K202	<10	<5	20	N	50	15	20	N	N	1,000	20	N
83K203	10	5	<20	N	<20	70	10	5	N	1,500	50	N
83K204	<10	<5	N	<5	50	15	50	N	N	2,000	15	N
83K207	N	10	100	<5	N	10	50	10	N	200	50	N
83K208	<10	5	100	N	<20	10	20	10	N	500	100	N
83K229	<10	<5	N	10	100	5	70	N	10	N	10	N
83K230	<10	<5	N	5	100	5	50	N	20	N	<10	N
83K230A	<10	<5	N	<5	50	<5	30	N	<10	N	<10	N
83K231	<10	10	20	<5	70	<5	70	<5	10	N	10	N
83K232	<10	7	20	<5	70	10	70	<5	10	N	20	N
83K233	<10	5	<20	10	70	15	70	N	<10	N	10	N
83K234	<10	<5	<20	10	70	10	100	<5	<10	N	<10	N
83K235	10	<5	<20	N	<20	15	20	5	N	500	20	N
83K236	<10	<5	N	10	50	<5	50	<5	<10	N	<10	N
83K237	<10	<5	N	5	50	<5	50	<5	<10	N	10	N
83K238	<10	<5	N	5	50	5	50	<5	<10	N	<10	N
83K239	<10	<5	N	10	70	10	50	<5	<10	N	<10	N
83K240	<10	<5	N	5	50	<5	30	<5	10	N	<10	N
83K247	100	20	20	N	<20	10	30	15	N	700	100	N
83K248	<10	<5	N	N	N	10	<10	N	N	N	20	N
83K249	<10	<5	<20	10	100	5	100	N	10	N	<10	N
83K250	<10	<5	20	10	100	<5	50	<5	10	N	10	N
83K251	<10	10	<20	200	70	5	100	N	N	<100	50	200
83K252	<10	<5	N	20	70	<5	50	N	N	N	<10	N
83K253	<10	<5	N	10	100	<5	30	N	N	N	<10	N
83K254	<10	<5	N	100	100	<5	50	N	N	N	20	150
83K255	20	5	100	<5	50	10	30	5	<10	<100	70	N
83K256	<10	5	N	10	70	<5	70	N	10	N	<10	N
83K257	<10	<5	N	10	70	<5	70	N	<10	N	<10	N
83K258	<10	<5	>1,000	10	70	15	70	N	N	N	10	N
83K259	<10	<5	20	15	50	15	70	<5	N	N	10	N
83K260	<10	<5	300	15	70	5	30	<5	N	N	20	N
83K261	<10	<5	>1,000	10	100	5	50	N	15	N	<10	N
83K262	<10	10	100	10	20	5	30	5	N	<100	50	N

APPENDIX A. ROCK DATA FROM THE BROKEN RIDGE AREA, UTAH--Continued

Sample	Y-ppm s	Zn-ppm s	Zr-ppm s	Li-ppm s	Th-ppm s	Cs-ppm s	Rb-ppm s	Au-ppm aa	As-ppm aa	F-ppm si	U-inst
83K188	50	2,000	50	300	N	30	300	N	N	4,400	.60
83K190	20	<200	200	7	N	N	200	N	N	400	.05
83K191	100	<200	100	100	N	N	500	N	N	2,200	2.40
83K192	70	<200	200	100	N	N	500	N	N	1,500	1.20
83K193	70	<200	100	100	N	N	700	N	N	1,800	2.20
83K194	100	<200	200	100	N	N	200	N	<5	1,500	1.40
83K195	100	<200	200	50	N	N	300	N	10	400	1.10
83K196	10	<200	100	100	N	N	700	N	N	400	.30
83K197	100	<200	200	100	N	N	700	N	N	2,400	1.80
83K198	100	<200	200	150	N	N	700	N	20	600	4.40
83K199	100	<200	200	150	N	<20	500	N	<5	2,800	1.70
83K202	70	<200	100	100	N	<20	300	N	5	500	.75
83K203	50	<200	200	150	N	N	200	N	N	1,900	1.20
83K204	70	<200	100	100	N	20	200	N	5	1,900	.70
83K207	50	<200	300	10	N	N	200	N	10	200	.70
83K208	50	<200	500	2	N	N	300	N	10	300	3.50
83K229	70	<200	100	200	N	<20	700	N	N	1,600	2.30
83K230	70	<200	150	200	N	20	700	.05	N	1,100	2.00
83K230A	20	<200	100	100	N	<20	500	.05	N	200	1.60
83K231	100	<200	150	300	N	20	500	.05	N	1,200	.55
83K232	100	<200	200	200	N	20	500	<.05	N	1,000	.40
83K233	100	<200	150	200	N	20	500	<.05	10	1,100	6.30
83K234	100	<200	100	150	N	N	500	<.05	10	5,200	7.10
83K235	20	<200	70	70	N	N	300	N	N	400	1.40
83K236	50	<200	100	150	N	<20	500	N	N	500	2.60
83K237	50	<200	100	200	N	<20	700	N	N	300	2.10
83K238	50	<200	100	70	N	N	500	N	N	6,200	6.50
83K239	50	<200	100	50	N	20	500	N	N	900	1.40
83K240	30	<200	100	50	N	N	300	N	N	600	4.50
83K247	20	<200	300	15	N	N	100	N	N	500	.35
83K248	10	<200	<10	30	N	<20	N	N	N	100	.25
83K249	100	<200	200	200	N	N	700	N	N	1,800	1.40
83K250	100	<200	200	200	N	N	1,000	<.05	<10	17,000	9.20
83K251	20	500	150	150	200	20	200	.40	10	2,200	2.10
83K252	<10	<200	150	200	N	N	500	.05	N	1,400	2.30
83K253	10	<200	200	200	N	N	20	.10	N	1,800	1.70
83K254	<10	<200	150	150	<100	N	20	<.05	10	400	.30
83K255	200	<200	200	20	<100	N	10	<.05	N	3,800	7.60
83K256	30	<200	150	100	N	N	500	<.05	N	800	1.40
83K257	10	<200	150	150	N	N	700	<.05	N	800	.95
83K258	>2,000	<200	150	100	N	20	700	<.05	N	4,300	4.70
83K259	200	<200	100	30	500	N	70	<.05	N	2,200	5.40
83K260	50	<200	200	150	1,000	N	15	N	10	2,800	4.10
83K261	1,000	<200	200	200	N	N	700	N	N	3,200	3.60
83K262	20	<200	500	15	N	20	200	N	10	300	1.80

APPENDIX A. ROCK DATA FROM THE BROKEN RIDGE AREA, UTAH--Continued

Sample	Latitude	Longitude	Fe-pct.	Mg-pct.	Ca-pct.	Ti-pct.	Mn-ppm	Ag-ppm	B-ppm	Ba-ppm	Be-ppm	Co-ppm
			%	%	%	%	%	%	%	%	%	%
83K263	38 2 34	113 37 0	2.00	.70	1.00	.200	500	N	<10	1,000	2.0	10
83K264	38 2 29	113 37 10	3.00	1.00	.70	.300	500	N	10	1,500	2.0	15
83K265	38 3 35	113 34 55	1.00	.05	.30	.070	1,000	N	50	N	10.0	<5
83K266	38 3 35	113 34 55	1.00	.50	1.00	.070	200	N	20	50	10.0	<5
83K267	38 3 35	113 34 55	.10	.05	.20	.010	100	N	30	<20	15.0	<5
83K268	38 3 35	113 34 55	1.00	.50	1.00	.070	700	N	10	50	15.0	<5
83K269	38 3 32	113 35 7	1.00	.07	.20	.050	1,000	N	20	<20	15.0	<5
83K274	38 7 7	113 38 12	.50	.20	.70	.020	1,000	N	50	200	10.0	<5
83K275	38 6 40	113 37 57	.70	.10	.50	.020	1,000	N	30	<20	15.0	<5
83K276	38 6 19	113 38 13	.70	.10	.20	.020	1,000	N	30	70	15.0	<5
83K277	38 5 7	113 38 7	.50	<.02	<.05	.070	70	N	10	20	20.0	<5
83K278	38 5 5	113 38 5	1.00	.10	.50	.070	300	N	20	20	10.0	<5
83K279	38 5 3	113 37 59	3.00	.02	<.05	.150	150	N	20	1,000	1.0	<5
83K280	38 5 4	113 37 58	.50	.10	.50	.500	100	N	20	500	1.0	<5
83K281	38 5 17	113 37 47	.50	.10	.20	.050	500	N	20	20	15.0	<5
84K319	38 3 43	113 35 40	.50	.20	.15	.010	300	N	20	N	5.0	N
84K327	38 4 25	113 35 15	1.00	.20	.20	.070	700	N	30	N	7.0	5
84K328	38 4 38	113 34 50	1.00	.20	.10	.100	1,000	N	30	N	7.0	5
84K331	38 4 45	113 34 23	1.00	.05	.20	.070	700	N	50	N	7.0	5
84K338	38 6 50	113 36 25	.70	.20	.30	.050	500	N	50	150	7.0	5
84K348	38 5 25	113 36 7	.70	.02	.50	.050	300	N	30	N	10.0	5
84K349	38 5 25	113 36 7	.70	.50	1.00	.050	500	N	20	N	50.0	<5
84K350	38 6 38	113 36 12	.20	.03	<0	.007	200	N	100	N	20.0	5
84K352	38 4 28	113 35 55	1.00	.10	.50	.070	1,000	N	20	N	2.0	5

APPENDIX A. ROCK DATA FROM THE BROKEN RIDGE AREA, UTAH--Continued

Sample	Cr-ppm	Cu-ppm	La-ppm	Mo-ppm	Nb-ppm	Ni-ppm	Pb-ppm	Sc-ppm	Sn-ppm	Sr-ppm	Y-ppm	W-ppm
83K263	20	10	50	N	N	5	30	10	N	700	100	N
83K264	30	20	50	N	N	10	30	10	N	700	100	N
83K265	<10	<5	20	10	70	5	70	<5	15	N	<10	N
83K266	<10	<5	<20	N	70	5	20	N	10	1,000	<10	N
83K267	<10	<5	N	N	20	5	<10	N	N	<100	<10	N
83K268	<10	<5	<20	N	50	5	70	N	10	700	<10	N
83K269	<10	<5	<20	5	100	<5	70	N	N	N	10	N
83K270	<10	<5	<20	5	100	5	100	N	10	N	10	N
83K275	<10	<5	<20	<5	100	5	100	N	<10	N	30	N
83K276	<10	<5	N	<5	70	5	100	N	<10	N	<10	N
83K277	<10	<5	N	<5	50	<5	N	N	N	N	<10	N
83K278	<10	<5	<20	<5	70	<5	70	5	N	N	<10	N
83K279	10	<5	N	20	N	7	20	N	N	N	50	N
83K280	20	<5	50	<5	50	<5	30	5	N	100	20	N
83K281	<10	<5	20	<5	70	5	50	N	N	N	<10	N
84K319	N	N	N	N	30	N	50	N	10	N	N	N
84K327	N	N	<20	15	70	10	70	N	N	N	10	N
84K328	N	N	50	7	70	N	70	N	N	N	N	N
84K331	N	N	70	10	50	N	70	N	10	N	N	N
84K338	N	N	N	<5	30	N	70	N	10	<100	N	N
84K348	N	N	<20	10	30	5	70	N	300	N	<10	N
84K349	N	N	50	<5	30	7	30	N	10	1,500	10	N
84K350	N	N	N	10	20	7	10	N	N	N	15	N
84K352	N	N	50	N	50	5	50	N	N	N	10	N

APPENDIX A. ROCK DATA FROM THE BROKEN RIDGE AREA, UTAH--Continued

Sample	Y-ppm s	Zn-ppm s	Zr-ppm s	Li-ppm s	Th-ppm s	Cs-ppm s	Rb-ppm s	Au-ppm aa	As-ppm aa	F-ppm sl	U-inst
83K263	20	<200	150	20	N	N	150	N	N	400	.45
83K264	20	<200	150	50	N	N	150	N	N	400	.45
83K265	100	<200	150	70	N	N	700	N	N	900	.15
83K266	70	<200	100	30	N	<20	500	N	N	100	1.10
83K267	20	<200	100	2	N	N	30	N	N	100	.60
83K268	50	<200	100	30	N	N	200	N	N	100	2.10
83K269	100	<200	100	200	N	N	700	N	<10	1,800	2.50
83K274	100	<200	100	200	N	N	700	N	20	1,400	2.30
83K275	100	<200	150	200	N	N	500	N	10	300	1.20
83K276	50	<200	150	200	N	N	700	N	N	700	1.50
83K277	<10	<200	150	50	N	N	30	N	N	100	.15
83K278	100	<200	150	70	N	N	500	N	<10	4,600	3.60
83K279	<10	<200	150	10	N	N	N	N	<10	100	.10
83K280	100	<200	200	10	N	N	20	N	<10	1,200	.55
83K281	100	<200	100	100	N	N	500	N	N	2,000	2.30
84K319	20	N	70	--	N	--	--	--	--	--	--
84K327	50	N	100	--	N	--	--	--	--	--	--
84K328	50	N	100	--	N	--	--	--	--	--	--
84K331	100	N	100	--	N	--	--	--	--	--	--
84K338	50	N	20	--	N	--	--	--	--	--	--
84K348	50	N	100	--	N	--	--	--	--	--	--
84K349	50	N	70	--	N	--	--	--	--	--	--
84K350	30	N	10	--	N	--	--	--	--	--	--
84K352	70	N	100	--	N	--	--	--	--	--	--

(200)
-452

OPEN-FILE REPORT 85-452

PLATE 1

TION

U.S. GEOLOGICAL SURVEY
RESTON, VA.
AUG 23 1985
LIBRARY

Quaternary

POCKET CONTAINS:
1 ITEMS

USGS LIBRARY-RESTON
3 1818 00063171 1